

**NASA CONTRACTOR
REPORT**



NASA-GRE

Q.1

0060536



TECH LIBRARY KAFB, NM

NASA CR-1399

EXPERIMENTAL VERIFICATION OF SURFACE VEHICLE DYNAMICS

*by B. D. Van Deusen, J. M. Sneyd, C. H. Hoppe,
and R. F. Hughes*

Prepared by
CHRYSLER CORPORATION
Detroit, Mich.
for

NASA CR-1399
TECH LIBRARY KAFB, NM



0060536

EXPERIMENTAL VERIFICATION
OF SURFACE VEHICLE DYNAMICS

By B. D. Van Deusen, J. M. Sneyd,
C. H. Hoppe, and R. F. Hughes

Distribution of this report is provided in the interest of information exchange. Responsibility for the contents resides in the author or organization that prepared it.

Prepared under Contract No. NASw-1607 by
CHRYSLER CORPORATION
Detroit, Mich.

for

NATIONAL AERONAUTICS AND SPACE ADMINISTRATION

For sale by the Clearinghouse for Federal Scientific and Technical Information
Springfield, Virginia 22151 - CFSTI price \$3.00



ABSTRACT

Under a previous contract (NASw-1287),⁽¹⁾ a technique was developed which allowed prediction of the dynamic response of vehicles traversing yielding and non-yielding rough surfaces. Virgin terrestrial and extraterrestrial surfaces were classified according to their frequency and amplitude distribution. A single parameter was defined which allowed accurate estimates of surface roughness. This classification determined the nature of a random input to an analog computer simulation of the vehicle and surface dynamic models. In addition, deterministic inputs were used, and a simplified linear model technique was presented using transfer function concepts.

The present study is the experimental verification of the above theoretical prediction techniques. A four wheeled truck and a specially designed single wheel trailer were instrumented and driven (pulled) across both yielding and non-yielding surfaces. The surface profile was measured on both surfaces and soil parameters were measured on the yielding surface. With this input information the theoretical prediction was compared with the physical measurements in a statistical fashion. The analog computer simulation was converted to a digital computer simulation to allow a more useful and versatile prediction technique.

ACKNOWLEDGMENT

The authors are grateful to Mr. Douglas Michel, NASA-OART and Dr. John P. Raney, NASA-Langley Research Center, for their guidance and suggestions in monitoring this research program.

This work was performed under the guidance and direction of Mr. B. D. Van Deusen, the Chrysler Program Manager. Other members of the Chrysler research team included: R. F. Hughes, J. M. Sneyd, C. H. Hoppe, D. H. Dieck, R. W. Hildebrand, and H. G. Ross. Acknowledgment is also due Mr. G. T. Cohron of Cohron Associates who contributed valuable assistance and consultation during the field tests, and Mr. J. W. Holzman of Dana Corporation for the use of the hydraulic vibration facility in vehicle vibration tests. Special acknowledgment is due Mr. C. S. Snyder, Manager of Engineering and Research and Dr. P. W. Lett, Operating Manager, Defense Engineering for their support of this study. The report was typed by Mrs. Bernice Wright.

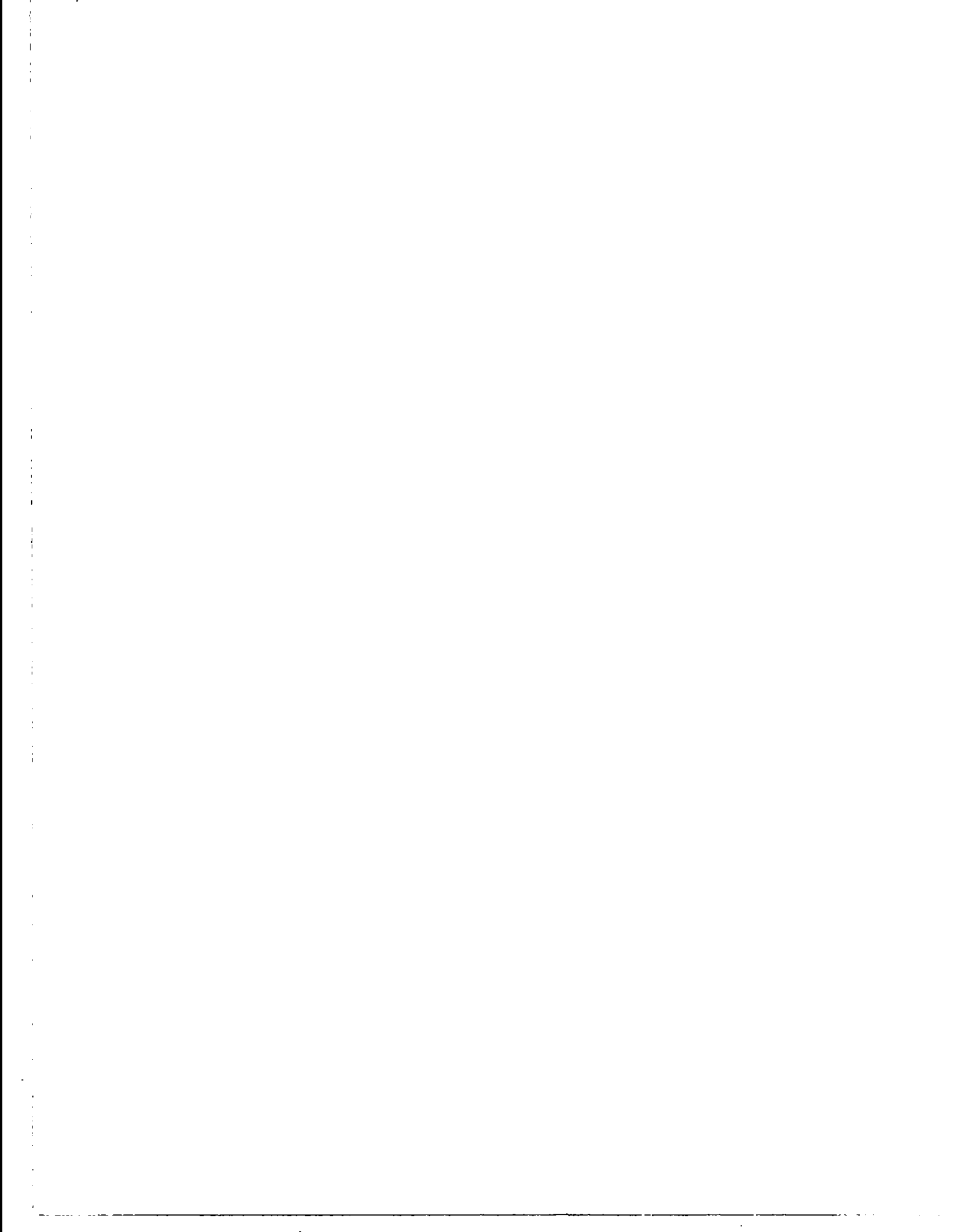


TABLE OF CONTENTS

	PAGE
ABSTRACT	iii
ACKNOWLEDGMENT	v
TABLE OF CONTENTS	vii
1.0 INTRODUCTION	1
2.0 VEHICLES	5
2.1 Truck	5
2.2 Trailer	5
3.0 SURFACES	8
3.1 Theory of Profile Analysis	8
3.2 Surface Profile Measurements	9
4.0 SOFT SOIL	11
4.1 Yielding Surface Dynamic Model	11
4.2 Soil Measurements	13
5.0 SIMULATION	15
5.1 Frequency Domain Approach for Vehicle Model Analysis	15
5.2 Shake Tests	16
5.3 Static Laboratory Measurements	21
5.4 Time Domain Simulation	22
6.0 VEHICLE FIELD TESTS	25
7.0 RESULTS	27
8.0 CONCLUSIONS	39
9.0 RECOMMENDATIONS	41
10.0 REFERENCES	42
APPENDIX A	A-1
APPENDIX B	B-1
APPENDIX C	C-1
APPENDIX D	D-1
APPENDIX E	E-1

1.0 INTRODUCTION

The effects of surface roughness on the design and operation of vehicles have been investigated for a number of years. The technical difficulty of the analytical approach to the problem and the relative ease of experimental procedures have tended to place little effort in developing meaningful mathematical models to simulate this situation.

When the problem of operating surface vehicles in extraterrestrial environments is considered, the analytical approach becomes a practical necessity. The cost and complexity associated with experimental testing in extraterrestrial environments precludes this approach to vehicular design. It thus becomes necessary to develop accurate analytical techniques which permit investigation of design parameters. With this object in mind the authors undertook a contract effort to develop such an analytical technique. The results of this effort were published in 1967.⁽¹⁾ This effort consisted basically of five parts.

1. Surface Roughness Classification: A statistical technique was devised to classify surface roughness in a concise and meaningful fashion usable for an input to vehicle simulation. This classification is based on a single parameter called the surface roughness coefficient.
2. Soil Model: An approximate soil model for vertical loading was devised which includes dynamic (time dependent) terms. This was based upon a combination of the excepted static (equilibrium) model used for vehicle mobility and the elastic vibrations model used in civil engineering for foundations.
3. Vehicle Models: Traditional linear vehicle models were used for the preliminary analysis. The procedure, however, allows the inclusion of non-linearities in the vehicle model as well as the soil model.
4. Vibrations Input: A technique was devised for exciting the vehicle and soil models based on random functions derived from the surface roughness coefficient.

5. Output Analysis: Techniques were developed for statistically analyzing the output random vibration, and presenting it in the form of frequency (power spectral density) and amplitude (amplitude probability distribution) plots.

Figure 1 shows a block diagram of the resulting simulation.

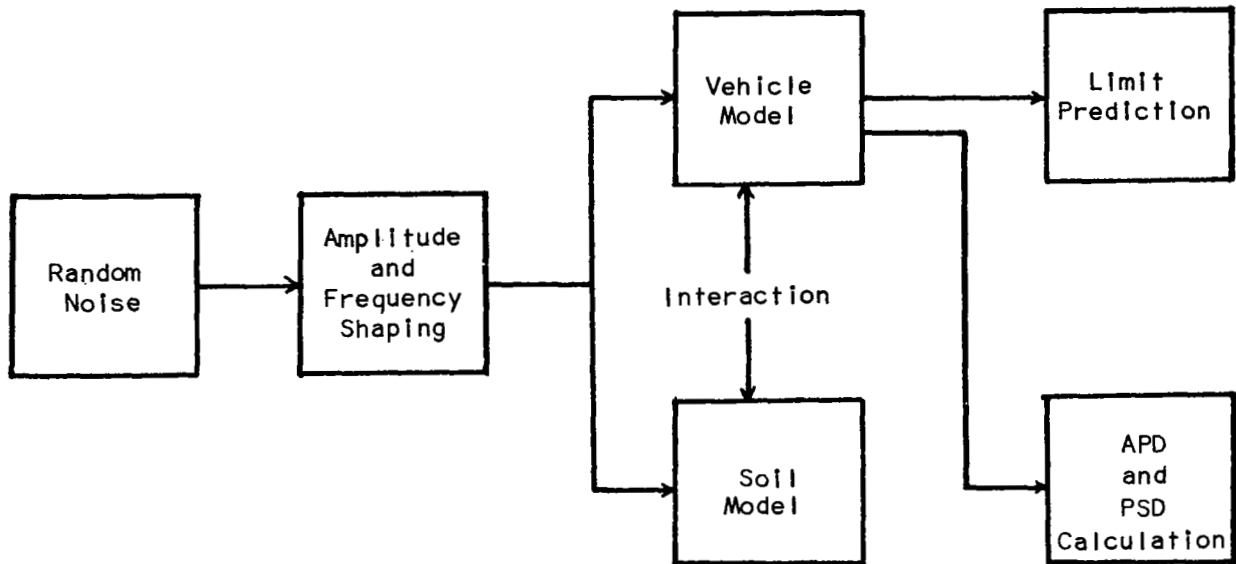


Figure 1 BLOCK DIAGRAM FOR NON-LINEAR SYSTEM ANALYSIS

Since the time the theoretical techniques were developed, a number of agencies have attempted to apply these techniques to evaluate alternate vehicle concepts and as a tool in vehicle design. Because of this interest it was deemed necessary to undertake at least a crude experimental verification of these techniques. The present study represents a rudimentary experimental verification. It must be recognized that a full investigation would involve a number of vehicles (or a number of design changes to a single vehicle) as well as a random sampling of terrain segments from a geographical area of consistent roughness.

The experimental verification program which was undertaken is outlined below.

1. Two vehicles were used for the testing. The first was a standard M37, 4 x 4 3/4 ton military cargo carrier. The second was a specially designed single wheel trailer. This was to allow a separate analysis of the coupling effects between wheels (4 wheel vehicle) and a simple system with one input (trailer). The trailer was designed to decouple its motions as much as possible from those of the towing vehicle.
2. Two separate surfaces were used for the testing. The first was a paved (non-yielding) surface and the second was a rough area of soft soil. This was to allow an analysis of the techniques with and without the added complexity of a dynamic soil model.
3. Profile height measurements were made prior to testing on the two surfaces using rod and transit techniques. The digital profile height data was processed to yield values of the power spectral density, surface roughness coefficient and amplitude probability distribution.
4. On the soft surface, soil parameters were measured to allow inclusion in the yielding surface model.
5. The vehicles were instrumented with accelerometers and driven over the surfaces at constant speeds. These instrumentation signals were recorded on f.m. magnetic tape and returned to the laboratory for processing on an analog computer to determine the power spectral density and amplitude probability distribution of vehicle vibration.
6. Simple linear vehicle models were developed. These were checked against laboratory shake tests of the vehicles. A digital simulation program was utilized to predict vehicle motion. The simulation allowed for the non-linearity of surface tire separation on both surfaces and soil model non-linearities on the soft surface. Both actual profile height measures and random measures based on the surface roughness coefficient, were used as inputs.
7. The output prediction from digital simulation was processed to yield the power spectral density and amplitude probability distribution. These predicted values were compared with the measured values of Item 5 above.

The main body of this report is written to give the reader an over view of the project and presents the significant results and conclusions. Additional details in specific phases of the project are presented in the five appendices.

- A. Profile Measurement and Analysis
- B. Soil Measurement and Analysis
- C. Vehicle Field Test Measurement and Analysis
- D. Linear Model Frequency Domain Analysis
- E. Time Domain Analysis

The reader who is concerned with additional information pertaining to the overall techniques, statistics and analytical details is referred to Reference (1) which presents the theory being verified here. The only major difference between Reference (1) and the present program is the translation of the analog computer network developed in Reference (1) to the digital simulation employed in the present project.

2.0 VEHICLES

Two different vehicles were used in this experimental program. A four wheel truck to account for multiple inputs and the coupling effects between inputs, and a single wheel trailer to allow analysis of a simple dynamic system with a single input.

2.1 Truck

The truck used in this test was a standard M37 3/4 ton, 4 x 4 military cargo carrier as shown in Figure 2. This vehicle was chosen since a good deal of information was available in the literature concerning dimensions and other characteristics of the vehicle, and previous dynamic tests have been performed by Chrysler and other investigators.^(23, 24) The technical military specifications and characteristics of this vehicle can be found in TM 9-500.

2.2 Trailer

The single wheel trailer was designed specifically to have a vehicle with dynamic simplicity. A picture of this trailer is shown in Figure 3. The long towing arm was selected to allow as much decoupling of the trailer body from the truck motions as possible. The c.g. of the trailer body was directly above the wheel carrier and the natural frequency of the trailer body was chosen to be between the truck body resonances and the truck wheel resonances to improve decoupling of motions. The single wheel was used so that the effect of multiple inputs would not have to be accounted for in computer simulation. A trailing arm suspension was employed as shown in Figure 4. A universal joint was used for the trailer hitch as shown in Figure 5. This allowed freedom of motion in the pitch and yaw directions, and the necessary rigidity in the roll direction to maintain balance of the trailer.

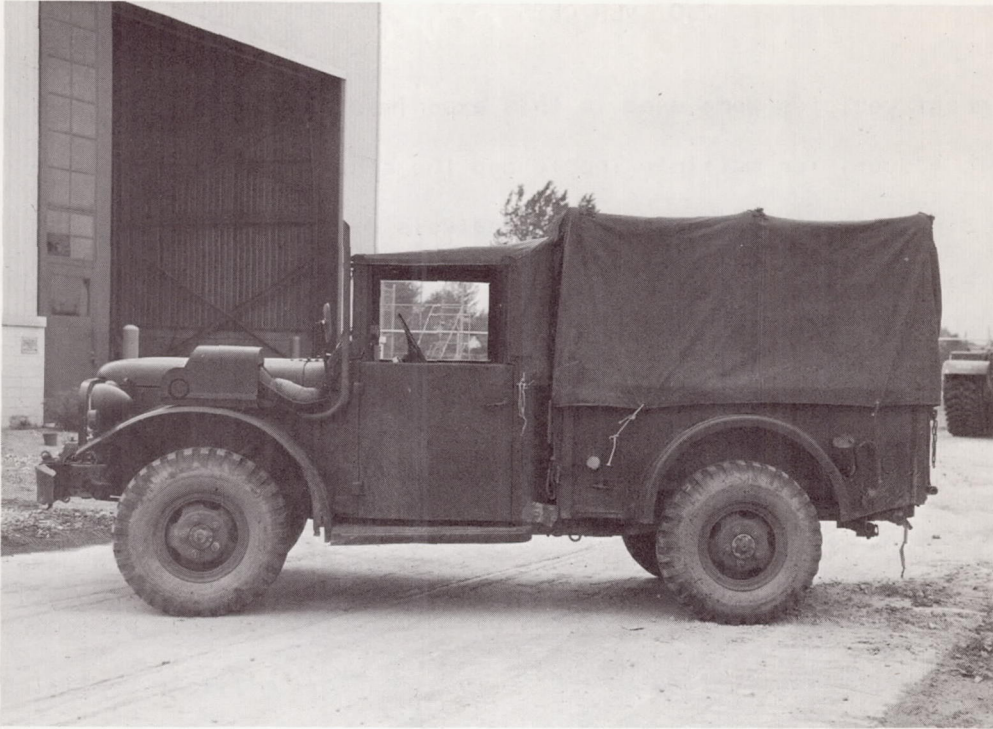


Figure 2 Standard M-37 3/4 Ton Military Cargo Carrier

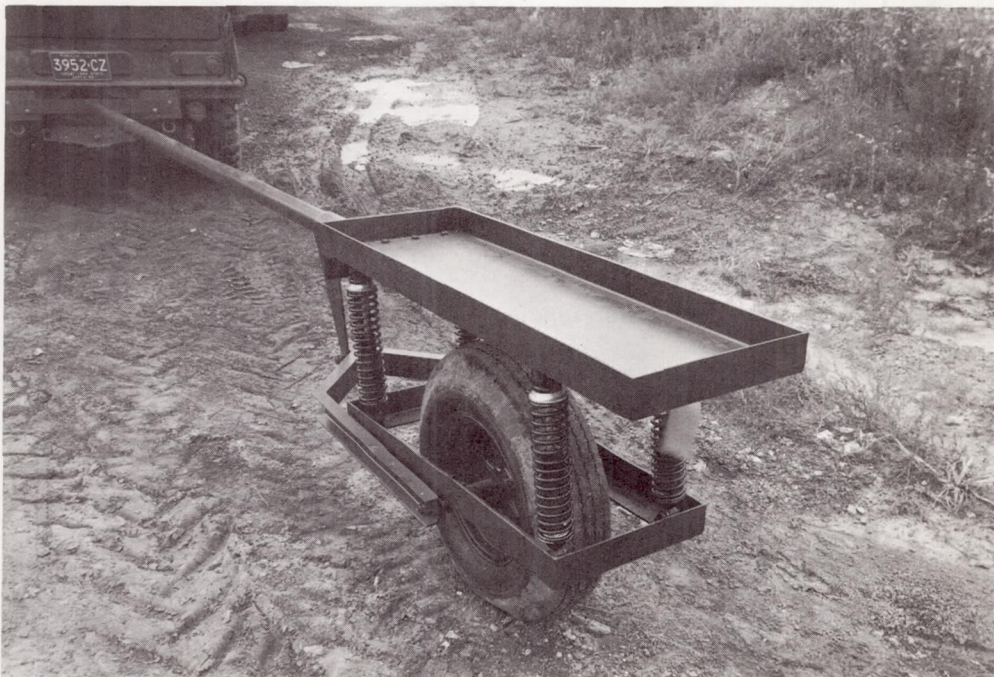


Figure 3 Specially Designed Single Wheel Trailer

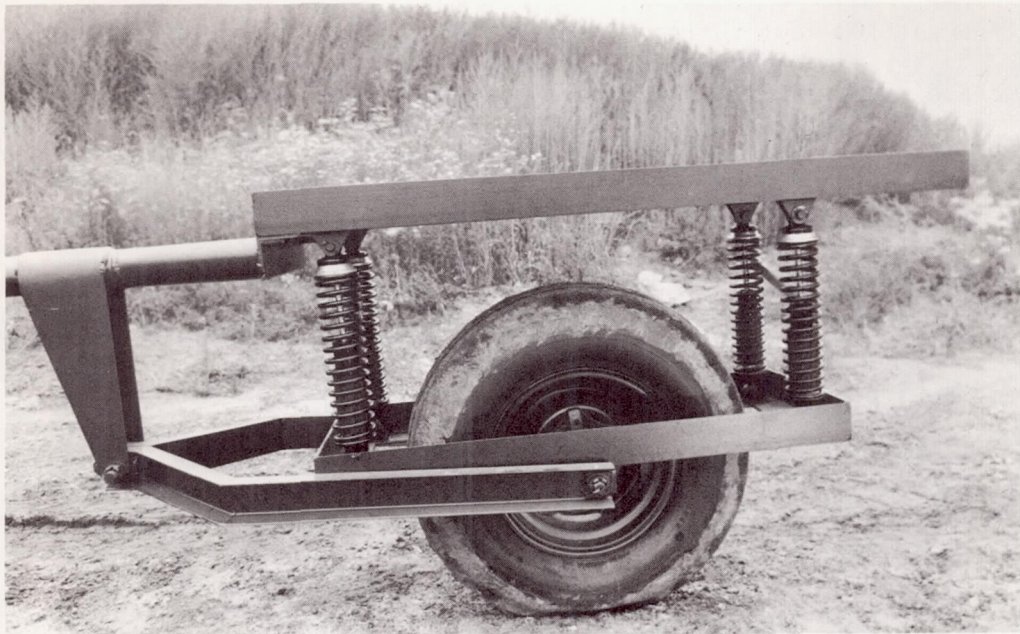


Figure 4 View Showing Single Wheel Trailer Suspension Design

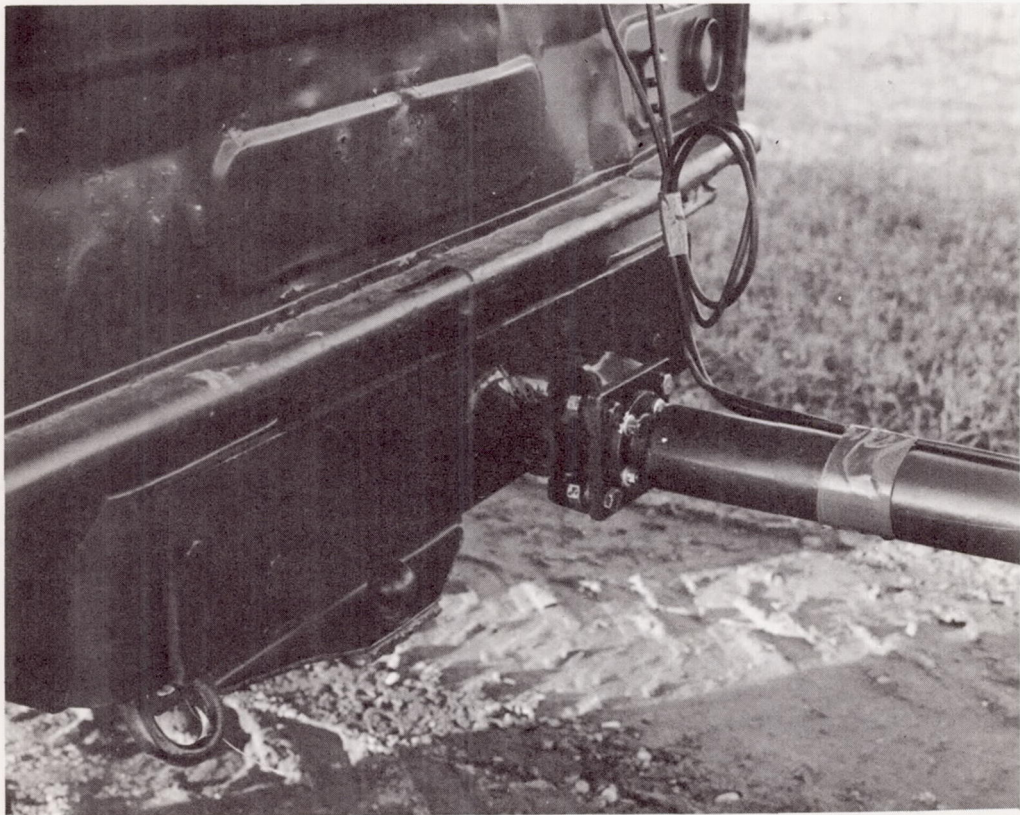


Figure 5 View Showing Universal Joint for Trailer Hitch

3.0 SURFACES

Two different 300 foot surfaces were used for the experimental program. The hard surface was a 300 foot section of the south tortuous road at the Chrysler proving ground (see map, Figure A-1, Appendix A). This road section was designed for automobile endurance testing and represents the roughest section of the proving ground endurance road. The soft surface was a 300 foot virgin section of terrain at the proving ground which had both the desired roughness and soil consistency to allow appreciable (approximately 2") sinkage of the vehicles.

3.1 Theory of Profile Analysis

It was shown in the previous study that the power spectral density (PSD) of virgin terrestrial and extraterrestrial surfaces can be approximated by the frequency content as depicted by Equation 1.

$$P(\Omega) = C\Omega^{-2} \quad (1)$$

Where $P(\Omega)$ is the power spectral density with units of length squared per cycle per unit length, C is the surface roughness coefficient with units of length, and Ω is a spatial frequency with units of cycles per unit length. C can be used to specify the roughness of representative profile traces in a statistical sense. An estimate of C can be accomplished by detrending, or filtering, a profile trace such that the frequency components of the order of, or longer than, the available data sample are filtered out. A special zero phase shift, 6 db per octave digital filter was developed⁽¹⁾ to accomplish this detrending. This is essentially an exponentially weighted filter with an exponential space constant λ (analogous to the time constant in the time domain). Once the data has been properly detrended with this filter,

a relationship exists between the variance of the digital profile height data, the surface roughness coefficient C , and the filter constant as given in Equation (2).

$$\text{Var} = \frac{C\pi^2\lambda}{2} \quad (2)$$

Thus, it is only necessary to detrend or filter the profile data from a representative trace with an appropriate filter constant λ and calculate the variance of the detrended data to obtain an estimate of the surface roughness coefficient C . Using this argument, the power spectral density estimate can be obtained from the value C and the amplitude probability distribution (assuming a Gaussian distribution) can be estimated from a knowledge of the variance.

3.2 Surface Profile Measurements

Digital profile heights were measured along the two test courses using standard rod and transit surveying techniques. These were measured at 15 inch intervals for the two truck lanes and at 5 inch intervals for the trailer lane. Details of these measurements, the actual data and analysis can be found in Appendix A.

A single number was used as an input for the surface roughness to computer models. The surface roughness coefficient was calculated for each trace and averaged to achieve a surface roughness coefficient for each surface. Table 1 lists the measured surface roughness coefficients from each of the traces from the hard and soft surfaces, together with the center portion of the hard surface which represents the center 300 feet. A value of 5 meters was chosen for the detrending constant λ in order to calculate these surface roughness coefficients.

Table 1 SURFACE ROUGHNESS COEFFICIENTS (FT.)			
	Soft Surface	Hard Surface	Center Portion of Hard Surface
Left Lane	.000243	.000151	.000019
Center Lane	.000238	.000149	.000012
Right Lane	.000214	.000136	.000012
Average	.000232	.000145	.000014

This constant is identical to that previously employed in Reference 1 for the analysis of Ranger photographic data and for lunar profile height analysis. The hard surface showed a significant trend which was apparent in the ends of the data even after filtering due to the end point contamination as reported in Figure A-3, page 59, of Reference 1. For this reason, a stretch of 400 feet was measured for the hard surface profile, with only 300 feet being used for the final analysis. Thus, after filtering, 50 feet were removed from each end of the data and new calculations for spectral estimates and amplitude probability distributions were determined. The hard surface analysis shows a predominant periodicity appearing at approximately .25 cycles per foot with second and third harmonics appearing at .5 and .75 cycles per foot respectively (see PSD plots in Appendix A). This periodicity was obvious in the analysis of the vehicle vibration data as well and in computer simulation where the actual input was used.

Estimates of the PSD and APD (see Appendix A) made from every third point of the data set, showed quite accurate surface roughness coefficient calculations at less resolution of the predominant frequency for the hard surface profiles.

4.0 SOFT SOIL

In addition to the surface profile measurement, measurements of soil properties were made for inclusion in the dynamic soil model.

4.1 Yielding Surface Dynamic Model

A dynamic model for the yielding or soft surface was developed under the previous contract and is essentially a spring-mass-damper system as shown in Figure 6 with a highly non-linear spring rate.

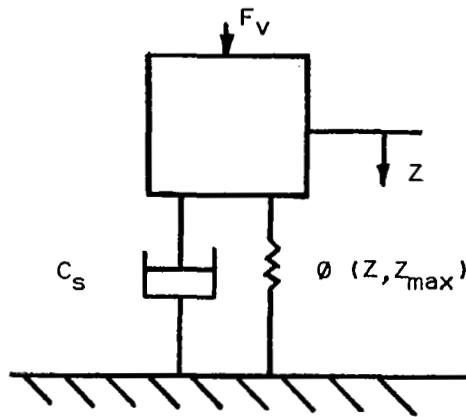


Figure 6 SOIL MODEL

The model of Figure 6 has the form of Equation (3).

$$m_e \ddot{Z} + C_s \dot{Z} + \phi(Z, Z_{max}) Z = F_v \quad (3)$$

Where F_v is the vertical dynamic force acting on the soil, Z (and its derivatives \dot{Z} and \ddot{Z}) is the soil deformation or sinkage, and m_e is the effective mass of the soil and represents the inertial effect of the soil in the proximity of the loading area. From elastic theory of soil mechanics derived from civil engineering, it was shown that m_e , the effective mass, has the form of Equation (4).

$$m_e = c_1 \rho \left(\frac{A}{\pi} \right)^{3/2} \quad (4)$$

C_s has, as a first approximation, the form of a linear viscous damping coefficient and represents the energy dissipation due to radiation damping (Pressure wave propagation in a semi-infinite medium) as given in Equation (5) from elastic theory.

$$C_s = \frac{A b_0}{\pi} \left(\frac{E \rho}{2 + 2\nu} \right)^{1/2} \quad (5)$$

$\emptyset (Z, Z_{\max})$ is the spring rate which is a function of the sinkage Z and the maximum penetration at that position of the surface Z_{\max} . If Z is less than Z_{\max} , then the function $\emptyset (Z, Z_{\max})$ is the elastic recovery rate as derived from civil engineering foundation analysis and given by Equation (6).

$$\emptyset (Z, Z_{\max}) \text{ for } Z < Z_{\max} = \frac{CE\sqrt{A}}{1 - \nu^2} \quad (6)$$

In Equations (4), (5), and (6):

A = area of wheel footprint

ρ = soil mass density

ν = Poisson's ratio for the soil

E = Young's modulus for the soil

c_1 & b_0 = soil constants depending upon ν

C = constant depending upon footprint area A

If $Z = Z_{\max}$ (consolidation), $\emptyset (Z, Z_{\max})$ is a non-linear rate derived from standard plate penetrometer measurements of sinkage versus pressure in soft soils.

4.2 Soil Measurements

In order to assess the soil consolidation rate, the trailer was used as a penetrometer. It was decided that this type of test would give a soil tire combination which was not easily achieved through plate penetration tests. Tests were made at six locations along the test course and five different loadings (ranging from 280 to 1486 pounds) for each test location.

Cone penetrometer measurements were made at random places throughout each segment of the test site. Details of the soil tests and the data is reported in Appendix B. Selected soil samples were also taken and brought back to the laboratory to measure soil density and assess the physical properties of the soil for estimating Young's modulus, Poisson's ratio, and other soil properties not directly measured. Table 2 lists a summary of soil

Table 2 SUMMARY OF SOIL MODEL PARAMETERS

Soil Property	Formula	Value	
		Truck	Trailer
Effective Mass	$c_1 \rho \left[\frac{A}{\pi} \right]^{3/2}$.0106 lb sec ² /in	.0073 lb sec ² /in
Damping	$\frac{A}{\pi} b_0 \sqrt{\frac{E \rho}{2(1-U)}}$	37 lb sec/in	29 lb sec/in
Consolidation Rate	Sinkage Tests	1000 lb/in	715 lb/in
Recovery Rate	$\frac{c E \sqrt{A}}{1-U^2}$	39,680 lb/in	35,000 lb/in

properties measured or estimated from the analysis of the soft soil test area. Details of the measurements made, and the data analysis, can be found in Appendix B. It should be noted (from Table 2) that the consolidation rate used was linear. Soil test information showed no indication of deviations from linearity. Attempts to fit curvature to the test data were non-conclusive. Two offsetting factors are acting here. The loading area (tire foot print) increases with load, and the soil stiffness decreases. It should also be noted that the recovery rate for the soil is considerably higher (approximately 40 times) than the consolidation rate. This gives a high degree of plasticity to the soil (i.e., deformations of 4 inches recover only 0.1 inch). This recovery rate is based on engineering estimates and published data. No attempt was made to measure Young's modulus or Poisson's ratio for the soil. At first this might appear as a severe limitation to the modeling. However, it was shown in computer runs that the recovery rate was encountered less than one percent of the time; and as such, large changes in this estimate had negligible effects on the results. The damping term is also dependent on estimates of Young's Modulus. Here it was shown that changes in this estimate of 2 to 1 (100% change) effected about a 10% change in the output. Thus it is obvious that the consolidation rate is by far, the dominant factor and most emphasis was placed on measuring this in the field.

5.0 SIMULATION

Two separate types of computer analyses were undertaken in this study. A linear model analysis using frequency domain (transfer function) techniques, and a true non-linear simulation which was the major program being verified.

5.1 Frequency Domain Approach for Vehicle Model Analysis

A frequency domain approach for analyzing vehicle motions was developed and implemented as a portion of the preceding contract.⁽¹⁾ This approach necessitates a linear vehicle model to analyze vehicle motions and uses transfer function concepts in the frequency domain (see Appendix D). The assumption of linearity requires a non-yielding surface or, at most, a linear yielding surface and also a vehicle speed below that which would cause surface vehicle separation. While this approach places rather severe restrictions on model analysis, it does allow a convenient solution which gives a good deal of insight into vehicular behavior. This approach has been used in the present effort to correlate laboratory sinusoidal excitation of the physical vehicles with the linear vehicle model, and secondly to validate the non-linear model excited in a linear fashion with a sine wave.

The linear frequency domain technique for analysis was also used to assess the coupling between the vehicles. The truck was shaken separately in the simulated program, and motions of the trailer were assessed. The reverse of trailer shaking and truck motion assessment was also done. This type of analysis showed that these vehicles had a minimal coupling so that they could be analyzed separately. In the succeeding analysis, both for time domain and frequency domain calculations, each vehicle was separately analyzed.

The linear frequency domain technique was also used to calculate power spectral density functions with random input. The transfer functions between

each of the inputs and the outputs of interest were calculated for both the trailer and the truck. These are measures of the amplitude and phase relationships between the center point of each tire and the output of interest. In the case of the truck, the three outputs were the bounce, or vertical motion of the c.g. of the body, pitch and roll of the truck body. In the case of the trailer, the outputs of interest were the vertical motion of the wheel spindle, the vertical motion of the c.g. of the vehicle body, and the pitch motion of the vehicle. This resulted in three transfer functions for the single wheel trailer and three times four or twelve transfer functions for the truck. Each of the trailer transfer functions were squared and weighted by the random input to yield output PSDs. The truck transfer functions were combined, taking into account time lags to yield output PSDs for multiple inputs. It was determined from the frequency domain analysis that the cross spectral density effects of lag between front and rear wheel, which were calculated theoretically as an input corresponding to time lag (see Equation (44), page 36 of Reference 1), gives a more pronounced resonant effect on the theoretical model than the actual vehicle. This showed up primarily at higher frequencies and might be attributed to the fact that the precise timing and characteristics of the real bumps are such that a statistical spread occurs, giving less resonant effect than observed in the theoretical model where time delays are mathematically precise. This effect can be seen in the detailed analysis presented in Appendix D of this report. The other obvious reason for smearing of higher frequencies in the field test data is the constant "Q" filter used in processing the data (see Appendix C).

5.2 Shake Tests

Sinusoidal shake tests were made on the actual vehicles in the laboratory

in an attempt to correlate actual vehicle measures with linear model prediction. Figure 7 shows the truck mounted on four hydraulic shakers, and Figure 8 shows the trailer mounted on a shaker. The trailer was subjected to 90 different inputs spanning a wide range of amplitude and frequency. Figure 9 is a summary of this input data. Basically, four different amplitudes were chosen; .1, .25, .5 and 1.2 inches peak to peak displacement. The frequency at each amplitude was started at .5 cps and increased in gradual steps. When the frequency was increased at constant amplitude, the acceleration increased as the square of frequency. When the input acceleration reached the 1 g level, the trailer was close to separating from the shake table, so a constant acceleration was maintained at this level for higher frequencies. The transfer functions shown in Figures 10 through 12 are dimensionless, i.e., they all represent the ratio of output acceleration to input acceleration. In making such plots, something has to be held constant as a function of frequency, since linearity cannot be assumed. Figures 10 and 12 show the measured transfer function from the tire input to the bounce motion of the vehicle body. The difference between these figures is the input parameter held constant. Figure 10 shows the measured tire patch to body transfer function with four different displacement level inputs. It can be seen that as the displacement level increases, the measured data agrees more closely with the linear model prediction. This increase in indicated resonances shows a non-linearity in the system which is suspected to be suspension system friction. Figure 12 shows the same data for constant acceleration input. Figure 11 shows the tire patch to vehicle wheel transfer function at four levels of displacement amplitude.

The tests on the truck were run at constant acceleration input levels (0.1 g and 0.3 g peak to peak). Figures 13 through 18 show this data compared

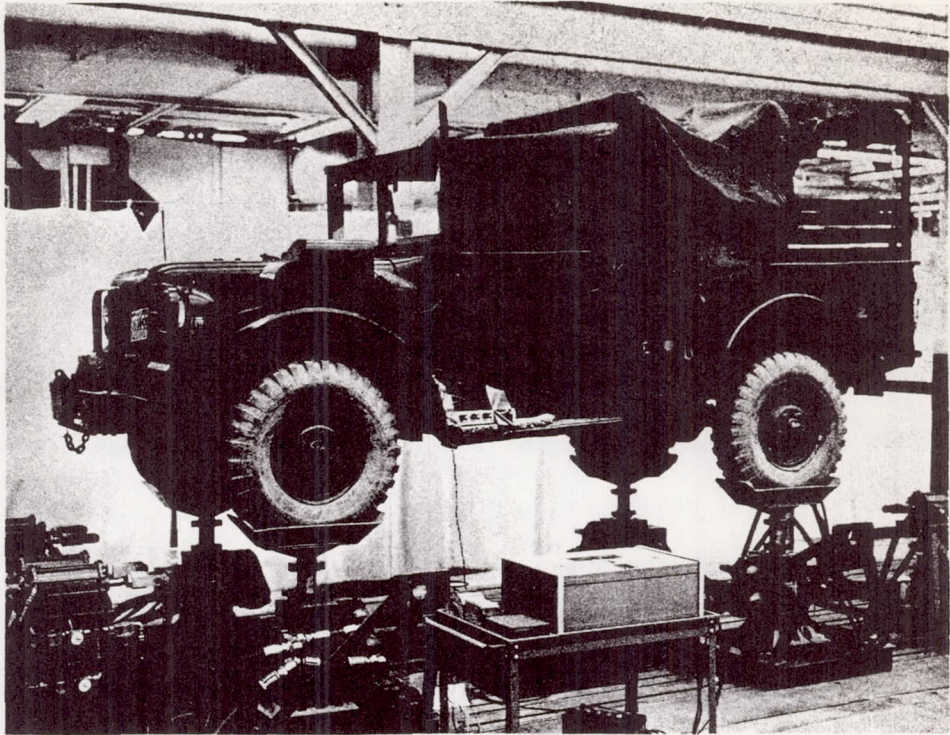


Figure 7 M-37 Mounted on Hydraulic Shakers

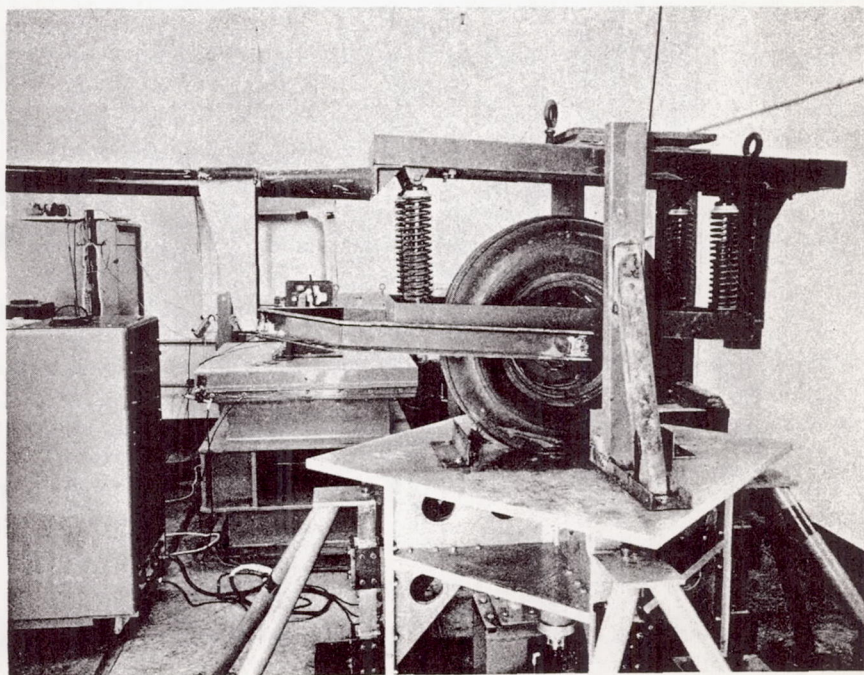


Figure 8 Single Wheel Trailer Mounted on Hydraulic Shaker

Figure 9 SUMMARY OF TRAILER VIBRATION TEST

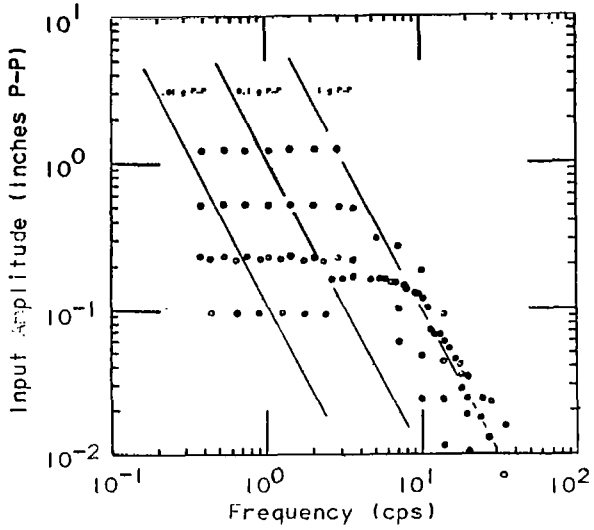


Figure 10 TRAILER CG BOUNCE TRANSFER FUNCTION FOR CONSTANT INPUT ACCELERATION AT TIRE PATCH

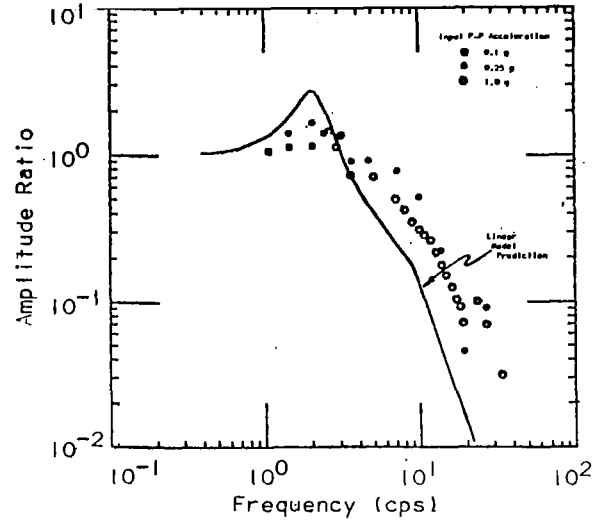


Figure 11 TRAILER WHEEL TRANSFER FUNCTION FOR CONSTANT INPUT DISPLACEMENT AT TIRE PATCH

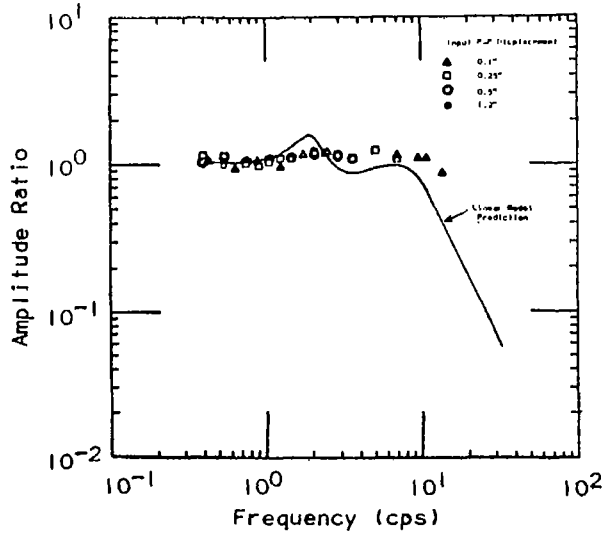
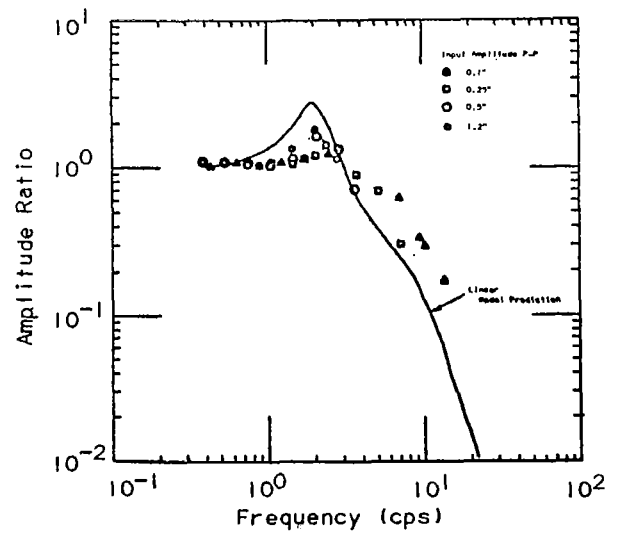


Figure 12 TRAILER CG BOUNCE TRANSFER FUNCTION FOR CONSTANT INPUT DISPLACEMENT AT TIRE PATCH

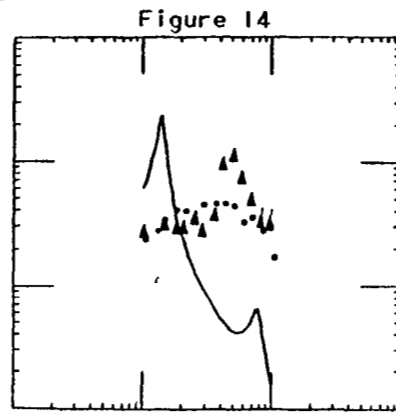
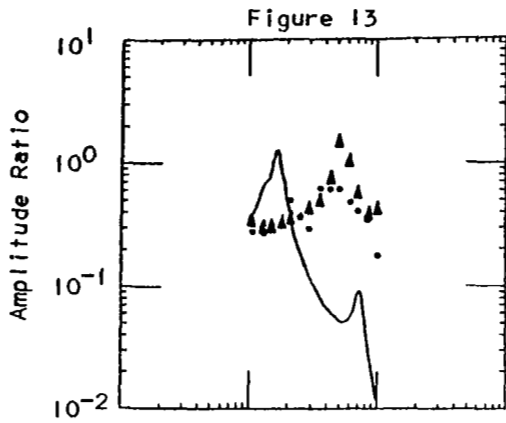


TRUCK TRANSFER FUNCTIONS

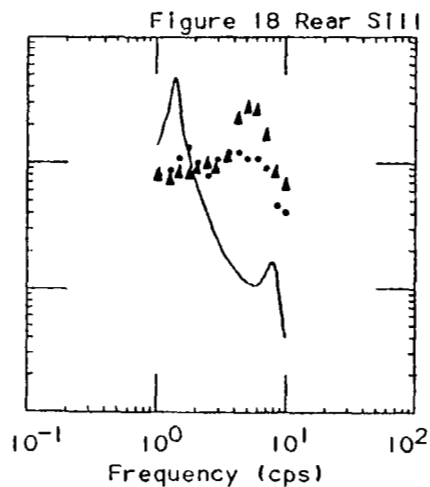
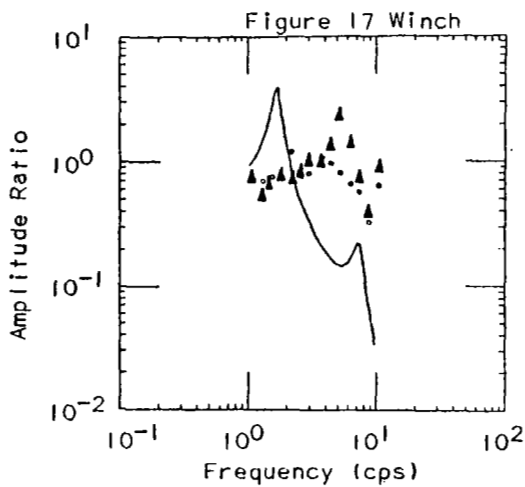
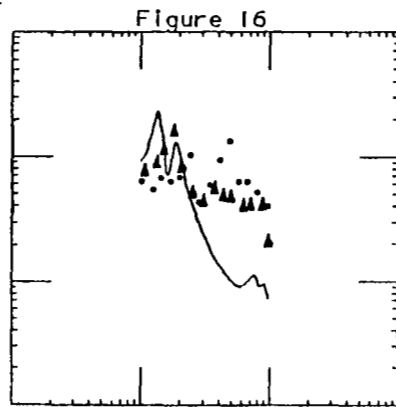
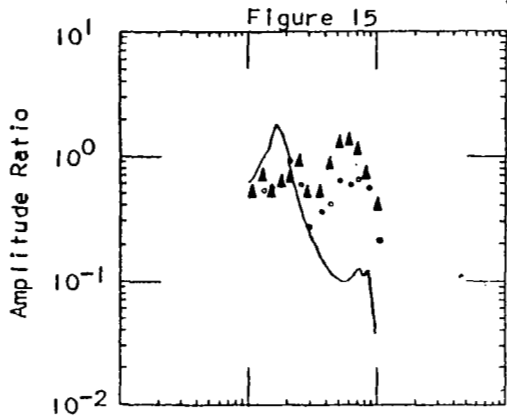
○ - .1g Peak to Peak
 △ - .3g Peak to Peak

○ △ Points Experimental Measures
 Solid Line Computer Prediction

-CG BOUNCE-



-RIGHT SILL-



to linear model prediction for both right front wheel and right rear wheel input. These data do not compare well with computer prediction. It appears that the vehicle is vibrating pretty much as a rigid body. This is expected to be due to the inter-leaf friction in the leaf springs. Better laboratory measurements could probably be made in this case using some technique to "break" inter-leaf friction. This might be impulse testing or the introduction of an additional high frequency signal during testing. It is obvious from Figures 10 through 18 that the trailer tests compared more favorably with linear model prediction than the truck tests.

5.3 Static Laboratory Measurements

The truck was weighted at each wheel location, and the data is summarized in Table 3.

Table 3 TRUCK WEIGHT	
Position	Weight
Left Front Wheel (unloaded)	1690 lbs.
Right Front Wheel (unloaded)	1650 lbs.
Left Rear Wheel (unloaded)	1380 lbs.
Right Rear Wheel (unloaded)	1250 lbs.
	Subtotal
	5970 lbs.
Instrumentation (Recorder)	120 lbs.
Driver and Passenger	350 lbs.
	Total
	6440 lbs.

Tilt tests of the truck were also made to determine the height of the c.g. The c.g. location is shown in Appendix C. Tire static spring rate measurements were made and compared to those supplied by the manufacturer. The remaining data was obtained from the literature^{(23) (24)} and from the U.S. Army Technical Manual for this vehicle.

The trailer was also weighted and it was found that unloaded, there was 279½ pounds on the tire, and 13½ pounds at the hitch point. A ballast weight of 430 pounds was added to the trailer bed and positioned to locate the c.g. directly above the center of the tire patch. Spring rate measurements of the tire and suspension springs were made, and shock absorber damping coefficients were supplied by the manufacturer.

5.4 Time Domain Simulation

In order to make the model developed as universally useful as possible, and also adhere as closely as possible to the previously developed analog computer techniques, a digital simulation language called MIMIC was utilized for this programming. MIMIC was developed at Wright Patterson Air Force Base⁽¹¹⁾ and has been adapted to a number of large scale digital computers. Versions of this program are generally available for most computing facilities.

Digital simulation is a programming technique which, by means of special subroutines, the digital computer is programmed to appear like an analog computer to the user. The special subroutines are predefined functional blocks from which the user can build a model of his system. These blocks perform the same functional operations as standard analog computer components - integrators, amplifiers, function generators, etc. Digital simulation programs are in a sense generalized programs which can be used to solve, on a digital computer, a general class of engineering or mathematical problems, primarily dynamic analysis or solution of ordinary differential equations. Generalized programs of this nature require a fixed notation or formatting of the input data. The notation can be considered a programming language such as FORTRAN or ALGOL.

The details of the time domain analysis are presented in Appendix E of

this report. Basically this solution was completely analogous to the analog computer solution previously reported.⁽¹⁾ Standard equations of motion representing linear springs and linear dampers were used for this simulation. The results of jounce and rebound bumpers were not included since it was felt the accelerations were not high enough to cause encounter of these limits. This linear vehicle model was used with two different types of inputs. The actual profile height data was recorded on digital magnetic tape, and points were read off directly into the simulation to allow assessment of the motions of the vehicle over the actual points. Since these points were spaced relatively far apart between digital integrations, it was necessary to extrapolate in some fashion. A linear extrapolation of the slope of the line was selected. Thus, the velocity input was piecewise continuous while the profile was a continuous straight-line segment profile. This technique caused some difficulty due to the discontinuity at the ends of the line segments. In order to minimize this effect, the high frequency components were filtered out with a 3 db per octave standard RC filter simulated in the MIMIC program. The cutoff frequency of the filter was set at 31.8 cps, which represents 200 radians per second. This filter minimized the effects of the end point discontinuities.

In the second simulation a random surface profile dictated by the surface roughness coefficient C was imposed between the vehicle model rim mass and an effective soil mass such that the wheel rim could not penetrate below the sum of the surface penetration and the profile input.⁽¹⁾ A Gaussian random number generator was used to generate the input digital points to replace the Gaussian white noise generator used for analog computer input. The mean value was selected as zero, and the standard deviation was selected as representative of the surface roughness. The output of the random number generator was

integrated using a MIMIC Integrator in a manner analogous to the integration on the analog computer of the white noise generator. Processing of the digital profile data resulting from this integration showed the desired frequency content of the profile information as depicted by Equation (1). This profile was inputted to the vehicle and a second profile representing the identical numbers was generated with the appropriate time delay from a second random number generator for the input to the rear wheel. The maximum penetration of the soil was time delayed using standard MIMIC time delay techniques to allow the surface penetration to be properly inputted to the rear wheel of the four-wheeled vehicle. The output was recorded on digital magnetic tape in the form of a time sample sequence, and these digital points were re-inputted to the digital computer to allow analysis and estimation of the power spectral density and amplitude probability distribution.

6.0 VEHICLE FIELD TESTS

Six dynamic test runs were made with the two vehicles instrumented with accelerometers as follows:

Soft Surface

Truck alone over rough yielding surface at 3 mph

Trailer towed by truck over rough off-road yielding surface at 3 mph

Hard Surface

Truck alone over rough non-yielding surface at both 3 and 6 mph - two consecutive runs

Trailer towed by truck over the same rough non-yielding surface at 3 and 6 mph - two runs

A single run was used on the soft surface since the profile measurements had to be made prior to each run, and the surface profile was significantly altered by the vehicle passage. The profiles were selected so that the truck wheels followed the same tracks whether carrying the trailer or not. In other words, the truck, while carrying the trailer over the soft surface, followed the same ruts it had left from the previous test, and the trailer followed between these ruts on a virgin profile.

Standard Kistler force-balance accelerometers were used to instrument both the towing vehicle and the trailer. The truck had five accelerometers mounted on it during Tests A-1 and B-1 as shown in Figure 5. One accelerometer was mounted on the floorpan of the truck at the location of the vehicle c.g. A second accelerometer was mounted at the front of the truck at the furthest point from the c.g. possible on the centerline of the truck. A

third accelerometer was mounted at the rear of the truck near the trailer hitch point. The other two accelerometers were mounted to the left and right of the c.g. location. With a proper combining of fore and aft, and left and right accelerometers, it was possible to calculate roll and pitch motions of the truck assuming rigid body motion. The assumption of rigid body motion was verified in the frequency range of interest by comparing the sum of the left and right accelerometers with twice the acceleration at the c.g. The same procedure was used to verify the bending mode of the vehicle by comparing the sum of the fore and aft accelerometers with twice the acceleration measured at the c.g. It was determined that the fundamental bending and torsional modes of the truck frame-body combination were above the dynamic range of interest in this study. The trailer had three accelerometers mounted on it during tests, as shown in Figure 6. One was at the front of the towing arm near the hitch point of the truck. One was mounted at the wheel spindle to measure wheel motions, and the third was at the c.g. directly above the center of the tire patch on the vehicle body. The output of all accelerometers during testing was recorded on f.m. instrumentation tape recorders and returned to the laboratory for analysis.

7.0 RESULTS

The purpose of this program was to make field measurements of vehicle vibration and compare them to predicted results from computer simulations. To this end, the detailed results of this program are statistical plots of vehicle vibration, and these are displayed in the appendices. Appendix C shows the results from the field measurements. Appendix D shows results from a linear frequency domain statistical computer program, and the non-linear time domain simulation is discussed in Appendix E with results.

One method of summarizing this information is to compare the square root of the area under the PSD curves or the RMS acceleration from each test. Table 4 shows such a comparison. The measured values were estimated from amplitude probability plots assuming Gaussian distribution. This technique is probably subject to some error. The linear model values were calculated by numerical integration under the PSD curve, and the simulation values were calculated by taking a true RMS of the digital time samples resulting from simulation. This table shows that computer prediction is, in general, higher than the actual measured values. The obvious question is "Why?". In order to investigate this, several other comparisons were made. The first was to input the actual measured profile to the computer simulation in place of the random profile generated from a calculated surface roughness coefficient. Table 5 shows the results of this comparison for the trailer. It can be seen that in most cases the actual profile gave a lower RMS value. In particular, the measured and predicted values for wheel and body vertical acceleration are very close for 3 mph on the hard surface. This would indicate that the techniques developed for defining a surface roughness coefficient in Appendix A of Reference 1, gives a value that is too large. This could also be due to

Table 4 COMPARISON OF MEASURED AND PREDICTED VALUES OF RMS ACCELERATION							
Surface	Speed MPH	TRUCK			TRAILER		
		Bounce (g's)	Pitch ($\frac{\text{Rad}}{\text{Sec}^2}$)	Roll ($\frac{\text{Rad}}{\text{Sec}^2}$)	Bounce (g's)	Pitch ($\frac{\text{Rad}}{\text{Sec}^2}$)	Wheel (g's)
SOFT	3						
Measured*		.062	.395	.428	.144	.206	.250
Simulation		.132	1.004	2.107	.342	.733	.796
Linear Model		.139	1.013	2.344	.304	.656	1.029
HARD	3						
Measured*		.038	.262	.312	.064	.212	.064
Simulation		.045	.360	.772	.109	.235	.274
Linear Model		.110	.254	.586	.077	.164	.257
HARD	6						
Measured*		.080	.580	.520	N/A	.638	.181
Simulation		.069	.444	1.135	.154	.331	.388
Linear Model		.137	.372	.880	.108	.230	.364

*Measured are data from field test

Table 5 COMPARISONS OF RMS ACCELERATION FROM SIMULATION WITH RANDOM AND ACTUAL INPUT						
Surface	Speed MPH	Type	Input	TRAILER MOTIONS		
				Bounce (g's)	Pitch ($\frac{\text{Rad}}{\text{Sec}^2}$)	Wheel (g's)
Soft	3	Simulation	Random	.342	.733	.796
Soft	3	Simulation	Actual	.219	.470	.209
Soft	3	Measured*	-	.144	.206	.250
Hard	3	Simulation	Random	.109	.235	.274
Hard	3	Simulation	Actual	.058	.122	.055
Hard	3	Measured*	-	.064	.212	.064
Hard	6	Simulation	Random	.154	.331	.388
Hard	6	Simulation	Actual	.173	.370	.153
Hard	6	Measured*	-	N/A	.638	.181

*Measured Type are data from field test

the statistical uncertainty derived from a finite number of points (2000) from the random number generation versus 720 points of actual profile.

Another comparison of interest is the effect of the soil model on computer predictions. In order to assess this, the computer simulation was run with and without (rigid) the soil model for the soft surface profile (both actual and random inputs). Table 6 shows a summary of this data. It can be seen that the soil model acts as a vibration isolation system. That is; in every case, the RMS acceleration is decreased when the soil model is introduced. Comparison of the frequency plots, with and without soil, show that the vehicle resonances are reduced in frequency by the soil; low frequency vibration, below 1.5 cps, is actually increased, and higher frequencies are reduced.

Table 6 COMPARISON OF RMS ACCELERATION FROM SIMULATION WITH AND WITHOUT SOIL MODEL (3 MPH on Soft Surface Profile)

Type	Input	Soft Soil	TRAILER MOTIONS		
			Bounce (g's)	Pitch ($\frac{\text{Rad}}{\text{Sec}^2}$)	Wheel (g's)
Simulation Simulation Measured*	Random	Yes	.342	.733	.796
	Random	No	.435	.933	1.091
	-	-	.144	.206	.250
Simulation Simulation Measured*	Actual	Yes	.219	.470	.209
	Actual	No	.274	.588	.315
	-	-	.144	.206	.250
TRUCK MOTIONS					
			Bounce (g's)	Pitch ($\frac{\text{Rad}}{\text{Sec}^2}$)	Roll ($\frac{\text{Rad}}{\text{Sec}^2}$)
Simulation Simulation Measured*	Random	Yes	.132	1.004	2.107
	Random	No	.180	1.470	3.049
	-	-	.062	.395	.428

*Measured are data from field test

Figures 19 through 54 show the comparison PSD plots for actual field measurements and computer simulation with random inputs. Each page shows the comparison of the three degrees of freedom of interest for one vehicle on one surface

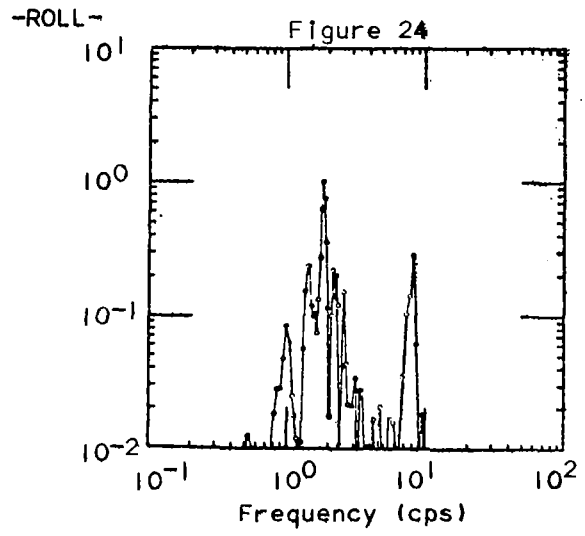
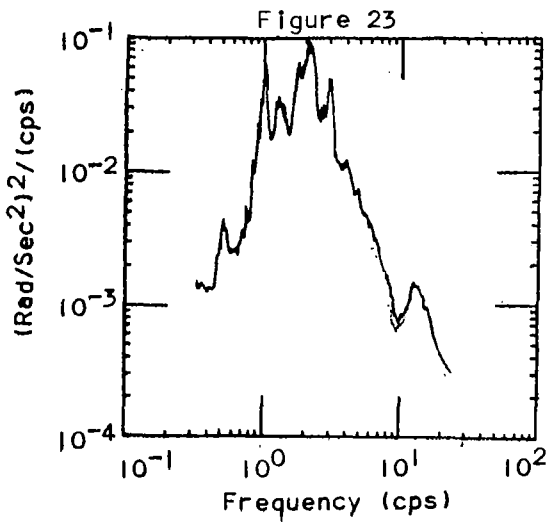
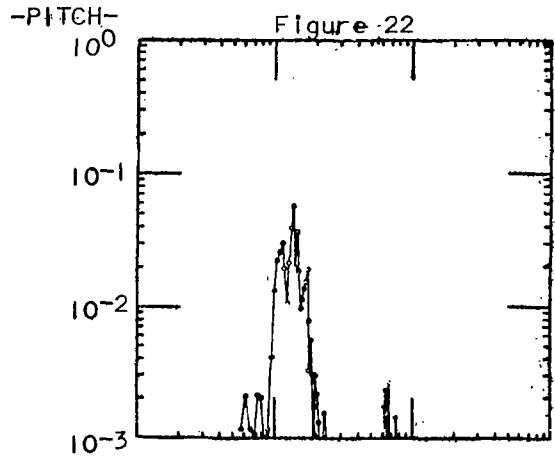
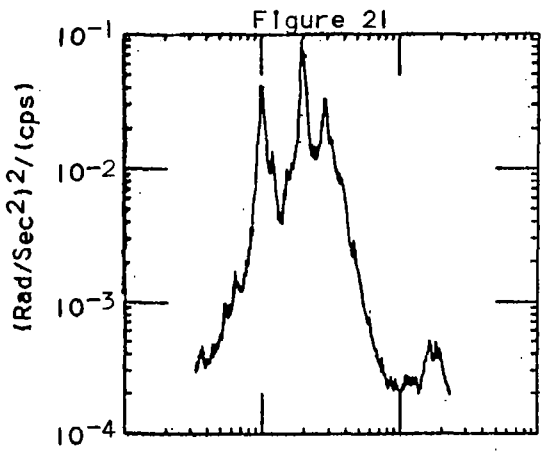
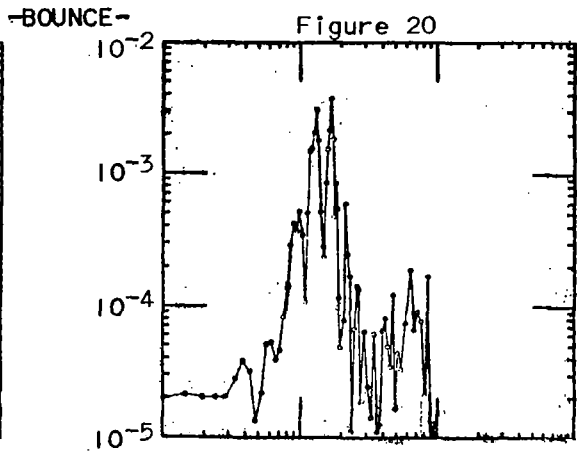
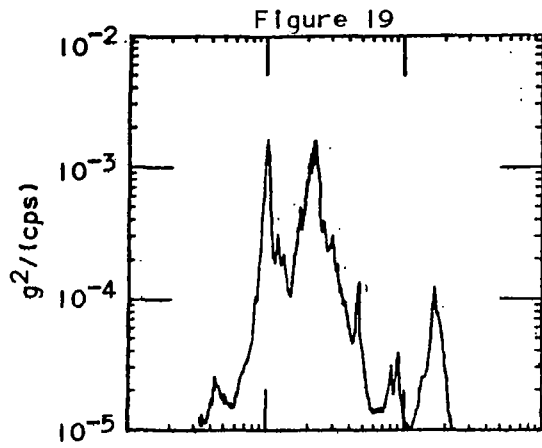
at one speed. The simulation had a precise mathematical time delay of profile height between front and rear wheels for the truck. The result is a sinusoidal perturbation on the PSD with frequency equal to the vehicle wheelbase over the vehicle speed. This is the principal reason for the large number of high frequency "resonances" noted in the simulation of the truck. In the physical measurements, the constant Q filter ($Q = 10$), used to process the data, smoothed this effect out. In the simulation, the other reasons for high frequency "noise" are digital integration errors, assumed linear extrapolation between profile points and random number generator statistical fluctuation with a finite data sample.

Figures 19 through 54 show reasonably good comparison between measured and predicted power spectral density, particularly for the bounce (or vertical motion) of the body of the vehicles. On the hard surface predominant frequencies were apparent in the input PSD and also the measured vehicle response. These obviously were not reproduced in the random input simulation. In general the trend for higher predictions than measurements was apparent as noted from the RMS acceleration comparison. The major vehicle resonances are well produced by the computer simulation although peaks in general seem to be higher and sharper in the computer simulation. It is suspected that this effect is due to friction in the physical system which was not included in the computer model.

Another type of prediction was that of the soil deformation under load. Figure 55 shows (in the upper half) a plot of the actual measured profile which was fed into the computer model, together with the computer predicted residual profile height after passage of the trailer wheel. This is plotted for a 10 foot span near the end of the course (240' - 250'). The difference

between these two traces is the wheel sinkage. The computer predicted sinkage and the actual measured sinkage are plotted in the lower half of Figure 55. The computer predicted a greater residual sinkage than actually measured. This would be expected from the data in Appendix B, since the computer used average soil parameters and the course was "firmer" near the end. Note that the computer predicted sinkage agrees fairly well with the measured sinkage, except at 2930 inches along the course. Here it appears that the actual trailer wheel hits hard on the back side of a 5" bump, and the computer did not predict such a hard encounter.

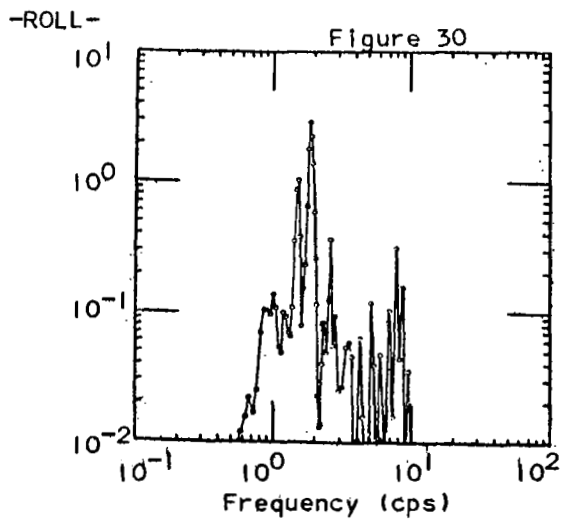
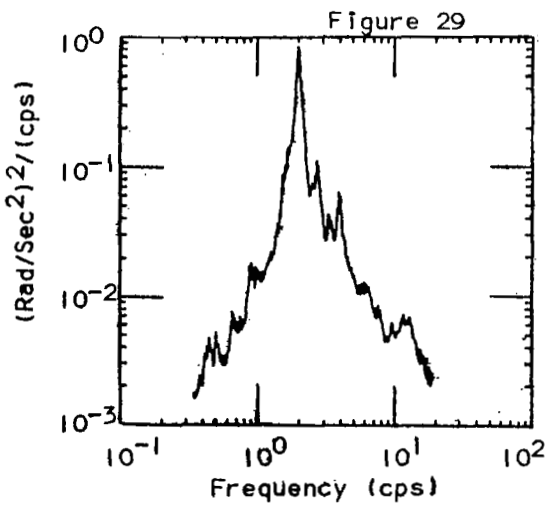
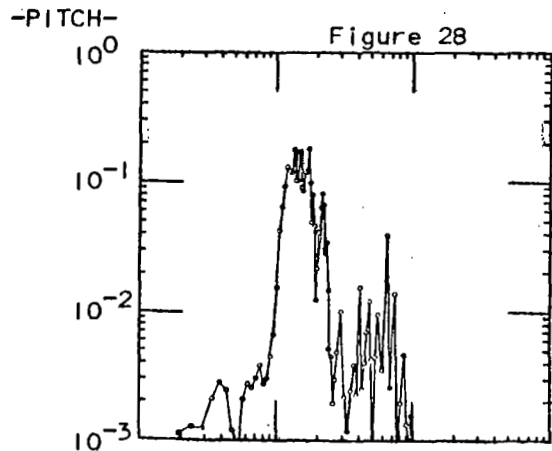
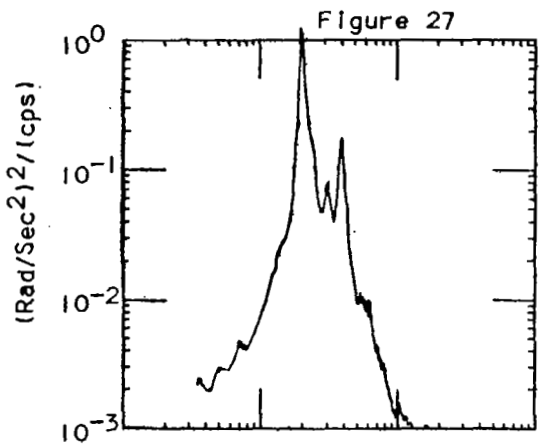
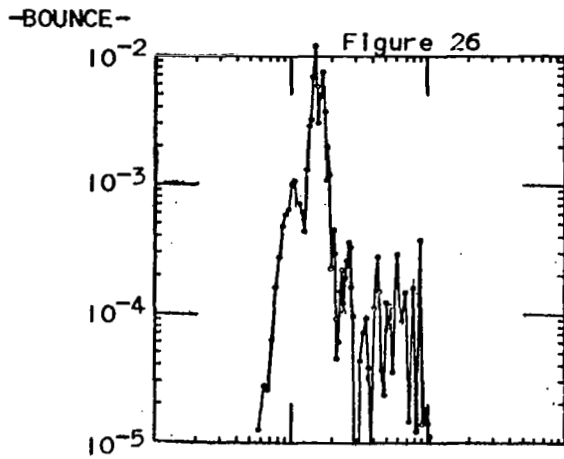
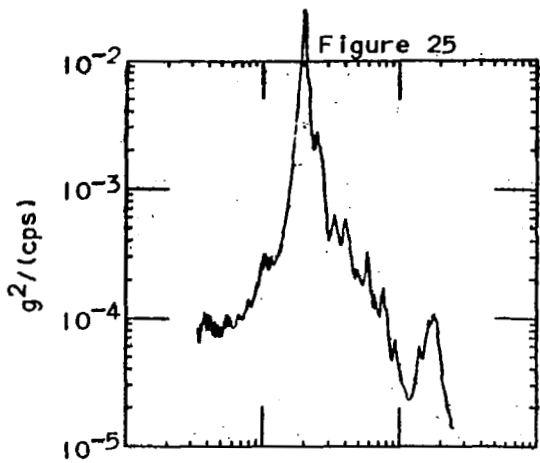
TRUCK PSD'S ON HARD SURFACE AT 3 MPH



MEASURED

TIME DOMAIN PREDICTION

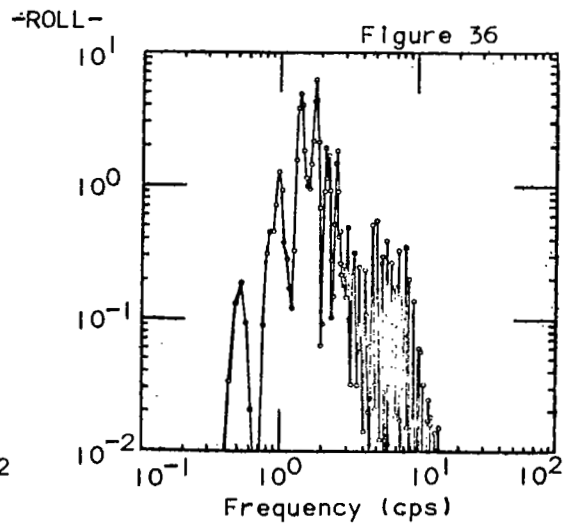
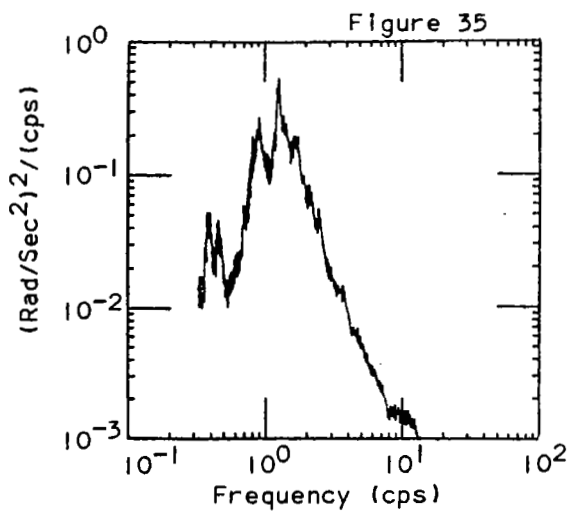
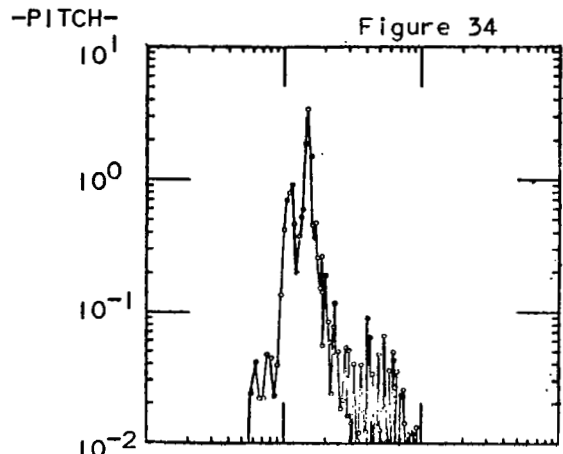
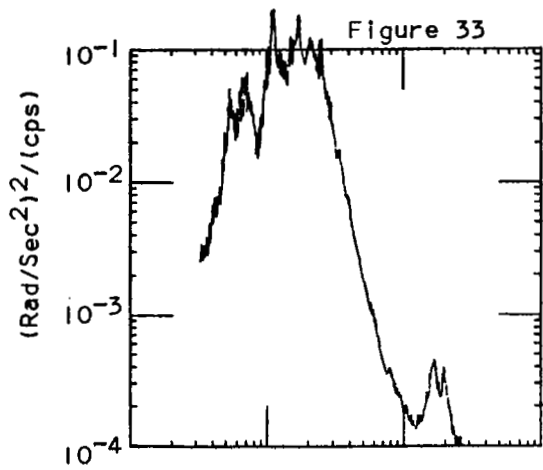
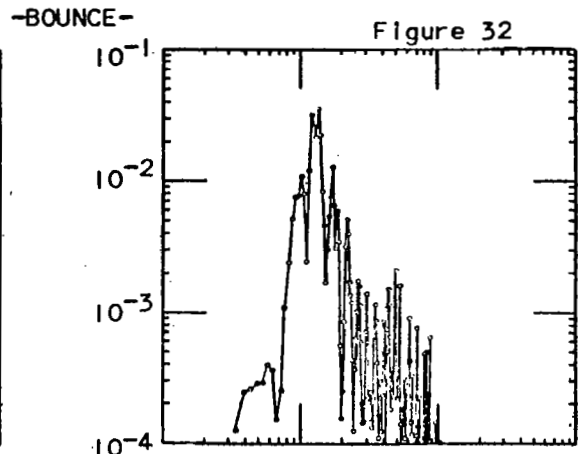
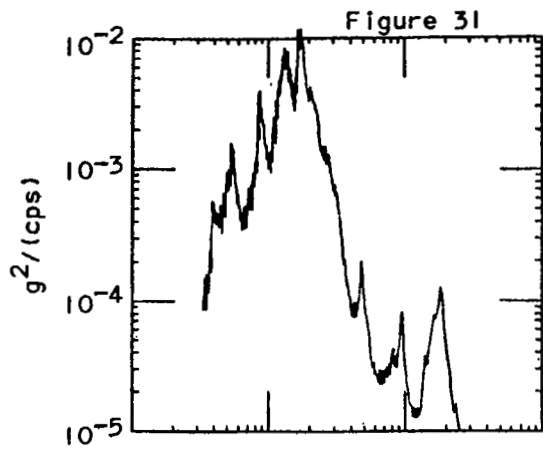
TRUCK PSD'S ON HARD SURFACE AT 6 MPH



MEASURED

TIME DOMAIN PREDICTION

TRUCK PSD'S ON SOFT SURFACE AT 3 MPH

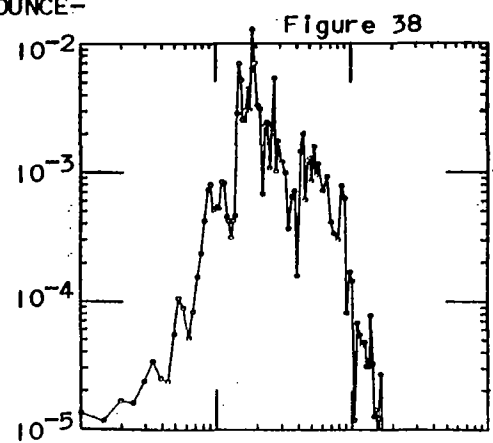
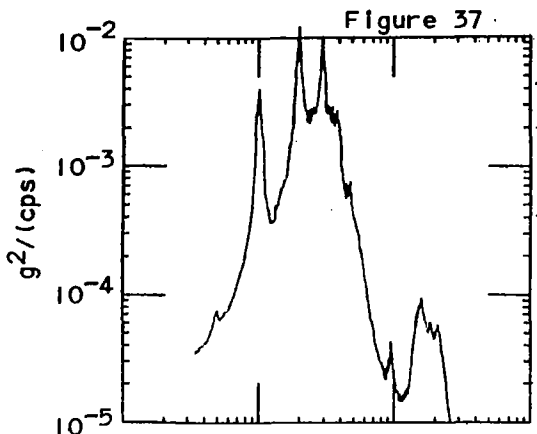


MEASURED

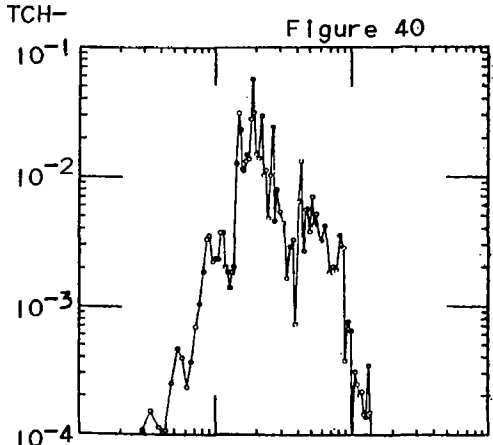
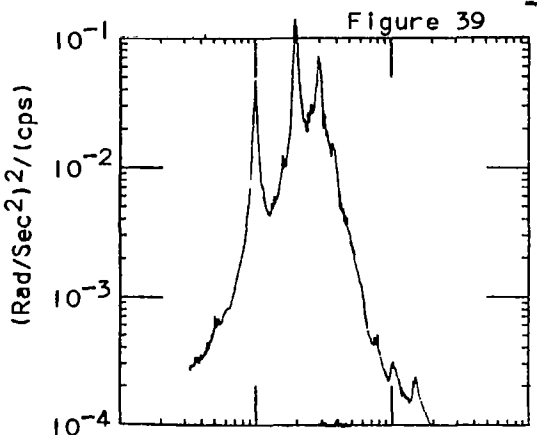
TIME DOMAIN PREDICTION

TRAILER PSD'S ON HARD SURFACE AT 3 MPH

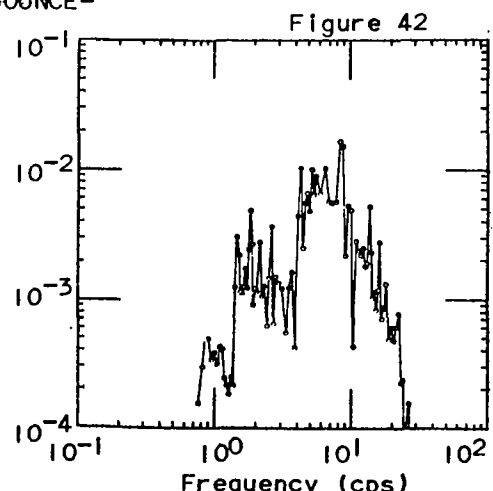
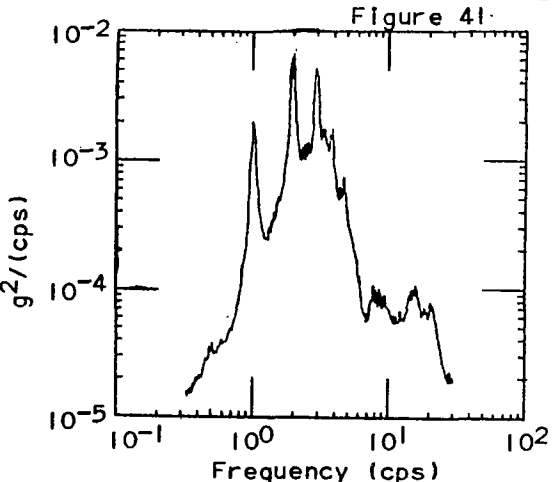
-CG BOUNCE-



-CG PITCH-



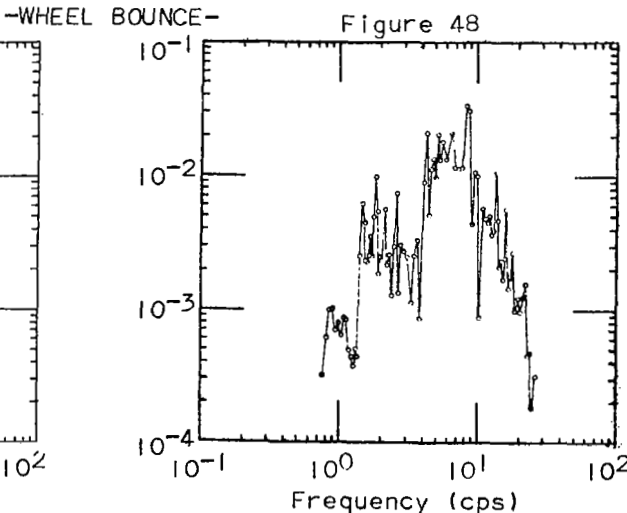
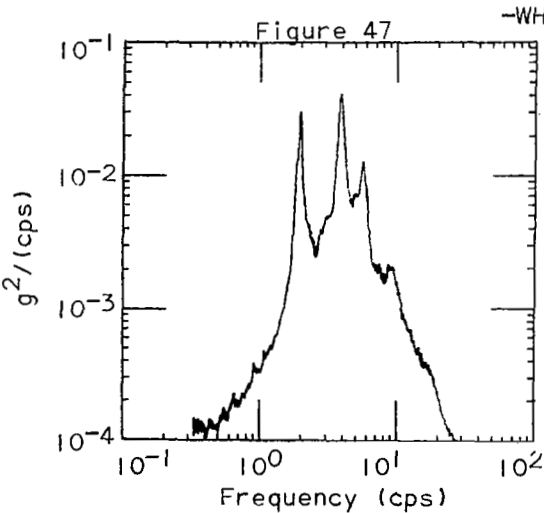
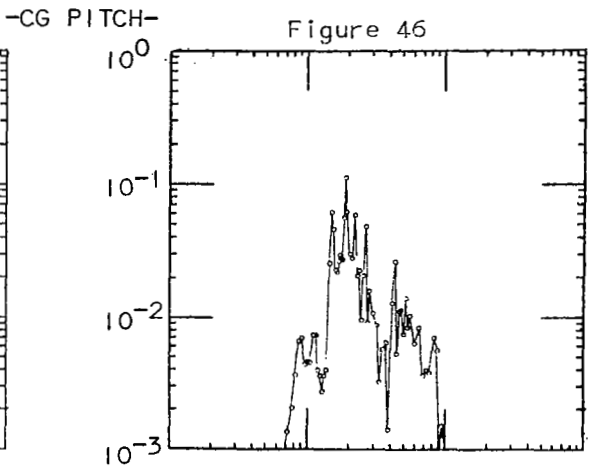
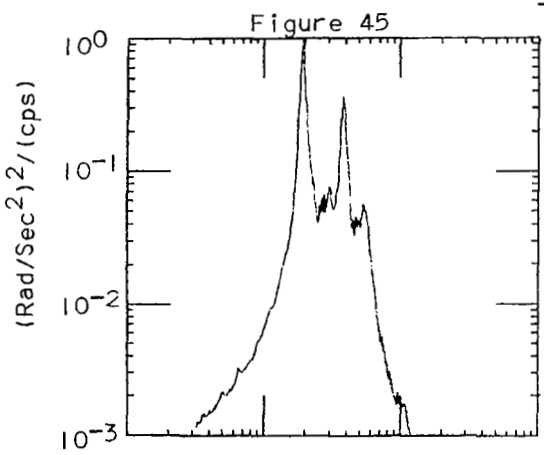
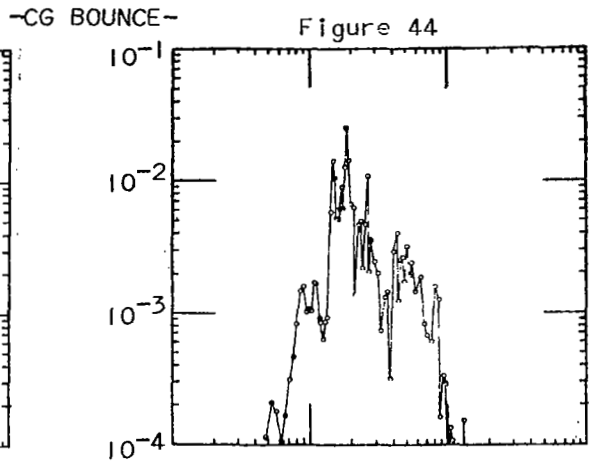
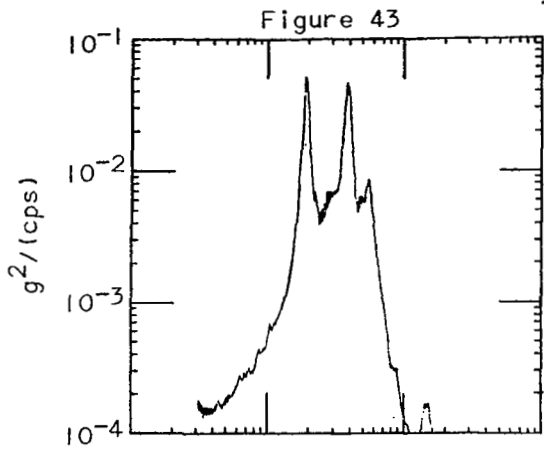
-WHEEL BOUNCE-



MEASURED

TIME DOMAIN PREDICTION

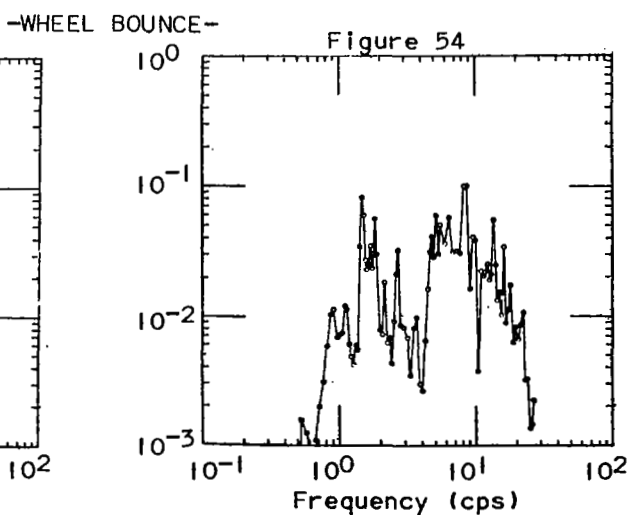
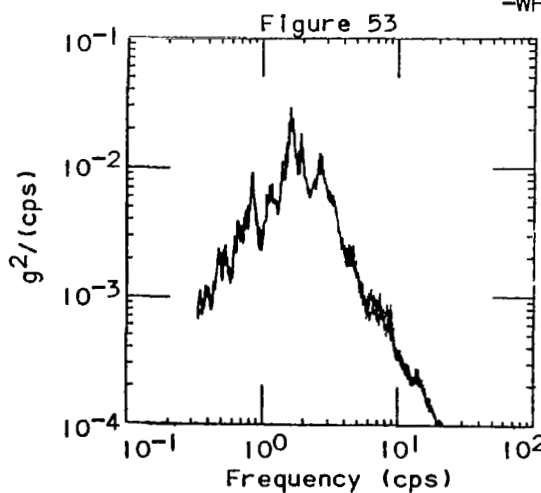
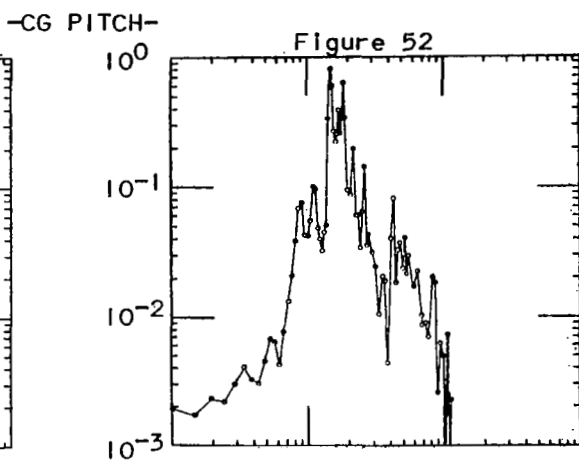
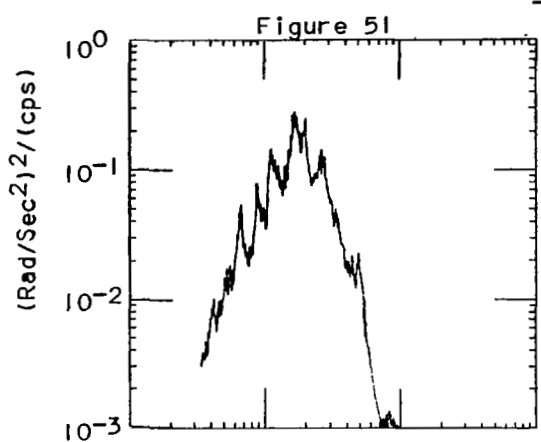
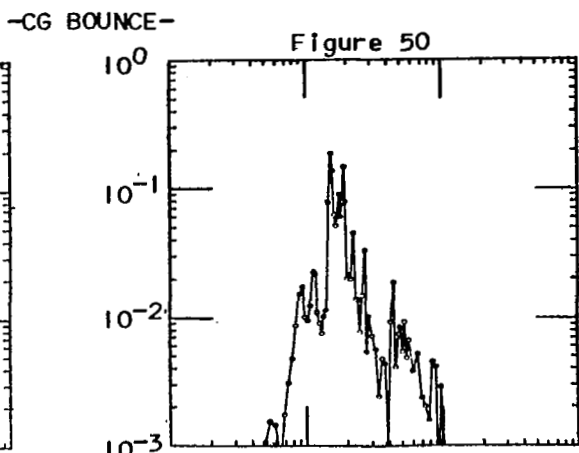
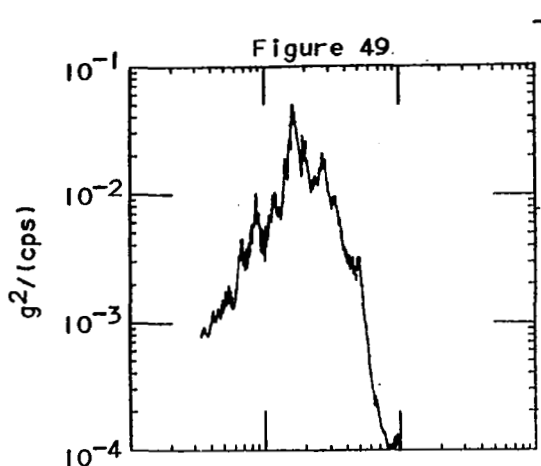
TRAILER PSD'S ON HARD SURFACE AT 6 MPH



MEASURED

TIME DOMAIN PREDICTION

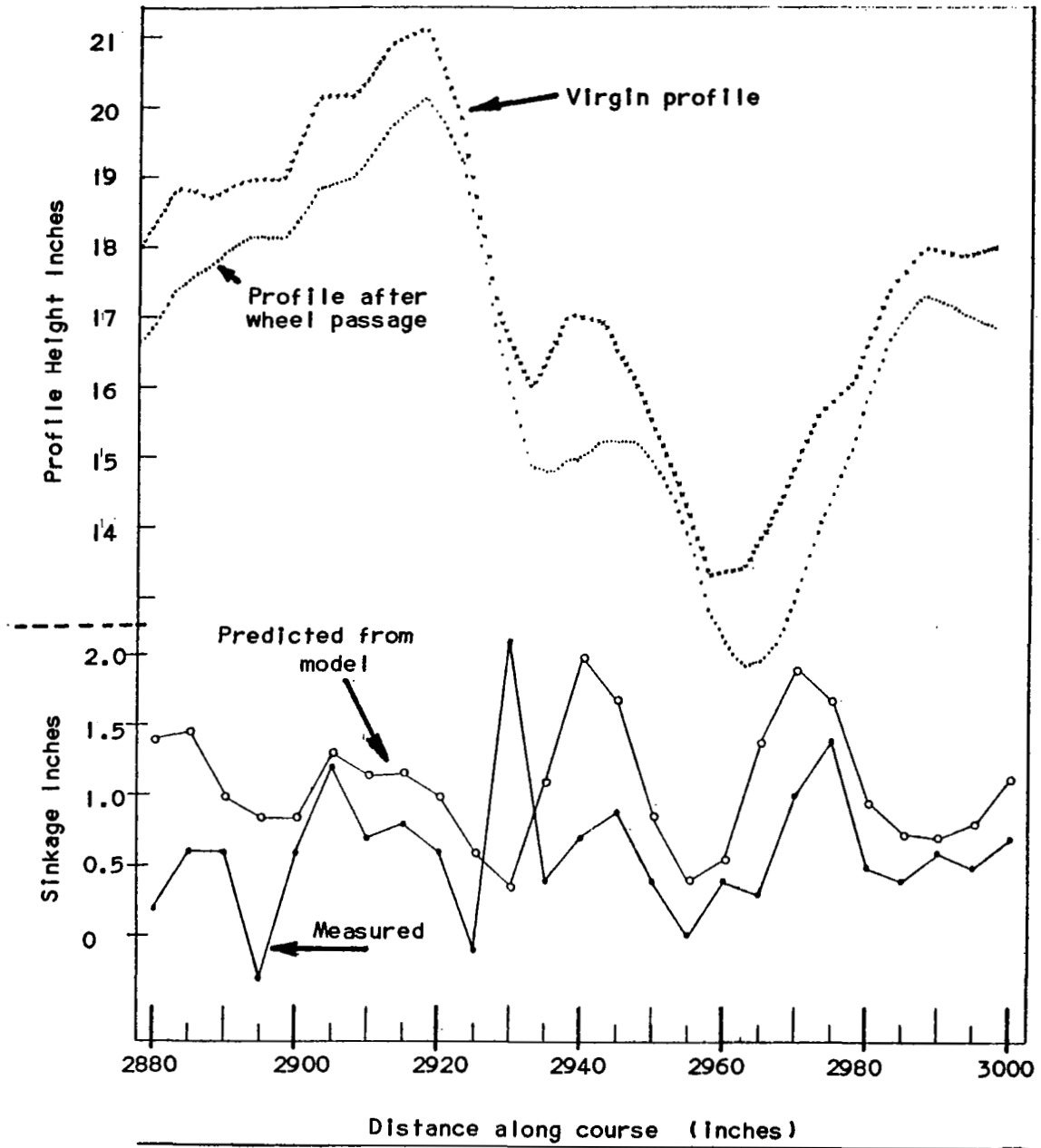
TRAILER PSD'S ON SOFT SURFACE AT 3 MPH



MEASURED

TIME DOMAIN PREDICTION

Figure 55 PLOT OF SOIL DEFORMATION UNDER LOAD



8.0 CONCLUSIONS

1. It is concluded from this study that the statistical techniques developed for the dynamic analysis of surface induced vehicle vibration are valid.
2. It is concluded that the vehicle models used in this study are not completely representative of the actual vehicles.

The first conclusion is based upon the fact that relatively good prediction of vehicle resonances occur. Estimates of vehicle vibration seem to be high, using the statistical technique which would indicate that modifications to the estimate of a surface roughness coefficient might be in order. The general shape of the virgin (soft surface) profile seems to be estimated quite well by the random distribution and surface roughness coefficient. Even the hard surface, where predominant periodicities occur, seems to have a "background roughness" dictated by the random spectral content. It is therefore concluded that if the problem is to match vehicle vibration with predicted values on a particular stretch of profile, then the actual profile input should be used for simulation. If the problem, however, is to design better vehicles or make vehicle concept trade-offs where no particular profile is of interest, then the statistical technique yields reasonable response estimates, and is the best technique known to exist. If this technique is not employed, there is a danger of designing a vehicle tailored to the resonances of a particular profile which will operate well on that profile and no place else.

The second conclusion is based on the fact that non-linearities and other effects occur in actual vehicles which are obviously not accounted for in this simple vehicle model. The correlation of laboratory shake tests of the vehicles

with vehicle models was extremely poor. Better correlation was achieved between the field tests and the vehicle simulation. One of the problems here is suspension system friction. Another very obvious drawback is the tire model used in this simulation. The point contact linear tire is a poor approximation. Tires are non-linear and smooth out short wavelength undulation through their ground contact area and distributed load. This tire "envelopment" would tend to decrease high frequency response of the vehicle. Another obvious simplification of the present vehicle modeling is the lack of fore-and-aft inputs and response. The tire geometry acts to put fore-and-aft or horizontal loads into the suspension system. This effect should probably be accounted for in modeling.

9.0 RECOMMENDATIONS

1. It is recommended that the time domain simulation (either analog or digital) be employed to estimate motions of vehicles designed to traverse random rough surfaces, and also be employed as a design tool in developing these vehicles or making concept trade-offs.
2. It is recommended that more emphasis be put into the area of developing more realistic vehicle models which include non-linearities, more realistic tires, and fore-and-aft (horizontal) vibration and input.
3. It is recommended that additional research be undertaken in the area of dynamic soil modeling for vehicles to develop accurate prediction.
4. It is recommended that a variable band pass window be developed for processing digital data. This would permit the band pass to be directly proportional to center frequency (Constant Q) which is normally of interest for vibration data processing.

10.0 REFERENCES

1. Van Deusen, B. D.: "A Statistical Technique for the Dynamic Analysis of Vehicles Traversing Rough Yielding and Non-Yielding Surfaces," NASA CR-659, March 1967.
2. Bodeau, A. C., Bollinger, R. H., and Lippin, L.: "Passenger Car Suspension Analysis," S.A.E. Trans., Vol. 64, 1956, pp. 273-283.
3. Kohr, R. H.: "Analysis and Simulation of Automobile Ride," S.A.E. Paper 144A, March 1960.
4. Grimes, C. K.: "Development of a Method and Instrumentation for Evaluation of Runway Roughness Effects on Military Aircraft, NATO AGARD," Report 119, 1957.
5. Thompson, W. E.: "Measurements and Power Spectra of Runway Roughness at Airports in Countries of the North Atlantic Treaty Organization," NACA TN 4303, 1958.
6. Silby, N. S.: "An Analytical Study of Effects of some Airplane and Landing Gear Factors on the Runway Roughness with Application to Supersonic Transports." NASA TN D-1492, December 1962.
7. Tung, C. C., Penzlen, J., Horonjeff, R.: "The Effect of Runway Unevenness on the Dynamic Response of Supersonic Transports." NASA CR-119, October 1964.
8. Van Deusen, B. D.: "A Study of the Vehicle Ride Dynamics Aspects of Ground Mobility - MERS Project." Vol. I "Summary," April 1965, U.S. Army Corps of Engineers, Waterways Experiment Station, CR-3-114.
9. Kozen, F., Cote, L. J., Bogdanoff, J. L.: "Statistical Studies of Stable Ground Roughness," Land Locomotion Laboratory Report No. 8391, November 1963.
10. Van Deusen, B. D.: "Data Acquisition and Statistical Analysis Using Analog Computer Techniques," 1963 S.A.E. Transactions, pp. 350-357.
11. Peterson, F. J. and Sansom, H. E.: "MIMIC Programming Manual." WPAFB Tech Report SEG-TR-67-31, July 1967.

12. McRae, J. L., Powell, C. J., Wismer, R. D.: "Performance of Soils Under Tire Loads." U.S. Army Engineer Waterways Experiment Station, Technical Report No. 3-666, Report 1, Vicksburg, Mississippi, January 1965.
13. Powell, C. J., and Green, A. J.: "Performance of Soils Under Tire Loads." U.S. Army Engineer Waterways Experiment Station, Technical Report No. 3-666, Report 2, Vicksburg, Mississippi, August 1965.
14. Smith, M. E., and Freitag, D. R.: "Deflection of Moving Tires." U.S. Army Engineer Waterways Experiment Station, Technical Report No. 3-516, Report 3, Vicksburg, Mississippi, May 1965.
15. Barkan, D. D.: Dynamics of Bases and Foundations, McGraw-Hill Book Co., 1962.
16. Hsieh, T. K.: "Foundation Vibrations." Proceedings Institution of Civil Engineers, Vol. 22, pp. 211-226, 1962.
17. Lysmer, J.: "Vertical Motion of Rigid Footings." U.S. Army Engineer Waterways Experiment Station, Contract Report No. 3-115, Vicksburg, Mississippi, June 1965.
18. Whitman, R. V.: "Analyses of Foundation Vibrations." M.I.T., Civil Engineering Department, Symposium on Man-Made Vibrations in Civil Engineering, International Association for Earthquake Engineering, London, April 1965.
19. Bekker, M. G.: Theory of Land Locomotion. University of Michigan Press, Ann Arbor, Michigan 1956.
20. Assur, A.: "Locomotion Over Soft Soil and Snow." Paper 782 F, Automotive Engineering Congress, S.A.E., Detroit, Michigan, January 1964.
21. Reece, A. R.: "Principles of Soil-Vehicle Mechanics." Proceedings Institution Mechanical Engineers, Vol. 180, Part 2A, 1965-66.
22. Cooper, D. H.: "Radial Stiffness of the Pneumatic Tyre." Transactions Institution Rubber Industry, Vol. 40, pp. 58-70, February 1964.
23. Van Deusen, B. D.: "A Study of the Vehicle Ride Dynamics Aspects of Ground Mobility - MERS Project." Vol. III "Theoretical Dynamics," U.S. Army Corps of Engineers, Waterways Experiment Station CR-3-114, April 1965.

24. FMC Corporation: "A Computer Analysis of Vehicle Dynamics while Traversing Hard Surface Terrain Profiles," U.S. Army Corps of Engineers, Waterways Experiment Station CR-3-1555, February 1966

APPENDIX A
PROFILE MEASUREMENT AND ANALYSIS

A.1 INTRODUCTION

The two sites selected for the field tests were a hard surface and a yielding surface at the Chrysler Proving Ground in Chelsea, Michigan (see map, Figure A-1). The hard surface was a 400 foot section of the south tortuous road designed and normally used for automobile endurance testing. The soft surface section was a cross-country area at the northeast corner of the Proving Ground outside the endurance road near the I-94 property line. This section represented a relatively rough surface which still had sufficient softness to allow a significant penetration (approximately 2 inches) of both the truck and trailer. This section at one time was a military tank proving ground, but for the last fifteen years it has been unused, and was assumed to be a more or less virgin surface. It was necessary to clear some vegetation from this area prior to measuring profile and conducting tests. This was accomplished without disturbing the profile.

A total of seven profile traces were measured from the two test sites for the purpose of computing statistics. Six of these traces represented the paths of the two test vehicles over the two test sites and the seventh was midway between the truck traces on the hard surface. This seventh trace was measured after the test with 5 inch increments to determine the effect of spacing on resolution of a predominant periodicity which appeared in the data. On the hard surface the trailer lane was close to the left lane of the truck. Table A-1 is a summary of the profile measurements.

Tables A-7 through A-13 at the end of this appendix exhibit the raw profile height data as recorded from rod and transit measurements for the

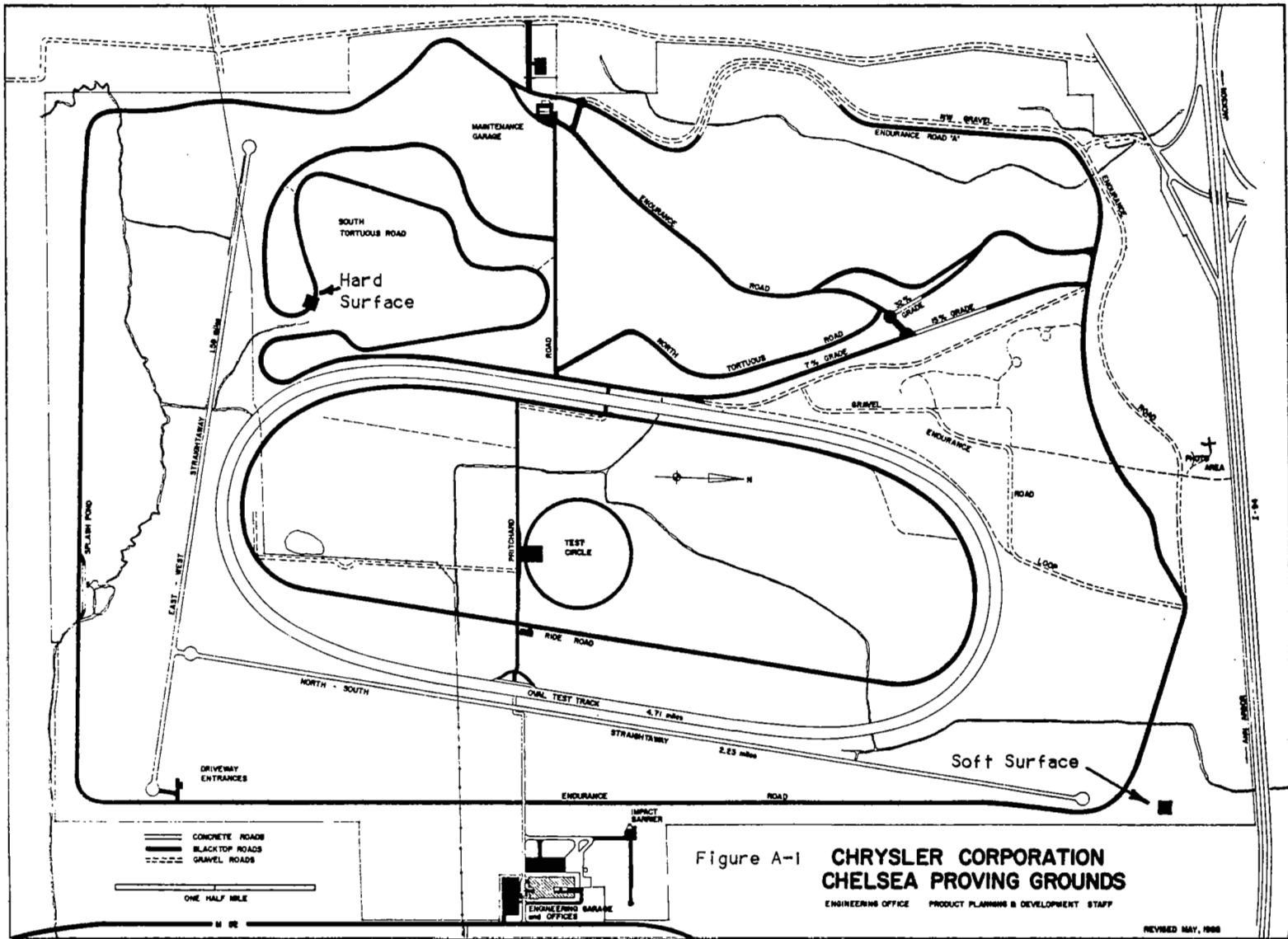


Figure A-1 CHRYSLER CORPORATION
CHELSEA PROVING GROUNDS

ENGINEERING OFFICE PRODUCT PLANNING & DEVELOPMENT STAFF

REVISED MAY, 1968

Table A-1 SUMMARY OF PROFILE MEASUREMENTS				
Surface	Lane	Distance	Spacing	No. of Points
Hard	Left	400'	15"	321
	Trailer	400'	15"	321
	Right	400'	15"	321
	Center	400'	5"	961
Soft	Left	300'	15"	241
	Center (Trailer)	300'	5"	721
	Right	300'	15"	241

seven surfaces in Table A-1.

A.2 ANALYSIS

The raw data from each trace was filtered (detrended) with the 6 db per octave, zero phase shift, digital filter described in Appendix A of Reference 1. The filter constant λ was chosen as 5 meters (16.4040 ft.) to agree with the previous work. To determine the effect of the filter constant on the estimate of the surface roughness coefficient C , the value of λ was varied from 1 to 10 meters for one surface. The results are summarized in Table A-2.

In addition to the C estimate, values of the RMS (standard deviation) and the arithmetic average (average of the absolute value) were computed. These averages for filtered profile data with a zero mean are defined by Equations A-1 and A-2.

$$\text{rms} = \left[\frac{1}{N} \sum_{n=1}^N Y_n^2 \right]^{\frac{1}{2}} \quad (\text{A-1})$$

$$\text{aa} = \frac{1}{N} \sum_{n=1}^N |Y_n| \quad (\text{A-2})$$

More important than the individual averages is their ratio. The ratio of the

Table A-2					
EFFECT OF λ ON ESTIMATE OF C (Soft Surface Center Lane 5" Spacing)					
λ		R.M.S. (Feet)	A.A. (Feet)	Ratio	C (Feet)
Meters	Feet				
1	3.2808	.0818	.0583	1.40	.000413
2	6.5617	.1015	.0719	1.41	.000318
3	9.8425	.1165	.0817	1.43	.000279
4	13.1234	.1288	.0898	1.43	.000256
5	16.4040	.1389	.0961	1.45	.000238
6	19.6850	.1461	.1007	1.45	.000220
7	22.9659	.1520	.1049	1.45	.000204
8	26.2467	.1570	.1089	1.44	.000190
9	29.5276	.1612	.1126	1.43	.000178
10	32.8084	.1650	.1163	1.42	.000168

arithmetic mean to RMS value can be used for comparing amplitude distributions against the Gaussian case. Table A-3 lists this ratio for several common waveforms. It is noted that the flatter the top of the peaks, the lower this ratio becomes. Most of the data in this investigation shows ratios above 1.24 (that of a Gaussian Distribution) indicating that large peaks exist beyond that predicted by a true Gaussian.

After filtering the hard surface data, which contained a large trend due to being on the side of a hill, end point contamination could be observed. This consisted of a trend of approximately 0.5 ft. variation over the first 50 ft. of data. While this value seems small, it was considerably larger than the undulations of the remaining detrended data (about .05 ft. peak to peak).

Table A-3

RATIO OF ARITHMETIC MEAN TO RMS
FOR COMMON WAVE FORMS

Waveform Description	RMS	Arithmetic Mean	Ratio
Sine Wave of Amplitude A	0.707A	0.637A	1.11
Square Wave of Amplitude A	A	A	1.00
Sawtooth Wave of Amplitude A	0.577A	0.500A	1.15
Triangular Wave of Amplitude A	0.577A	0.500A	1.15
Gaussian Distribution with Standard Deviation σ	σ	0.806 σ	1.24

This contamination was anticipated and was the main reason for measuring 400 ft. of hard surface data. By eliminating the 50 ft. of detrended data at either end, a reduced (300 ft.) data set produced lower values of C which were used as inputs for computer simulation. Table A-4 shows the effect of this end point contamination on estimates of the surface roughness coefficient. It also indicates that the C estimates obtained by using the data at 15 inch spacing are virtually unchanged when increased to the resolution of 5 inch spacing.

Estimates of the amplitude probability distribution and power spectral density were obtained from the detrended data using the techniques described in Reference 1. Figure A-2 shows the PSD of the hard surface data computed from the center lane data with a hamming window (or frequency domain filter). The other profile traces produced very similar PSD plots. The hamming window is used in all digital PSD plots in this report with the exception of Figure A-3. This figure shows the same Fourier series data which produced Figure A-2 with the exponential window introduced in Reference 1. On either Figure A-2 or A-3 it can be seen that a predominant periodicity exists in the hard profile at

Table A-4

SUMMARY OF SURFACE ROUGHNESS

Surface	Section	Spacing	No. of Points	RMS (feet)	AA (feet)	Ratio	C (feet)
Hard	Left Lane (400')	15"	321	.1105	.0544	2.03	.000151
Hard	Trailer Lane (400')	15"	321	.1100	.0546	2.01	.000149
Hard	Right Lane (400')	15"	321	.1050	.0571	1.84	.000136
Hard	Center Lane (400')	5"	961	.1074	.0545	1.97	.000143
Hard	Center Lane (every 3rd point from above)	15"	320	.1073	.0543	1.98	.000142
Hard	Left Lane (center 300')	15"	240	.0315	.0252	1.25	.000012
Hard	Trailer Lane (center 300')	15"	240	.0317	.0265	1.20	.000012
Hard	Right Lane (center 300')	15"	240	.0394	.0299	1.32	.000019
Hard	Center Lane (center 300')	5"	720	.0349	.0278	1.26	.000015
Soft	Left Lane	15"	241	.1402	.0911	1.54	.000243
Soft	Center Lane (Trailer)	5"	721	.1389	.0961	1.45	.000238
Soft	Right Lane	15"	241	.1317	.0880	1.50	.000214
Soft	Center Lane (every 3rd point)	15"	240	.1338	.0924	1.45	.000221

Figure A-2 PSD OF HARD SURFACE CENTER LANE

5" spacing - 300 feet of filtered data
Filter "time constant" 16.404 feet (5 meters)
PSD computed from 320 harmonics and hamming filter

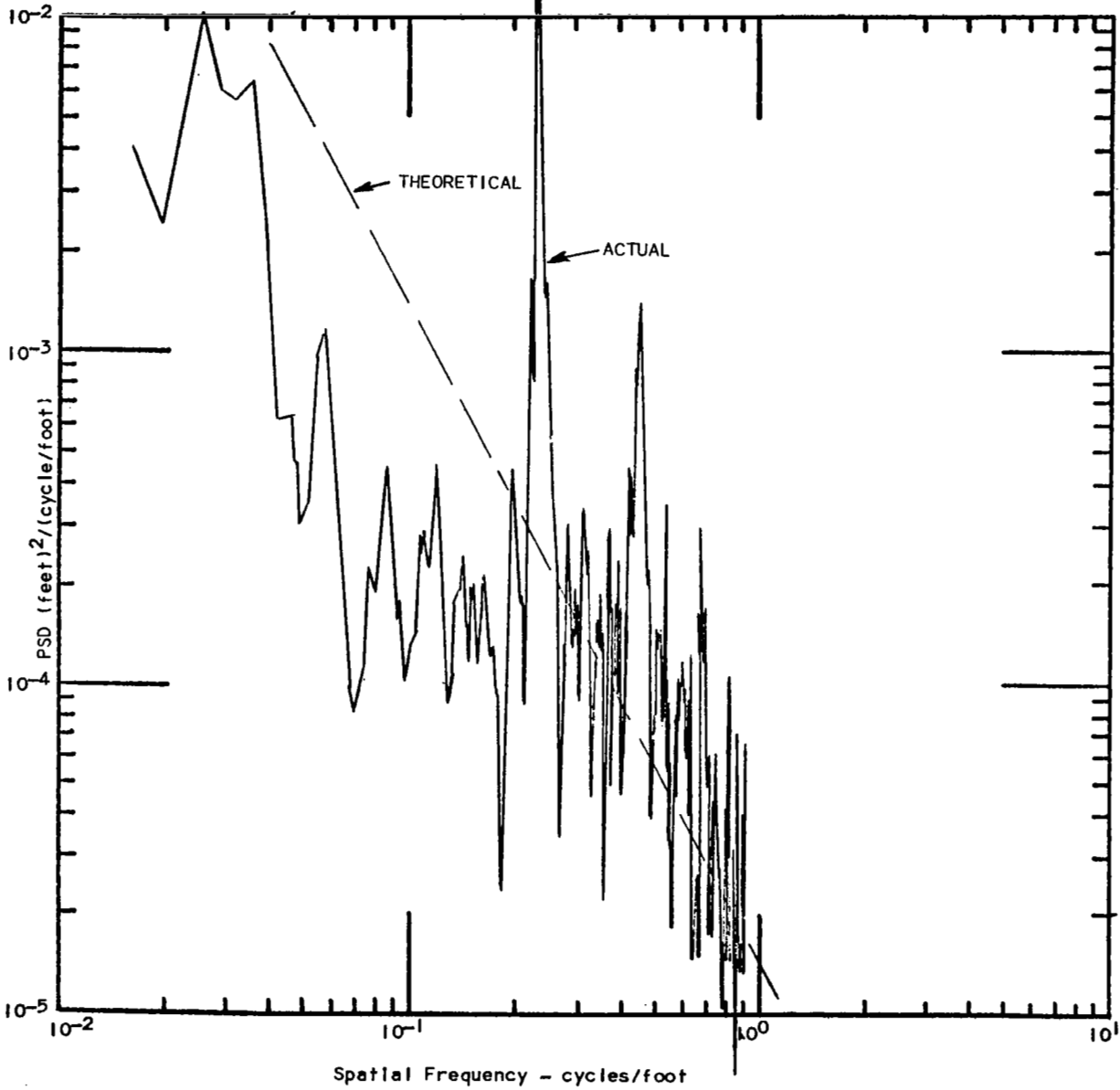


Figure A-3 PSD OF HARD SURFACE CENTER LANE
USING EXPONENTIALLY WEIGHTED FILTER

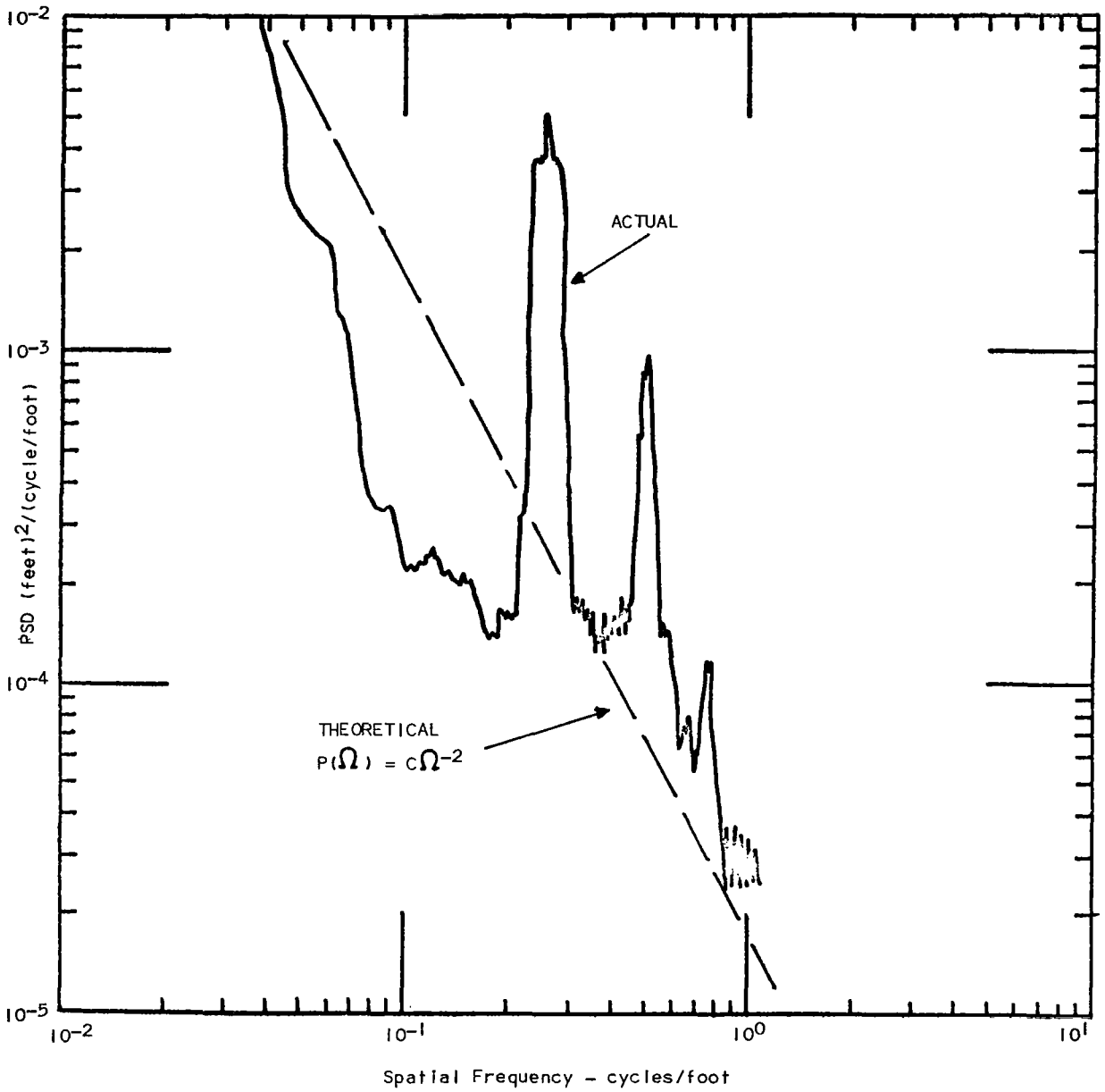
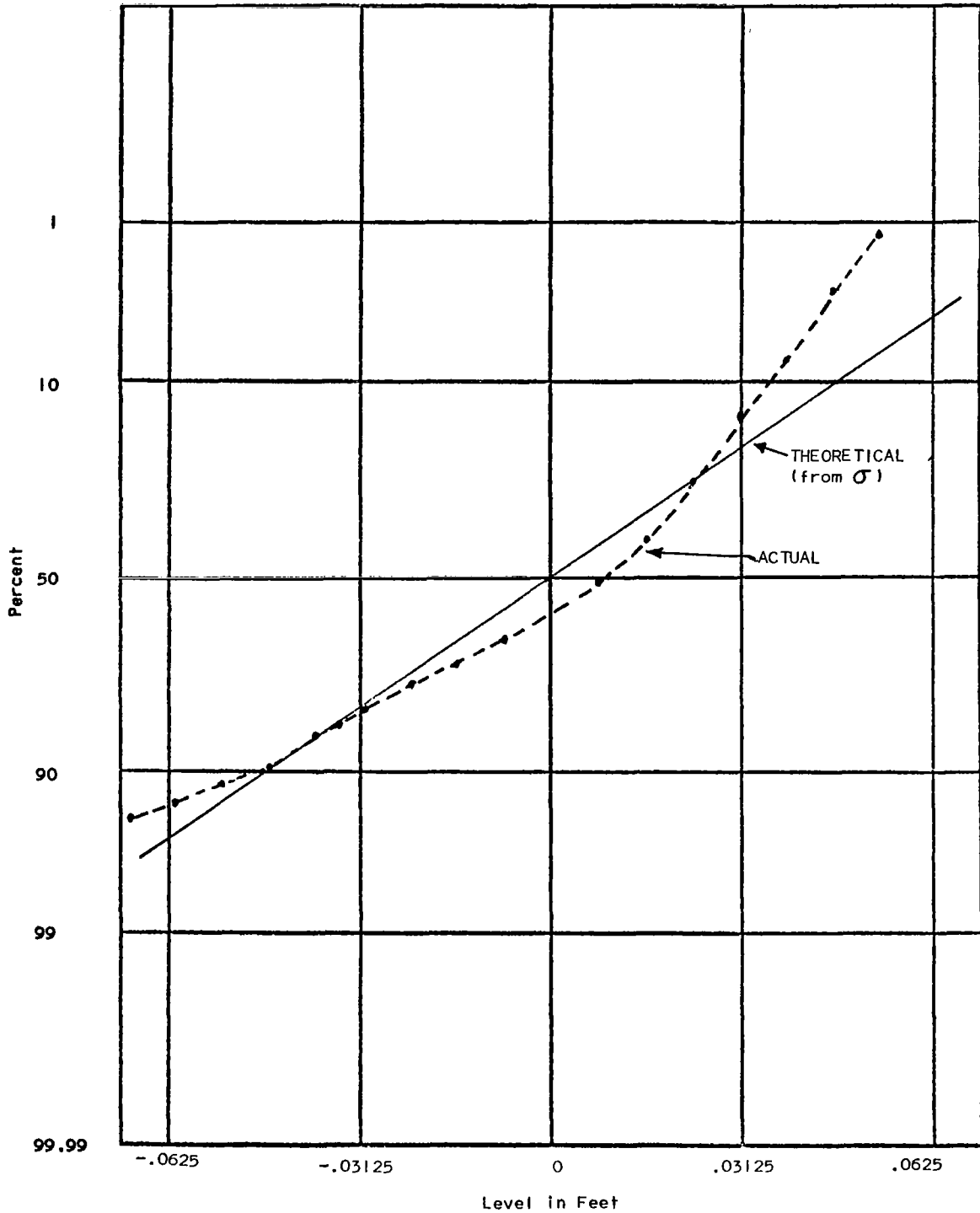


Figure A-4 AMPLITUDE PROBABILITY DISTRIBUTION FOR HARD SURFACE
(Center Lane - 300' - 5" spacing)



0.25 cycles per foot (4 ft/cycle). Second and third harmonics of this periodicity also exist at 0.5 and 0.75 cycles respectively. The effect of this periodicity is clearly evident in the vehicle vibration measurements of Appendix C. The APD for the hard surface is shown in Figure A-4 together with the Gaussian curve (straight line on normal probability paper) computed from the standard deviation. It can be seen that the positive probability is less than that predicted by the Gaussian while the negative is greater. This would indicate that sharp depressions exist in the profile. Indeed when observing the profile, it is obvious that "cracks" about 1 inch wide exist at relatively regularly spaced four foot intervals.

The soft surface PSD is shown in Figure A-5. The effect of the filter can be seen in the low frequency end of this plot. Figure A-6 shows the APD for this surface.

A.3 CROSS CORRELATION

In order to determine the interaction of profile between the left and right lanes of the truck, the cross power spectral density was computed from the detrended soft surface profile, and the center 300 feet of the detrended hard surface profile. The detailed normalized cross spectral density for the soft surface is given in Table A-14, and for the hard surface in Table A-15. These tables list both the real (in-phase, co-spectral) and imaginary (out-of-phase, quadrature spectral) density. Table A-5 is a summary of this data in terms of correlation coefficients.

The reason for this computation was to check the assumption made in Reference 1 that these could be considered independent (i.e. uncorrelated) random traces. Table A-5 shows that this is a reasonable assumption for the

Figure A-5 PSD OF SOFT SURFACE PROFILE TRAILER LANE

(5" spacing) 300' of Filtered Data
Filter Constant = 16.4040 feet

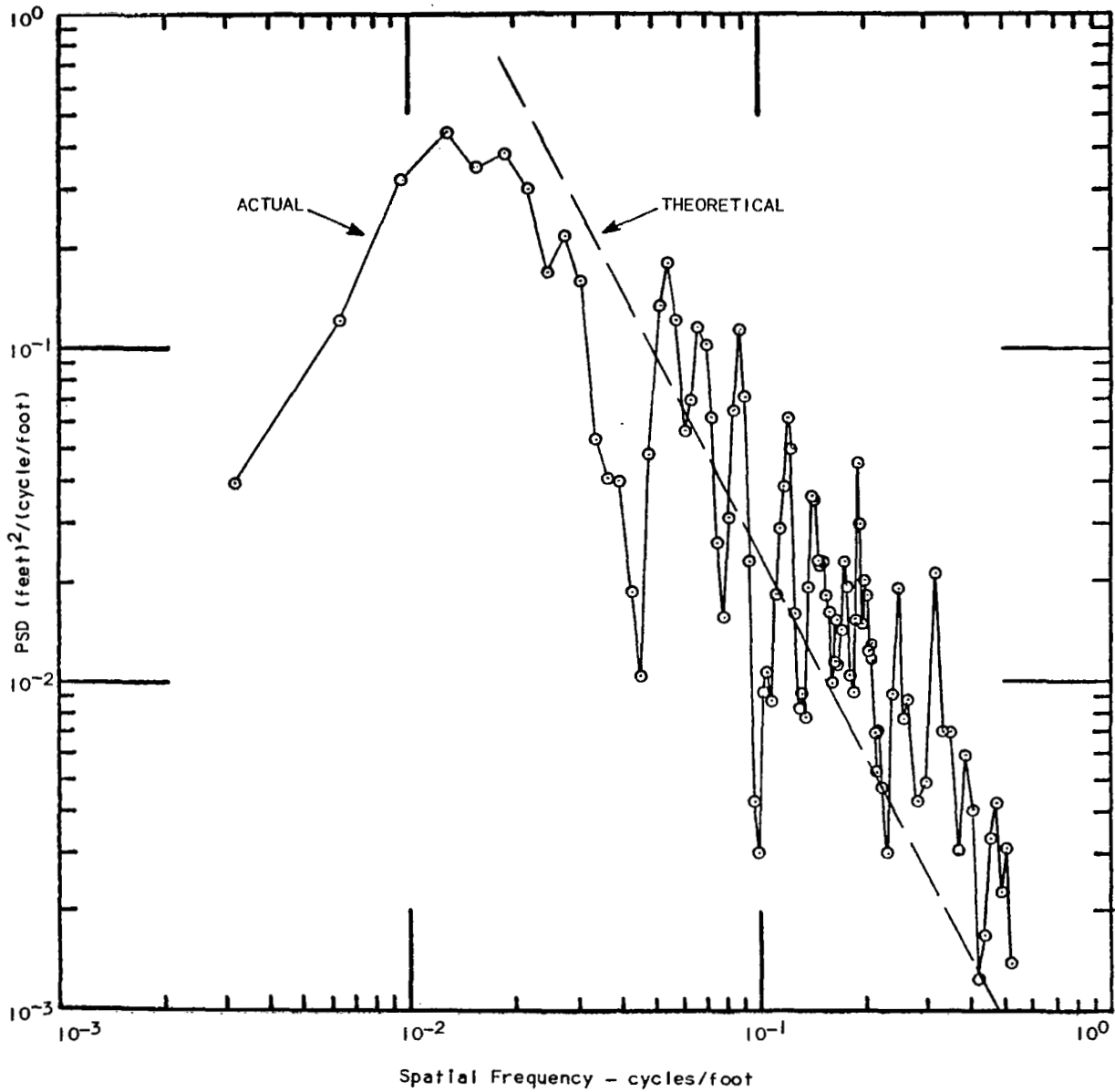


Figure A-6 AMPLITUDE PROBABILITY DISTRIBUTION FOR SOFT SURFACE
 (Center Lane - 300' - 5" Spacing)

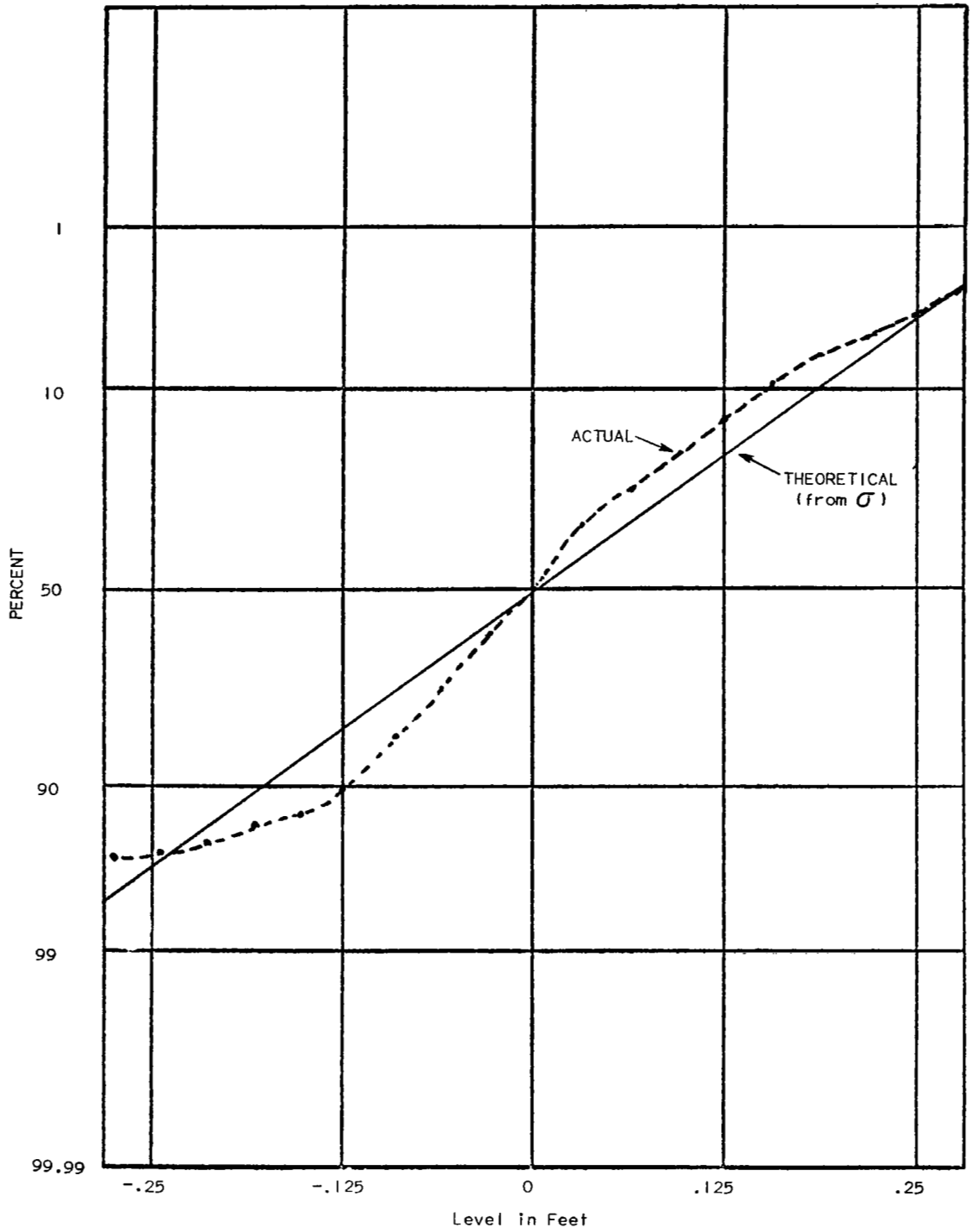


Table A-5 CORRELATION COEFFICIENTS BETWEEN PROFILE LANES		
Lanes	Hard Surface	Soft Surface
Left Center	.798	.390
Center Right	.788	.350
Left Right	.574	.285

soft (virgin) surface, and not as good an assumption for the hard (man-made) surface. Table A-6 shows the normalized (to zero correlation) effect of this assumption on linear vehicle vibration. This table is based upon the analysis of a simple two-wheel vehicle having left and right wheels. The pitch motion for such a vehicle would be directly related to bounce motion. In a realistic four-wheel vehicle, the time lag effect between front and rear inputs would have an effect on this simple analysis.

Table A-6 EFFECT OF PROFILE CORRELATION ON VEHICLE VIBRATION		
Left to Right Correlation Coefficient	Normalized Vehicle Response	
	Roll	Bounce
+1	0	1.414
0	1.0	1.0
-1	1.414	0

The effect of left to right profile correlation from Table A-6 would indicate that the pitch and bounce motions of the vehicle body (M37) would be underestimated by the assumed zero correlation techniques used for the computer predictions in Appendices D and E and the roll motion would be over-estimated. This tendency can be observed in detailed comparison of predicted plots of Appendices D and E with the actual measurements of Appendix C.

Table A-7

RAW DATA ELEVATIONS IN FEET

NASA FIELD TEST DATA-LEFT LANE-HARD SURFACE-15 INCH SPACING

321 POINTS

19.1900	19.0900	19.0400	18.9700	18.8800	18.8400	18.7700
18.6700	18.6200	18.5600	18.4800	18.4000	18.3300	18.2700
18.1600	18.1200	18.0400	17.9500	17.8900	17.8300	17.7300
17.6700	17.6200	17.5400	17.4700	17.4100	17.3400	17.2500
17.1800	17.1200	16.9900	16.9500	16.8800	16.7500	16.7200
16.6500	16.5700	16.4700	16.4100	16.3400	16.2200	16.1900
16.1200	16.0200	15.9700	15.9000	15.8200	15.7600	15.7000
15.6100	15.5200	15.4600	15.3900	15.3000	15.2500	15.1700
15.0700	15.0200	14.9300	14.8600	14.8000	14.7200	14.6000
14.5800	14.5200	14.4000	14.3700	14.3100	14.2100	14.1700
14.1200	14.0500	13.9800	13.9300	13.8800	13.7500	13.7300
13.6700	13.5500	13.5200	13.4500	13.2900	13.2700	13.2000
13.1100	13.0400	12.9500	12.8700	12.7800	12.7400	12.6900
12.5800	12.5500	12.4900	12.3700	12.3500	12.2800	12.2100
12.1400	12.0900	12.0300	11.8900	11.8900	11.8200	11.7200
11.6900	11.6200	11.4800	11.4800	11.4200	11.3100	11.2900
11.2300	11.1100	11.0800	11.0400	10.9500	10.9300	10.8800
10.8200	10.7200	10.7000	10.6300	10.5500	10.5100	10.4500
10.3400	10.3100	10.2600	10.1600	10.1200	10.0800	9.9900
9.9600	9.9100	9.8600	9.7900	9.7400	9.6900	9.5900
9.5700	9.5200	9.4300	9.4000	9.3600	9.2900	9.2500
9.2000	9.1400	9.0600	9.0300	8.9700	8.8600	8.8600
8.8200	8.7400	8.7200	8.6800	8.6100	8.6000	8.5500
8.5800	8.5200	8.5100	8.4700	8.3800	8.3700	8.3500
8.2700	8.2600	8.2700	8.2100	8.1300	8.1300	8.1000
8.0200	8.0300	8.0000	7.9200	7.9300	7.9100	7.8700
7.8600	7.8500	7.8200	7.7900	7.7800	7.7700	7.7100
7.7300	7.7200	7.6400	7.6700	7.6600	7.6000	7.6100
7.6100	7.5800	7.5300	7.5600	7.5300	7.4800	7.4900
7.4700	7.4100	7.4300	7.4100	7.3300	7.3700	7.3600
7.3000	7.3200	7.3000	7.2500	7.2700	7.2600	7.2200
7.2100	7.2100	7.2000	7.1400	7.1700	7.1500	7.0900
7.1300	7.1200	7.0500	7.0800	7.0700	7.0500	7.0200
7.0300	7.0100	6.9500	6.9900	6.9800	6.9100	6.9500
6.9500	6.8800	6.9200	6.9100	6.9100	6.9000	6.9000
6.8500	6.8600	6.8300	6.8500	6.8500	6.8500	6.8400
6.7900	6.8300	6.8200	6.7600	6.8100	6.8000	6.7400
6.7800	6.7700	6.7200	6.7500	6.7400	6.6800	6.7200
6.7200	6.6800	6.7000	6.7100	6.6700	6.6800	6.6900
6.6900	6.6300	6.6800	6.6800	6.6300	6.6700	6.6700
6.6600	6.6400	6.6600	6.6300	6.6400	6.6500	6.6400
6.5900	6.6200	6.6200	6.6000	6.6100	6.6100	6.5900
6.5500	6.5800	6.5700	6.5200	6.5500	6.5500	6.4600
6.5300	6.5300	6.4600	6.5000	6.5000	6.4900	6.4700
6.4600	6.4500	6.3800	6.4200	6.4100	6.3400	6.3700
6.3700	6.3000	6.3300	6.3100	6.2500	6.2700	

Table A-8

RAW DATA ELEVATIONS IN FEET

NASA FIELD DATA-TRAILER LANE-HARD SURFACE-15 INCH SPACING

321 POINTS

19.2000	19.1100	19.0500	18.9900	18.8900	18.8500	18.7900
18.6800	18.6400	18.5800	18.5000	18.4200	18.3500	18.2800
18.1800	18.1400	18.0600	17.9600	17.9100	17.8500	17.7500
17.7000	17.6400	17.5700	17.4900	17.4300	17.3600	17.2700
17.2100	17.1400	17.0200	16.9800	16.9100	16.7700	16.7400
16.6700	16.5900	16.4900	16.4300	16.3600	16.2400	16.2100
16.1500	16.0300	15.9900	15.9300	15.8300	15.7900	15.7200
15.6200	15.5300	15.4900	15.4100	15.3200	15.2700	15.1900
15.0900	15.0400	14.9500	14.8800	14.8200	14.7400	14.6100
14.5900	14.5300	14.4100	14.3800	14.2200	14.2200	14.1900
14.1300	14.0600	13.9900	13.9400	13.8700	13.7500	13.7400
13.6700	13.5500	13.5300	13.4600	13.3000	13.3100	13.2300
13.1600	13.0800	12.9900	12.9000	12.7800	12.7800	12.7100
12.5900	12.5700	12.5200	12.4000	12.3700	12.3100	12.2300
12.1600	12.1100	12.0300	11.9100	11.9100	11.8500	11.7300
11.7100	11.6400	11.5100	11.4900	11.4400	11.3400	11.3100
11.2400	11.1600	11.0800	11.0500	10.9600	10.9300	10.8900
10.8400	10.7300	10.7100	10.6500	10.5500	10.5100	10.4600
10.3200	10.3000	10.2500	10.1800	10.0900	10.0700	9.9900
9.9400	9.9000	9.8400	9.7800	9.7400	9.6900	9.5900
9.5700	9.5200	9.4200	9.4100	9.3600	9.3000	9.2400
9.2100	9.1500	9.0500	9.0400	8.9800	8.8700	8.8800
8.8400	8.7400	8.7400	8.7100	8.6200	8.6100	8.5900
8.5500	8.5400	8.5000	8.4400	8.4200	8.3900	8.3300
8.2900	8.2900	8.2500	8.2300	8.1700	8.1300	8.0500
8.0600	8.0400	7.9700	7.9500	7.9400	7.9100	7.8700
7.8600	7.8400	7.7900	7.8000	7.7800	7.7200	7.7300
7.7200	7.6500	7.6700	7.6700	7.6200	7.6100	7.6200
7.6000	7.5400	7.5600	7.5500	7.4900	7.5000	7.4800
7.4000	7.4400	7.4200	7.3400	7.3800	7.3700	7.3100
7.3300	7.3200	7.2600	7.2800	7.2600	7.2500	7.2200
7.2200	7.2100	7.1500	7.1800	7.1600	7.1000	7.1300
7.1300	7.0700	7.1000	7.0900	7.0700	7.0200	7.0500
7.0400	6.9700	7.0000	6.9900	6.9100	6.9200	6.9200
6.9000	6.9400	6.9300	6.8800	6.9200	6.9100	6.8800
6.8900	6.8800	6.8700	6.8600	6.8600	6.8500	6.8000
6.8400	6.7800	6.7700	6.8100	6.8100	6.7400	6.7900
6.7800	6.7200	6.7600	6.7500	6.6900	6.7300	6.7200
6.6900	6.7100	6.7100	6.6900	6.6800	6.6900	6.6800
6.6300	6.6700	6.6700	6.6300	6.6600	6.6600	6.6500
6.6500	6.6600	6.6200	6.6300	6.6400	6.6400	6.5800
6.6100	6.6100	6.5900	6.6000	6.5900	6.5900	6.5400
6.5700	6.5600	6.4900	6.5300	6.5300	6.4500	6.5100
6.5200	6.4300	6.4900	6.4800	6.4600	6.4500	6.4600
6.4400	6.3600	6.4100	6.3900	6.3200	6.3600	6.3600
6.3000	6.3200	6.3100	6.2600	6.2800	6.2700	

Table A-9

RAW DATA ELEVATIONS IN FEETNASA FIELD TEST DATA-RIGHT LANE-HARD SURFACE- 15 INCH SPACING

321 POINTS

19.0400	18.9600	18.9200	18.8600	18.7800	18.7300	18.6900
18.6300	18.5600	18.5000	18.4500	18.3900	18.3100	18.2500
18.1800	18.1100	18.0500	17.9800	17.9000	17.8500	17.7600
17.6900	17.6200	17.5900	17.4700	17.4400	17.3800	17.2700
17.2300	17.1700	17.0900	17.0200	16.9500	16.8800	16.7600
16.7200	16.6500	16.5800	16.4900	16.4300	16.3500	16.2600
16.2100	16.1200	16.0400	15.9800	15.9000	15.8000	15.7500
15.6800	15.5800	15.4900	15.4300	15.3100	15.2700	15.1900
15.0600	15.0000	14.9200	14.8000	14.7600	14.7000	14.6400
14.5300	14.4800	14.4100	14.3200	14.2700	14.2100	14.0800
14.0700	14.0200	13.9200	13.8900	13.8200	13.7100	13.6400
13.5800	13.5100	13.3900	13.3800	13.2900	13.2000	13.1500
13.0600	12.9600	12.9200	12.8400	12.7200	12.7000	12.6500
12.5700	12.5000	12.4500	12.3900	12.2600	12.2400	12.1900
12.1000	12.0600	12.0000	11.9400	11.8200	11.8000	11.7600
11.6700	11.6400	11.5700	11.4600	11.4500	11.3900	11.2900
11.2600	11.1900	11.1000	11.0500	11.0100	10.9200	10.8900
10.8400	10.7500	10.6600	10.6100	10.5100	10.4400	10.3900
10.3000	10.2600	10.2100	10.1600	10.0400	10.0100	9.9600
9.8900	9.8200	9.7700	9.7100	9.6600	9.6000	9.5400
9.4300	9.4000	9.3500	9.2500	9.2200	9.1700	9.1000
9.0300	8.9800	8.9100	8.8300	8.7900	8.7400	8.6100
8.5900	8.5400	8.4500	8.4000	8.3900	8.3200	8.3100
8.3100	8.2300	8.2100	8.1900	8.1400	8.1100	8.0900
8.0600	7.9900	7.9700	7.9500	7.9000	7.8700	7.8600
7.7600	7.7600	7.7600	7.7400	7.6700	7.6700	7.6700
7.6200	7.6100	7.6000	7.5500	7.5500	7.5600	7.5600
7.5100	7.5100	7.5100	7.4500	7.4600	7.4500	7.4000
7.4100	7.4000	7.3600	7.3600	7.3700	7.3300	7.3200
7.3100	7.2600	7.2500	7.2400	7.2200	7.1700	7.1800
7.1500	7.1100	7.1200	7.1000	7.0500	7.0600	7.0500
7.0100	7.0100	7.0100	6.9800	6.9400	6.9500	6.9400
6.9100	6.9200	6.8900	6.8300	6.8600	6.8700	6.8200
6.8300	6.8200	6.8100	6.7600	6.7800	6.7600	6.6900
6.7200	6.7100	6.6700	6.6600	6.6800	6.6300	6.6400
6.6500	6.6000	6.6000	6.6200	6.6000	6.5900	6.6000
6.6000	6.5500	6.5700	6.5700	6.5400	6.5500	6.5400
6.5000	6.5300	6.4900	6.4800	6.4900	6.4900	6.4600
6.4700	6.4800	6.4400	6.4800	6.4800	6.4500	6.4900
6.5000	6.4600	6.4700	6.4700	6.4700	6.4300	6.4900
6.4900	6.4400	6.4500	6.4700	6.4200	6.4600	6.4400
6.3900	6.4200	6.4400	6.3900	6.4100	6.4400	6.4500
6.4400	6.4300	6.4100	6.3700	6.3600	6.3700	6.3800
6.3400	6.3300	6.3300	6.3100	6.3000	6.3000	6.2600
6.2600	6.2900	6.2500	6.1600	6.2000	6.2000	6.1600
6.1800	6.1300	6.1300	6.1300	6.1000	6.0500	

Table A-10

RAW DATA ELEVATIONS IN FEET

HARD SURFACE	CENTER LANE	5 INCH SPACING				
961 POINTS						
19.1400	19.0800	19.0400	19.0400	19.0300	19.0200	19.0000
18.9800	18.9700	18.9400	18.9100	18.8700	18.8400	18.8400
18.8200	18.8000	18.7800	18.7600	18.7400	18.7200	18.7000
18.6800	18.6200	18.6200	18.6100	18.5900	18.5700	18.5500
18.5300	18.5000	18.4800	18.4600	18.4200	18.3700	18.3700
18.3600	18.3500	18.3200	18.3000	18.2800	18.2800	18.2300
18.1900	18.1400	18.1500	18.1300	18.1100	18.0900	18.0800
18.0600	18.0200	17.9800	17.9100	17.9100	17.9100	17.8900
17.8700	17.8400	17.8300	17.8000	17.7700	17.7100	17.7100
17.7000	17.6800	17.6700	17.6400	17.6200	17.6000	17.5800
17.5600	17.5100	17.4800	17.4800	17.4700	17.4500	17.4200
17.4000	17.3800	17.3500	17.3100	17.2800	17.2700	17.2500
17.2300	17.2100	17.1900	17.1500	17.1400	17.1000	17.0400
17.0200	17.0200	17.0000	16.9800	16.9600	16.9300	16.9100
16.8900	16.8500	16.8000	16.7600	16.7600	16.7300	16.7200
16.7000	16.6800	16.6500	16.6300	16.6000	16.5800	16.5100
16.4900	16.4800	16.4600	16.4400	16.4200	16.3900	16.3700
16.3300	16.2600	16.2600	16.2600	16.2400	16.2200	16.2000
16.1800	16.1600	16.1300	16.0800	16.0600	16.0400	16.0300
16.0100	15.9900	15.9700	15.9500	15.9200	15.8900	15.8400
15.8100	15.8000	15.7800	15.7700	15.7500	15.7200	15.7000
15.6700	15.6400	15.5600	15.5200	15.5400	15.5200	15.5000
15.4800	15.4600	15.4400	15.4000	15.3400	15.3300	15.3300
15.3100	15.2800	15.2600	15.2300	15.2100	15.1700	15.1000
15.0800	15.0800	15.0500	15.0300	15.0300	15.0100	14.9700
14.9500	14.9200	14.8500	14.8500	14.8200	14.8100	14.7800
14.7500	14.7300	14.7100	14.6900	14.6400	14.5900	14.5900
14.5900	14.5700	14.5400	14.5300	14.4900	14.4700	14.3800
14.3700	14.3800	14.3700	14.3500	14.3300	14.3100	14.2800
14.2500	14.2100	14.1700	14.1400	14.1400	14.1500	14.1200
14.0900	14.0800	14.0600	14.0400	14.0100	13.9600	13.9400
13.9600	13.9400	13.9100	13.8800	13.8800	13.8600	13.8200
13.7800	13.7200	13.7200	13.7100	13.7000	13.6800	13.6600
13.6300	13.6200	13.5900	13.5400	13.4900	13.4900	13.4900
13.4700	13.4500	13.4200	13.3900	13.3700	13.3300	13.2700
13.2600	13.2700	13.2400	13.2200	13.2000	13.1800	13.1500
13.1200	13.0600	13.0400	13.0300	13.0100	12.9800	12.9500
12.9300	12.9100	12.8800	12.8500	12.7900	12.7500	12.7500
12.7600	12.7500	12.7300	12.7100	12.7000	12.6700	12.6300
12.5800	12.5700	12.5700	12.5600	12.5400	12.5200	12.5000
12.4800	12.4600	12.4300	12.3600	12.3400	12.3500	12.3400
12.3300	12.3100	12.2900	12.2700	12.2500	12.2200	12.1600
12.1500	12.1500	12.1300	12.1100	12.0900	12.0700	12.0500
12.0200	12.0000	11.9300	11.9000	11.9000	11.9000	11.8900
11.8700	11.8400	11.8200	11.8000	11.7700	11.7200	11.6900
11.7000	11.7000	11.6700	11.6500	11.6200	11.6000	11.5600
11.4800	11.4700	11.4900	11.4900	11.4700	11.4500	11.4300
11.4100	11.3800	11.3300	11.3100	11.3200	11.3000	11.2800

Table A-10
(Continued)

RAW DATA ELEVATIONS IN FEET

11.2700	11.2400	11.2200	11.2000	11.1700	11.1000	11.0600
11.0900	11.0800	11.0700	11.0500	11.0300	11.0000	10.9500
10.9400	10.9400	10.9300	10.9200	10.9000	10.8800	10.8600
10.8400	10.8200	10.7700	10.7300	10.7200	10.7300	10.7100
10.7000	10.6800	10.6600	10.6300	10.5800	10.5300	10.5300
10.5300	10.5100	10.5000	10.4700	10.4500	10.4300	10.3800
10.3300	10.3300	10.3400	10.3300	10.3100	10.2900	10.2700
10.2500	10.2400	10.2100	10.1700	10.1100	10.1000	10.1100
10.1000	10.0900	10.0700	10.0500	10.0300	10.0100	9.9600
9.9500	9.9400	9.9300	9.9200	9.9000	9.8800	9.8600
9.8400	9.7900	9.7700	9.7700	9.7600	9.7400	9.7200
9.7100	9.6800	9.6600	9.6500	9.6200	9.5700	9.5500
9.5500	9.5400	9.5300	9.5000	9.4900	9.4700	9.4400
9.4000	9.3800	9.3900	9.3700	9.3600	9.3400	9.3200
9.3000	9.2800	9.2600	9.2100	9.1800	9.1900	9.1700
9.1600	9.1400	9.1200	9.1000	9.0800	9.0400	8.9900
8.9700	8.9700	8.9700	8.9500	8.9400	8.9100	8.9000
8.8800	8.8400	8.7700	8.7600	8.7800	8.7800	8.7700
8.7400	8.7300	8.7200	8.7000	8.6600	8.6100	8.5900
8.5900	8.6100	8.6000	8.5900	8.5700	8.5600	8.5300
8.5100	8.5100	8.5100	8.5000	8.4800	8.5000	8.4900
8.4800	8.4600	8.4400	8.3900	8.3800	8.3900	8.3900
8.3800	8.3700	8.3600	8.3500	8.3300	8.2700	8.2400
8.2500	8.2700	8.2600	8.2600	8.2500	8.2300	8.2200
8.2000	8.1400	8.1200	8.1400	8.1500	8.1400	8.1400
8.1200	8.1100	8.1000	8.0800	8.0500	8.0200	8.0200
8.0300	8.0300	8.0200	8.0200	8.0000	7.9800	7.9300
7.9100	7.9100	7.9200	7.9200	7.9100	7.9000	7.9000
7.8900	7.8800	7.8500	7.8000	7.8000	7.8200	7.8200
7.8200	7.8100	7.8100	7.8100	7.8000	7.7700	7.7400
7.7500	7.7600	7.7600	7.7500	7.7500	7.7500	7.7400
7.7200	7.6900	7.6900	7.7100	7.7100	7.7100	7.7000
7.7000	7.6900	7.6800	7.6800	7.6400	7.6200	7.6300
7.6500	7.6500	7.6500	7.6400	7.6400	7.6300	7.6100
7.5500	7.5400	7.5700	7.5900	7.5900	7.5800	7.5800
7.5700	7.5600	7.5200	7.5000	7.5100	7.5300	7.5300
7.5400	7.5300	7.5300	7.5200	7.5100	7.4600	7.4300
7.4300	7.4700	7.4700	7.4800	7.4700	7.4600	7.4500
7.4200	7.3900	7.4000	7.4200	7.4300	7.4200	7.4100
7.4100	7.3900	7.3500	7.3300	7.3300	7.3500	7.3600
7.3500	7.3500	7.3400	7.3300	7.3100	7.2600	7.2600
7.2700	7.2900	7.2900	7.2900	7.2800	7.2800	7.2700
7.2300	7.2100	7.2000	7.2300	7.2400	7.2400	7.2300
7.2200	7.2200	7.1800	7.1700	7.1800	7.1900	7.1900
7.1900	7.1900	7.1800	7.1800	7.1700	7.1300	7.1200

Table A-10
(Continued)

RAW DATA ELEVATIONS IN FEET

7.1300	7.1400	7.1400	7.1400	7.1300	7.1300	7.1200
7.1100	7.1000	7.0600	7.0500	7.0600	7.0800	7.0900
7.0800	7.0800	7.0700	7.0600	7.0200	7.0100	7.0200
7.0400	7.0400	7.0400	7.0400	7.0300	7.0200	6.9800
6.9700	6.9700	6.9800	6.9900	7.0000	6.9900	6.9900
6.9800	6.9700	6.9600	6.9100	6.9100	6.9300	6.9500
6.9500	6.9500	6.9400	6.9300	6.9300	6.9200	6.9000
6.8500	6.8600	6.8800	6.9000	6.8900	6.8900	6.8800
6.8600	6.8300	6.8000	6.8200	6.8400	6.8600	6.8600
6.8500	6.8500	6.8400	6.8000	6.7800	6.7900	6.8100
6.8200	6.8200	6.8200	6.8200	6.8100	6.8000	6.7700
6.7700	6.7900	6.8000	6.8000	6.8000	6.8000	6.8000
6.7900	6.7800	6.7400	6.7200	6.7500	6.7700	6.7700
6.7700	6.7700	6.7700	6.7600	6.7300	6.7200	6.7400
6.7400	6.7500	6.7500	6.7500	6.7500	6.7400	6.7300
6.7000	6.6700	6.7000	6.7200	6.7300	6.7300	6.7300
6.7300	6.7200	6.6900	6.6600	6.6800	6.6900	6.7100
6.7100	6.7000	6.7000	6.6900	6.6700	6.6300	6.6600
6.6700	6.6800	6.6800	6.6800	6.6800	6.6600	6.6300
6.6300	6.6500	6.6600	6.6500	6.6500	6.6600	6.6400
6.6400	6.6000	6.5800	6.6000	6.6200	6.6300	6.6300
6.6300	6.6300	6.6200	6.6100	6.5700	6.5900	6.6000
6.6100	6.6200	6.6200	6.6300	6.6300	6.6200	6.5800
6.5500	6.5600	6.6000	6.6100	6.6100	6.6200	6.6200
6.6200	6.6100	6.5800	6.5500	6.5600	6.5900	6.6000
6.6000	6.6000	6.6000	6.6000	6.5900	6.5500	6.5600
6.5600	6.5800	6.5900	6.6000	6.6000	6.6000	6.6000
6.6000	6.5900	6.5600	6.5600	6.5600	6.5800	6.5900
6.5900	6.5900	6.5800	6.5500	6.5500	6.5700	6.5800
6.5900	6.5900	6.5800	6.5800	6.5700	6.5500	6.5200
6.5200	6.5400	6.5400	6.5500	6.5600	6.5600	6.5500
6.5100	6.5200	6.5300	6.5500	6.5500	6.5500	6.5400
6.5500	6.5500	6.5500	6.5500	6.5500	6.5300	6.5000
6.4900	6.5000	6.5200	6.5200	6.5200	6.5100	6.5100
6.5000	6.4900	6.4600	6.4700	6.4900	6.4900	6.4900
6.4900	6.4900	6.4900	6.4800	6.4600	6.4200	6.4200
6.4500	6.4600	6.4600	6.4700	6.4600	6.4500	6.4300
6.4000	6.4100	6.4300	6.4400	6.4400	6.4400	6.4400
6.4400	6.4400	6.4700	6.3800	6.3900	6.4100	6.4100
6.4100	6.4100	6.4100	6.4000	6.4000	6.3800	6.3400
6.3300	6.3400	6.3600	6.3600	6.3600	6.3500	6.3500
6.3300	6.2800	6.2700	6.2900	6.3100	6.3200	6.3200
6.3100	6.3100	6.2800	6.2500	6.2400	6.2500	6.2600
6.2500	6.2400	6.2400	6.2300	6.2200	6.2000	6.1700
6.1600	6.1600					

Table A-11

RAW DATA ELEVATIONS IN FEET

LEFT LANE- SOFT SURFACE- ELEVATIONS, 15 INCH SPACING

241 POINTS

.5800	.5900	.6500	.5900	.6300	.6200	.6800
.7000	.7100	.6300	.6300	.6300	.6900	.6900
.7100	.7400	.6900	.7500	.6800	.7700	.8200
.7000	.8000	.8900	.7500	.7600	.7400	.7400
.7000	.7500	.8100	.6600	.7500	.7200	.7000
.6900	.6900	.6900	.7200	.7200	.8100	.7300
.7400	.7000	.6900	.7400	.7000	.7200	.7400
.7400	1.3000	.7000	.8000	.7600	.8200	.8700
.8700	.7600	.7300	.7100	.8800	.9200	.7600
1.1200	.8400	.8100	.8500	.8000	.8600	.9700
.7900	1.2900	.9500	.9500	.8800	1.0500	.9600
1.0100	.9300	.9700	.9300	1.0600	.9300	.8900
.9900	.9900	1.0800	1.0200	1.1300	1.0900	1.0600
1.2200	1.1000	1.2400	1.1200	1.2500	1.1800	1.1900
1.0500	1.1600	1.3200	1.2300	1.2100	1.1600	1.3100
1.1600	1.1900	1.3100	1.2300	1.3300	1.2200	1.3800
1.2300	1.3500	1.3800	1.3700	1.3800	1.3400	1.3300
1.3600	1.2900	1.3100	1.3800	1.3200	1.3200	1.4800
1.3600	1.3300	1.3500	1.3700	1.3800	1.4000	1.5300
1.4900	1.5000	1.5100	1.4900	1.5800	1.6100	1.5700
1.6100	1.6100	1.6500	1.6000	1.5700	1.5600	1.5700
1.5100	1.5200	1.4400	1.3800	1.4300	1.4000	1.4000
1.3600	1.3400	1.4100	1.3400	1.3700	1.3600	1.3500
1.3300	1.3200	1.3300	1.3800	1.4100	1.4100	1.3400
1.3300	.8600	.9500	.9700	1.2800	1.4300	1.3700
1.5100	1.3100	1.4700	1.3200	1.3100	1.1400	1.0700
1.2400	1.2100	1.3100	1.2400	1.5100	1.5300	1.4900
1.4700	1.4900	1.5400	1.4000	1.3900	1.5100	1.4800
1.3700	1.3500	1.3800	1.3900	1.4600	1.4100	1.4200
1.4200	1.3800	1.4600	1.3800	1.5700	1.7500	1.7900
1.8300	1.6900	1.8400	1.8300	2.0000	2.2100	2.3500
2.2000	2.0000	1.9100	2.1000	1.7400	1.6100	1.6000
1.3500	1.5000	1.3500	1.4500	1.1800	.9900	.9400
1.0800	1.4500	1.3700	1.3100	1.2300	1.3200	1.4000
1.2800	1.5300	1.6200				

Table A-12

RAW DATA ELEVATIONS IN FEET

SOFT SURFACE CENTER LANE 5 INCH SPACING

721 POINTS

.5500	.5500	.5400	.5200	.5700	.6450	.6700
.5900	.5900	.6200	.6400	.5900	.6200	.6200
.6700	.6000	.6150	.6300	.6000	.7000	.6200
.5800	.6100	.6350	.7200	.6400	.6200	.5900
.5700	.6000	.5800	.6000	.6600	.6700	.6300
.6400	.6400	.7800	.7300	.6600	.6700	.6550
.5800	.5700	.6300	.6500	.6700	.6300	.6700
.7100	.7000	.6600	.6800	.6800	.6600	.7000
.6600	.7300	.8100	.8300	.7900	.7200	.7500
.7200	.7000	.6700	.7700	.9300	.7000	.7500
.7200	.7400	.7300	.7500	.7200	.7200	.6800
.8100	.8300	.8200	.7400	.7000	.6700	.7100
.7400	1.0800	.7900	.7000	.6400	.6500	.6000
.8100	.7300	.8700	.7400	.6500	.6500	.7100
.7400	.7200	.7400	.7200	.6700	.7100	.7000
.7100	.6700	.8500	.7300	.7200	.7000	.7000
.6300	.6200	.6000	.5900	.6100	.6300	.6500
.5800	.5800	.5800	.6000	.7200	.7000	.7300
.7400	.7000	.6900	.6800	.6600	.7000	.7000
.7700	.7300	.7200	.7300	.7700	.7300	.7000
.6700	.6800	.6700	.7400	.7400	.8800	1.0000
.7400	.6500	.6800	.6900	.8400	.7400	.7100
.7300	.7000	.6400	.7000	1.0700	.9600	.8600
.8800	.7500	.7200	.7200	.8000	.7500	.7600
.7700	.8900	1.0200	.7300	.7900	.8100	.7200
.7500	.8500	.9600	.8900	.8900	.9400	1.0400
.8700	.9900	.8100	.8600	.8700	.8400	.9900
.8500	.8400	.8300	.8500	.8600	.7800	.8300
.8800	.8100	.8700	.8100	.8200	.8600	.8500
.9500	.9900	.7800	.7500	.8000	.8700	.8300
.8300	1.0500	1.2000	.8000	.9500	.9400	.9700
1.0200	.9100	.8400	.8800	.9700	.9800	.9300
.9300	.9700	.8400	.9000	.9000	.9600	.9100
1.0200	1.0500	1.2100	1.0900	.9850	.9600	1.0500
1.1000	1.2400	1.2600	.9200	.9900	1.1000	1.0600
1.0700	.9800	.9900	1.0500	1.0200	.9800	1.1000
1.0200	.9200	.9900	1.0200	1.1600	1.2900	1.3400
1.0800	1.1700	.9800	1.0000	1.2000	1.2300	1.0200
1.1300	1.2500	1.2100	1.1500	1.2500	1.2700	1.0800
1.1000	1.3000	1.2800	1.2700	1.1500	1.1500	.9600
1.2600	1.3000	1.2700	1.0300	1.2100	1.0700	1.1100
1.2000	1.1900	1.2700	1.2100	1.1400	1.1700	1.2200
1.3100	1.3000	1.1900	1.2600	1.2800	1.3300	1.3500
1.3500	1.2500	1.2300	1.2500	1.2500	1.3000	1.3100
1.2100	1.2800	1.2900	1.3200	1.2700	1.2500	1.2500
1.3500	1.3800	1.3400	1.3200	1.3100	1.3100	1.2300
1.2900	1.2800	1.4100	1.4100	1.2800	1.2400	1.3500
1.3300	1.3900	1.4300	1.4100	1.3200	1.2500	1.3400

Table A-12
(Continued)

RAW DATA ELEVATIONS IN FEET

1.4000	1.4100	1.3900	1.4500	1.4000	1.3700	1.4300
1.3600	1.3400	1.4200	1.4100	1.3400	1.3400	1.4500
1.4700	1.4200	1.4300	1.4700	1.4400	1.4000	1.4600
1.4800	1.4300	1.4800	1.5400	1.4100	1.4200	1.3900
1.4600	1.4300	1.4200	1.4000	1.4100	1.4100	1.3800
1.4000	1.3500	1.3600	1.4200	1.3800	1.4100	1.4000
1.3500	1.3600	1.4000	1.4000	1.3900	1.3900	1.4100
1.4100	1.3900	1.3900	1.3900	1.3900	1.4300	1.4200
1.3900	1.3900	1.3900	1.4300	1.4500	1.4300	1.4600
1.5300	1.5400	1.4900	1.5100	1.5300	1.5900	1.5300
1.6000	1.6000	1.6400	1.6300	1.6600	1.7200	1.7600
1.7100	1.7200	1.7500	1.7200	1.7000	1.7100	1.7100
1.6800	1.7000	1.7000	1.7000	1.7600	1.8000	1.7600
1.7200	1.7400	1.7200	1.7400	1.7400	1.7100	1.6800
1.7000	1.7500	1.7300	1.7000	1.7100	1.7000	1.7300
1.7500	1.7200	1.7100	1.7000	1.6500	1.6400	1.6400
1.6700	1.6100	1.6000	1.5800	1.6000	1.5800	1.5800
1.5600	1.5700	1.5600	1.5900	1.5800	1.5600	1.5500
1.5500	1.5400	1.5100	1.5100	1.5400	1.5600	1.5800
1.5600	1.4900	1.5400	1.5500	1.4900	1.5100	1.4800
1.4800	1.4600	1.4700	1.4700	1.4800	1.5000	1.5000
1.4900	1.4800	1.4300	1.4500	1.4600	1.4800	1.4700
1.4500	1.4400	1.4000	1.4100	1.4700	1.4800	1.4400
1.4700	1.4500	1.4200	1.4200	1.4300	1.4500	1.4800
1.4700	1.5300	1.5400	1.5400	1.5500	1.5100	1.4900
1.4700	1.4600	1.4100	1.2100	1.0400	.9500	.9500
.9900	.9500	.9900	1.0000	1.0700	1.1900	1.3200
1.4000	1.5400	1.5700	1.6000	1.5600	1.5000	1.5100
1.5500	1.5600	1.5300	1.4900	1.4700	1.5000	1.5400
1.5700	1.5800	1.6100	1.5500	1.4500	1.4100	1.3500
1.2700	1.1500	1.0100	1.0400	1.0100	1.2600	1.4000
1.3200	1.1700	1.1100	1.1400	1.2500	1.2900	1.2600
1.2800	1.3100	1.3700	1.3700	1.4000	1.4600	1.4900
1.5000	1.4600	1.5000	1.5200	1.5900	1.5700	1.5200
1.5100	1.4700	1.5000	1.5700	1.5600	1.5800	1.5800
1.6800	1.6800	1.7400	1.7600	1.6500	1.4200	1.3300
1.4200	1.4100	1.3300	1.2300	1.1100	1.1200	1.2000
1.3000	1.3400	1.4500	1.5000	1.4900	1.5000	1.5100
1.5800	1.5700	1.4500	1.4500	1.5200	1.6100	1.6100
1.6500	1.6200	1.5800	1.5400	1.5000	1.5700	1.4900
1.5600	1.5500	1.5500	1.5200	1.5100	1.4900	1.6100
1.6800	1.6900	1.6000	1.5500	1.6400	1.6700	1.7400
1.8000	1.9200	1.9800	2.0000	1.9800	1.9800	1.9700
1.9900	1.9700	1.9100	1.8500	1.8300	1.9000	1.9700
1.9900	1.9700	1.8900	1.9400	1.9900	2.0600	2.1300
2.1400	2.1300	2.1000	2.1200	2.2300	2.2800	2.2500
2.2500	2.2800	2.2600	2.1500	2.1300	2.0900	2.1000
2.0700	1.9500	1.8300	1.7800	1.7700	1.7900	1.8000
1.8200	1.8400	1.7500	1.7400	1.8000	1.8200	1.8100
1.5500	1.3800	1.3900	1.3600	1.3500	1.5300	1.6500
1.7000	1.7100	1.6900	1.6900	1.5800	1.4900	1.3900
1.3600	1.4300	1.5000	1.6100	1.6100	1.5700	1.5700
1.5000	1.3100	1.2500	1.3000	1.4500	1.5200	1.5300
1.4500	1.4700	1.4900	1.5000	1.4900	1.4200	1.2600
1.1200	1.1000	1.1000	1.1900	1.2400	1.4000	1.6100

Table A-13

RAW DATA ELEVATIONS IN FEET

RIGHT LANE -SOFT SOIL-ELEVATIONS, 15 INCH SPACING

241 POINTS

.5500	.6000	.6200	.5400	.6400	.6100	.6500
.6400	.5600	.7400	.6500	.7600	.7000	.6300
.6200	.7100	.7900	.6500	.6700	.6800	.6800
.6600	.6700	.7500	.7500	.7000	.7400	.6900
.7000	.6500	.6500	.6700	.6100	.7000	.6800
.6700	.7100	.6100	.6800	.6100	.6200	.6300
.6900	.6700	.6600	.6500	.6500	.8100	.8500
1.0200	.9000	.7300	.7600	.8000	.7100	.7800
.7600	.7200	.6700	.7100	.8900	.7600	.8000
.7600	.8400	.7500	.7900	.7900	1.1500	.7500
1.0300	.7900	.8100	1.0000	.8400	.9700	.9300
.9100	.8900	.9300	1.0100	.8900	.8800	1.0900
.9100	.9800	.9500	1.1200	1.0400	1.0100	1.0200
1.0300	1.1000	1.1200	1.0100	1.0500	1.1100	1.0600
1.0900	1.1700	1.1700	1.2200	1.2800	1.1300	1.2900
1.2400	1.2500	1.2500	1.2200	1.3100	1.2400	1.2700
1.3000	1.2800	1.3400	1.3200	1.3300	1.3200	1.4300
1.3600	1.4100	1.4900	1.4100	1.3400	1.3600	1.3300
1.3400	1.3400	1.4600	1.3000	1.2600	1.3200	1.2900
1.3700	1.3900	1.3900	1.4500	1.5000	1.5700	1.5500
1.5600	1.6300	1.6900	1.7100	1.7700	1.7300	1.7100
1.6900	1.6800	1.7000	1.6600	1.6200	1.6100	1.5200
1.5100	1.5800	1.5500	1.4800	1.4900	1.4600	1.5000
1.5100	1.5100	1.4400	1.4400	1.4100	1.4000	1.3900
1.4000	1.5400	1.4400	1.4200	1.4300	1.4300	1.2500
.8500	.8100	1.0500	1.3800	1.3800	1.3900	1.4500
1.4500	1.5400	1.1600	1.2100	1.3800	1.0300	.9500
1.1100	1.0400	1.2300	1.3500	1.4000	1.4400	1.5500
1.5300	1.6700	1.6400	1.1900	1.4600	1.4300	1.3200
1.4200	1.4900	1.5000	1.5900	1.5800	1.5800	1.7200
1.6000	1.6000	1.6700	1.7100	1.9500	1.9000	1.8500
1.8500	1.8800	2.0600	2.1000	2.2600	2.0800	1.9300
1.8500	1.7400	1.6700	1.6800	1.7600	1.3900	1.2700
1.5300	1.6100	1.5100	1.5400	1.3200	1.1300	1.2500
1.3200	1.4500	1.1900				

Table A-14 SOFT SURFACE CROSS SPECTRAL DENSITY

CO-LR	QUD-LR	CO-LT	QUD-LT	CO-RT	QUD-RT	FREQ
9.64E-01	1.06E-01	9.92E-01	-5.70E-04	9.86E-01	-1.11E-01	.0033
8.71E-01	4.21E-01	9.68E-01	1.95E-01	9.62E-01	-2.45E-01	.0067
8.27E-01	5.60E-01	9.42E-01	3.27E-01	9.65E-01	-2.58E-01	.0100
8.78E-01	3.88E-01	9.53E-01	2.97E-01	9.66E-01	-1.08E-01	.0133
9.44E-01	1.54E-01	9.66E-01	2.54E-01	9.63E-01	9.25E-02	.0167
9.19E-01	3.13E-01	9.54E-01	2.96E-01	9.81E-01	-2.62E-02	.0200
7.30E-01	5.91E-01	9.49E-01	3.09E-01	8.61E-01	-3.23E-01	.0233
3.78E-01	8.65E-01	9.42E-01	3.09E-01	6.18E-01	-6.93E-01	.0267
3.12E-01	9.34E-01	9.36E-01	4.04E-01	6.64E-01	-7.22E-01	.0300
3.64E-01	8.87E-01	8.57E-01	4.85E-01	7.79E-01	-6.14E-01	.0333
1.79E-02	9.33E-01	7.70E-01	6.14E-01	6.17E-01	-7.32E-01	.0367
-1.41E-02	7.80E-01	7.35E-01	2.98E-01	3.47E-01	-9.08E-01	.0400
3.76E-01	5.73E-01	7.38E-01	-3.36E-01	1.58E-01	-9.40E-01	.0433
-1.24E-01	5.81E-01	6.04E-01	-5.34E-02	-5.62E-02	-9.36E-01	.0467
-8.17E-01	2.41E-01	1.37E-01	6.99E-01	2.02E-02	-9.62E-01	.0500
-9.08E-01	2.47E-01	3.02E-01	8.20E-01	-9.10E-02	-9.75E-01	.0533
-7.65E-01	5.65E-01	6.94E-01	6.07E-01	-2.13E-01	-9.72E-01	.0567
-8.64E-01	4.68E-01	5.29E-01	7.65E-01	-1.01E-01	-9.88E-01	.0600
-9.33E-01	5.54E-02	1.39E-01	9.58E-01	-8.99E-02	-9.83E-01	.0633
-8.20E-01	-4.44E-01	-1.51E-02	9.85E-01	-4.11E-01	-8.16E-01	.0667
-7.34E-01	-5.46E-01	8.15E-02	9.82E-01	-5.67E-01	-6.42E-01	.0700
-8.72E-01	-2.58E-01	-5.75E-02	9.70E-01	-1.74E-01	-8.52E-01	.0733
-8.86E-01	-3.81E-01	-4.48E-01	8.17E-01	9.92E-02	-9.74E-01	.0767
-6.97E-01	-6.58E-01	-3.57E-01	4.13E-01	1.98E-01	-4.86E-01	.0800
-2.73E-01	-8.79E-01	1.95E-01	2.12E-01	-1.89E-01	2.51E-01	.0833
-6.54E-02	-9.17E-01	-1.29E-01	6.32E-01	-6.86E-01	-1.32E-01	.0867
-4.62E-01	-7.81E-01	-1.95E-01	9.44E-01	-7.33E-01	-6.46E-01	.0900
-5.92E-01	-7.46E-01	7.61E-04	9.82E-01	-7.72E-01	-6.06E-01	.0933
-4.27E-01	-5.48E-01	-1.46E-01	9.73E-01	-5.01E-01	-4.64E-01	.0967
-3.06E-01	2.50E-01	-3.34E-03	6.44E-01	2.91E-01	-6.16E-01	.1000
4.06E-01	5.96E-01	2.16E-01	9.82E-02	2.05E-01	-4.83E-01	.1033
5.95E-01	1.24E-01	-4.95E-01	2.10E-01	-2.89E-01	-6.10E-02	.1067
-1.85E-01	-3.84E-01	-7.14E-01	4.84E-01	-9.35E-02	-6.02E-01	.1100
-4.68E-01	-2.86E-01	-2.44E-01	8.29E-01	-1.05E-01	-6.69E-01	.1133
3.21E-01	-3.75E-01	5.37E-02	9.26E-01	-2.89E-01	1.49E-01	.1167
8.12E-01	-3.40E-01	2.20E-01	8.27E-01	-4.61E-02	5.11E-01	.1200
7.45E-01	-5.48E-01	-2.13E-01	4.69E-01	-3.70E-01	3.61E-02	.1233
8.11E-01	-5.22E-01	-6.49E-01	-2.25E-01	-4.70E-01	-5.24E-01	.1267
9.26E-01	-9.62E-02	-8.87E-01	-8.58E-02	-6.82E-01	-1.17E-01	.1300
9.19E-01	3.00E-01	-9.54E-01	2.03E-01	-7.80E-01	4.55E-01	.1333
8.29E-01	8.76E-02	-9.74E-01	2.60E-03	-7.34E-01	9.47E-02	.1367
6.93E-01	-2.91E-01	-9.36E-01	-2.77E-01	-6.13E-01	-5.07E-01	.1400
6.29E-01	2.73E-01	-8.30E-01	-5.24E-01	-7.58E-01	-1.68E-01	.1433
7.73E-02	5.35E-01	-8.44E-01	-4.29E-01	-4.11E-01	2.08E-01	.1467
-3.60E-01	-2.29E-01	-5.88E-01	-2.47E-01	5.08E-01	-9.28E-02	.1500
2.20E-01	-6.79E-01	-8.25E-02	-2.51E-01	5.05E-01	8.01E-02	.1533
4.65E-01	-2.05E-01	-2.38E-01	-4.53E-02	-4.68E-01	3.84E-01	.1567
6.14E-02	1.95E-01	-3.35E-01	-3.04E-01	-8.81E-01	2.55E-01	.1600
6.66E-02	-5.08E-02	-5.10E-01	-2.81E-01	-8.18E-01	4.08E-02	.1633
-1.35E-01	4.09E-01	-2.71E-01	-6.92E-01	-7.46E-01	2.20E-01	.1667
2.99E-01	6.24E-01	-5.91E-02	-5.40E-01	-6.77E-01	1.82E-01	.1700
6.98E-01	3.85E-01	-2.69E-01	2.03E-01	-4.63E-01	6.06E-01	.1733
5.82E-01	4.23E-01	-6.07E-01	1.91E-01	-5.69E-01	7.88E-01	.1767
4.35E-01	2.25E-01	-4.22E-01	1.52E-01	-7.45E-01	6.56E-01	.1800
1.34E-01	3.08E-01	-7.53E-02	-5.60E-01	-6.01E-01	1.95E-01	.1833
6.09E-01	1.31E-01	-1.32E-02	-5.37E-01	-1.89E-02	-2.11E-01	.1867
7.13E-01	-1.05E-01	2.47E-01	2.68E-01	2.84E-01	4.94E-01	.1900
1.72E-01	-6.90E-01	7.57E-01	2.32E-01	4.84E-02	9.52E-01	.1933
-9.55E-02	-5.50E-01	8.47E-01	3.79E-01	-7.89E-02	5.28E-01	.1967

Table A-14 (Continued)

-3.21E-01	4.55E-01	6.44E-01	7.34E-01	2.84E-01	-4.47E-01	.2000
-2.02E-01	6.27E-01	3.63E-01	8.67E-01	2.34E-01	-4.79E-01	.2033
5.34E-01	1.36E-02	1.83E-01	8.38E-01	-1.99E-02	5.33E-01	.2067
4.10E-01	-5.60E-01	4.01E-01	7.35E-01	-1.23E-01	5.89E-01	.2100
-1.83E-02	-5.22E-01	6.28E-02	4.70E-01	-4.76E-01	-3.48E-01	.2133
5.99E-01	-1.10E-01	-3.57E-01	9.10E-03	-5.51E-01	-3.62E-01	.2167
7.28E-01	-2.10E-01	-2.23E-01	1.09E-01	-4.79E-02	4.13E-01	.2200
-7.94E-02	-4.47E-01	-1.27E-01	-4.99E-01	5.20E-01	6.00E-01	.2233
-3.86E-01	1.47E-01	-4.18E-01	-4.75E-01	4.04E-01	8.13E-01	.2267
2.19E-01	2.66E-01	-2.05E-01	2.99E-01	2.19E-01	9.75E-01	.2300
3.13E-01	-5.76E-01	3.87E-01	4.59E-02	3.63E-01	7.39E-01	.2333
-1.58E-01	-7.00E-01	3.09E-01	-6.93E-01	3.98E-01	3.35E-01	.2367
-5.03E-01	1.39E-01	3.27E-01	-9.03E-01	-3.99E-01	2.71E-01	.2400
-3.85E-01	5.05E-01	3.10E-01	-9.38E-01	-6.74E-01	2.28E-01	.2433
-7.03E-01	-1.61E-02	4.48E-01	-6.91E-01	-4.09E-01	4.58E-01	.2467
-9.55E-01	-2.57E-01	3.82E-01	-1.67E-01	-2.96E-01	1.48E-01	.2500
-9.44E-01	-2.98E-01	-6.95E-02	-8.49E-02	7.46E-02	-7.58E-02	.2533
-7.96E-01	-4.19E-01	2.52E-01	1.59E-01	-5.02E-01	-5.48E-02	.2567
-5.30E-01	-7.20E-01	2.09E-01	3.25E-01	-6.60E-01	-8.17E-04	.2600
-2.98E-01	-4.19E-01	6.74E-02	-3.76E-01	-3.55E-01	4.39E-01	.2633
1.59E-01	9.44E-03	-4.99E-02	-5.78E-01	-5.19E-01	5.06E-01	.2667
-1.55E-01	-4.59E-01	3.83E-01	-4.59E-04	-3.71E-01	3.60E-01	.2700
-5.87E-01	-2.25E-01	5.05E-02	4.78E-01	-2.56E-01	-9.79E-03	.2733
-3.59E-01	6.59E-01	-3.77E-01	-1.78E-02	-2.58E-01	2.26E-01	.2767
-3.35E-01	8.48E-01	-1.35E-01	-4.48E-01	-2.31E-01	4.40E-02	.2800
-3.01E-01	4.01E-01	-1.92E-01	-6.23E-02	4.99E-01	1.97E-01	.2833
2.34E-01	-2.07E-01	3.67E-01	4.39E-01	4.39E-01	3.93E-01	.2867
1.90E-01	-6.93E-01	6.85E-01	5.67E-01	-1.72E-01	3.22E-01	.2900
5.10E-01	-6.88E-01	4.19E-01	2.27E-01	-4.27E-02	3.10E-01	.2933
4.89E-01	-5.71E-01	-2.42E-01	3.16E-01	-5.46E-01	-1.12E-01	.2967
-2.69E-01	-7.02E-01	-2.10E-01	3.71E-01	-4.64E-01	-3.50E-01	.3000
-5.16E-01	-8.48E-01	-4.01E-01	-8.83E-02	3.02E-01	-3.94E-01	.3033
-4.45E-01	-8.88E-01	-7.61E-01	1.78E-01	1.86E-01	-7.84E-01	.3067
-1.50E-01	-9.15E-01	-5.40E-01	3.58E-01	7.60E-03	-5.35E-01	.3100
1.82E-01	-9.18E-01	3.08E-01	1.95E-01	9.97E-02	4.56E-01	.3133
-1.80E-02	-5.16E-01	6.72E-01	-1.56E-01	4.24E-01	3.67E-01	.3167
-4.11E-01	2.21E-01	3.59E-01	4.23E-02	5.62E-01	-3.45E-01	.3200
-3.60E-01	3.23E-02	-9.44E-02	-1.11E-01	8.37E-01	-2.03E-01	.3233
3.35E-01	8.43E-02	4.69E-01	-4.40E-02	9.46E-01	-1.78E-01	.3267
2.18E-01	2.81E-01	6.76E-01	5.49E-01	4.20E-01	-3.42E-01	.3300
-9.61E-02	-6.39E-02	2.14E-01	4.82E-01	-5.62E-01	6.42E-03	.3333
-1.59E-01	1.41E-01	-4.46E-01	-1.93E-01	-5.90E-01	7.29E-02	.3367
-1.31E-01	-6.54E-02	-5.93E-01	1.25E-01	2.36E-01	-2.00E-01	.3400
5.46E-01	1.23E-01	5.35E-02	7.50E-01	6.57E-01	3.48E-01	.3433
8.71E-01	3.62E-01	5.90E-01	7.26E-01	6.97E-01	4.23E-01	.3467
3.57E-01	3.33E-01	4.89E-01	4.89E-01	6.13E-01	-3.92E-01	.3500
-9.26E-02	-4.77E-02	-8.05E-02	6.56E-01	4.21E-01	-4.92E-01	.3533
2.39E-01	2.44E-01	2.25E-01	5.60E-01	1.93E-01	5.79E-02	.3567
-1.78E-01	4.48E-01	4.98E-01	1.82E-01	-3.47E-01	-3.80E-01	.3600
-7.22E-01	7.70E-02	1.40E-01	6.34E-01	-2.53E-01	-8.73E-01	.3633
-8.40E-01	2.40E-01	3.00E-01	8.60E-01	-5.00E-02	-8.50E-01	.3667
-9.39E-01	2.35E-01	4.61E-01	7.23E-01	-2.36E-01	-7.23E-01	.3700
-9.66E-01	5.01E-02	1.90E-01	4.64E-01	1.41E-02	-3.80E-01	.3733
-9.43E-01	-2.16E-01	7.45E-02	-2.73E-01	1.78E-01	3.45E-01	.3767
-8.70E-01	-4.12E-01	-1.52E-01	-4.94E-01	4.42E-01	5.17E-01	.3800
-6.95E-01	-6.65E-01	4.79E-01	-3.86E-01	4.16E-02	7.54E-01	.3833
-3.74E-01	-7.87E-01	8.74E-01	1.14E-02	-4.22E-01	8.81E-01	.3867
2.79E-01	-8.08E-01	5.50E-01	6.38E-01	-5.10E-01	8.36E-01	.3900
2.43E-01	-6.19E-01	3.34E-01	8.26E-01	-7.11E-01	4.70E-01	.3933
-6.18E-01	-2.08E-01	2.80E-01	5.88E-01	-4.76E-01	-1.79E-01	.3967
-8.63E-01	1.96E-01	-3.84E-01	5.70E-01	4.81E-01	-3.28E-01	.4000

Table A-15 HARD SURFACE CROSS SPECTRAL DENSITY

CO-LR	QUD-LR	CO-LT	QUD-LT	CO-RT	QUD-RT	FREQ
9.84E-01	1.32E-01	9.90E-01	9.97E-02	9.99E-01	-3.32E-02	.0033
9.62E-01	1.62E-01	9.76E-01	1.32E-01	9.98E-01	-3.14E-02	.0067
9.62E-01	-9.76E-02	9.85E-01	1.60E-02	9.75E-01	1.11E-01	.0100
7.39E-01	-7.65E-04	7.84E-01	2.52E-01	9.44E-01	2.38E-01	.0133
4.24E-01	3.34E-01	4.90E-01	6.33E-01	8.90E-01	2.54E-01	.0167
6.73E-01	2.01E-02	7.39E-01	4.97E-01	7.97E-01	4.25E-01	.0200
9.08E-01	1.59E-01	9.36E-01	2.94E-01	8.92E-01	1.21E-01	.0233
9.32E-01	3.63E-01	9.53E-01	-2.77E-02	8.80E-01	-3.73E-01	.0267
8.97E-01	1.21E-01	9.31E-01	-3.25E-01	7.96E-01	-4.01E-01	.0300
8.58E-01	-2.49E-01	9.47E-01	-2.95E-01	8.87E-01	-9.22E-03	.0333
4.86E-01	-1.28E-01	9.83E-01	-8.63E-02	5.16E-01	-1.78E-02	.0367
-7.70E-02	-5.53E-02	9.35E-01	2.13E-01	-1.47E-01	1.03E-01	.0400
5.13E-01	5.95E-02	8.29E-01	2.73E-01	2.76E-01	1.68E-01	.0433
9.07E-01	3.57E-01	7.84E-01	-3.02E-01	4.88E-01	-5.32E-01	.0467
8.23E-01	1.86E-01	6.72E-01	-3.35E-01	1.60E-01	-5.08E-01	.0500
7.40E-01	-1.93E-01	6.48E-01	1.85E-01	8.19E-03	9.77E-02	.0533
7.99E-01	2.26E-01	8.38E-01	2.27E-02	4.48E-01	-3.07E-01	.0567
6.06E-01	1.92E-01	9.20E-01	-1.05E-01	7.37E-01	-1.69E-01	.0600
-1.28E-01	-3.50E-01	8.17E-01	-4.33E-01	2.60E-01	5.34E-01	.0633
-6.28E-01	1.20E-01	7.83E-01	-5.13E-01	-3.94E-01	2.80E-01	.0667
-3.63E-01	3.44E-01	7.99E-01	-3.32E-01	-8.81E-02	-3.04E-01	.0700
-2.50E-01	-4.30E-01	6.59E-01	-5.99E-01	3.45E-01	2.14E-01	.0733
-2.41E-01	-5.35E-01	7.65E-01	-4.65E-01	1.85E-01	6.84E-01	.0767
9.90E-02	-2.05E-01	5.16E-01	-1.25E-01	5.80E-01	5.68E-01	.0800
-8.47E-02	-4.20E-02	-4.87E-02	-9.54E-02	8.24E-01	5.58E-01	.0833
5.38E-01	-4.91E-02	4.58E-01	1.24E-01	8.13E-01	4.25E-01	.0867
8.35E-01	-2.63E-01	7.08E-01	-2.67E-01	9.13E-01	-5.50E-02	.0900
3.31E-01	-3.03E-01	4.73E-01	-6.50E-01	6.55E-01	-4.06E-01	.0933
-3.99E-02	7.53E-02	4.45E-01	-5.24E-01	2.09E-01	-6.71E-01	.0967
-4.47E-02	-8.80E-02	-2.24E-01	-6.00E-01	3.36E-01	-2.65E-01	.1000
-2.63E-01	1.67E-01	-7.82E-01	-2.35E-01	1.64E-01	1.90E-01	.1033
-4.60E-01	1.38E-01	-4.03E-01	2.14E-01	3.88E-02	-5.24E-01	.1067
-4.04E-02	1.96E-01	4.15E-01	-2.20E-01	1.71E-01	-7.86E-01	.1100
4.62E-01	-3.56E-01	5.45E-01	-7.44E-01	7.04E-01	-3.81E-01	.1133
4.48E-01	-2.57E-01	5.72E-01	-4.12E-01	8.12E-01	-4.36E-01	.1167
-1.19E-01	5.60E-01	6.76E-01	2.31E-01	3.41E-01	-8.10E-01	.1200
-1.32E-02	9.17E-01	8.45E-01	-6.06E-02	-4.85E-02	-9.69E-01	.1233
3.12E-01	9.15E-01	9.10E-01	-2.72E-01	4.18E-02	-9.78E-01	.1267
3.60E-01	8.66E-01	7.51E-01	2.53E-01	3.55E-01	-5.69E-01	.1300
6.90E-01	5.59E-01	4.11E-01	7.95E-01	5.80E-01	3.67E-01	.1333
5.42E-01	3.41E-02	4.60E-01	5.32E-01	4.29E-01	8.44E-01	.1367
-8.10E-02	-1.12E-01	7.19E-01	-1.60E-01	2.03E-01	5.48E-01	.1400
-5.23E-02	1.49E-01	7.89E-01	-3.10E-01	4.04E-01	1.76E-02	.1433
-2.06E-01	2.19E-02	5.82E-01	-6.52E-01	2.03E-01	1.51E-01	.1467
-1.73E-02	1.41E-01	3.38E-01	-4.28E-01	-5.18E-01	-1.89E-01	.1500
-1.13E-02	-1.53E-01	1.78E-01	2.50E-01	-9.19E-01	-2.80E-01	.1533
-4.67E-01	-9.51E-02	3.78E-01	-1.83E-01	-5.14E-01	-1.48E-01	.1567
-4.07E-01	-1.13E-01	3.10E-01	-6.34E-01	2.86E-01	-1.95E-01	.1600
-6.19E-02	5.62E-01	6.39E-01	-1.42E-01	3.39E-01	-6.41E-01	.1633
-1.57E-01	8.73E-01	3.80E-01	3.23E-01	5.75E-01	-4.56E-01	.1667
-3.05E-01	6.41E-01	-1.85E-01	-2.44E-02	6.64E-01	-8.18E-02	.1700
3.50E-01	6.37E-01	3.61E-01	-5.09E-01	2.83E-01	-6.37E-01	.1733
3.57E-01	5.54E-01	3.10E-01	-4.77E-01	2.69E-01	-7.90E-01	.1767
-4.96E-01	4.39E-01	-1.78E-01	1.24E-01	5.15E-01	-5.13E-01	.1800
-7.98E-01	4.06E-01	3.50E-01	5.74E-01	6.48E-03	-7.18E-01	.1833
-5.47E-01	2.36E-01	3.85E-01	7.96E-01	-2.91E-01	-4.07E-01	.1867
-1.26E-01	2.78E-01	-3.27E-01	6.95E-01	3.19E-01	1.71E-01	.1900
-5.35E-01	3.34E-02	-8.53E-01	1.60E-01	7.32E-01	7.11E-02	.1933
-6.13E-01	-6.55E-02	-6.27E-01	-3.48E-01	7.71E-01	3.53E-01	.1967

Table A-15 (Continued)

-2.87E-01	-5.22E-01	2.80E-01	-4.63E-01	4.38E-01	4.00E-01	.2000
-6.30E-01	-3.85E-01	5.60E-01	1.75E-01	-1.45E-01	3.27E-02	.2033
-4.57E-01	9.62E-02	2.69E-01	5.94E-01	3.88E-01	-2.74E-01	.2067
1.02E-01	6.41E-02	5.68E-01	4.65E-01	6.21E-01	-2.58E-01	.2100
-9.20E-02	1.46E-01	6.33E-01	3.26E-01	1.36E-01	-6.79E-01	.2133
4.63E-01	3.74E-01	3.25E-01	-1.70E-02	9.35E-02	-4.99E-01	.2167
4.30E-01	3.92E-01	-7.37E-02	4.58E-01	-6.62E-02	1.17E-01	.2200
-4.66E-01	-6.56E-02	-1.22E-01	6.85E-01	-1.67E-01	-4.61E-01	.2233
-7.06E-01	-3.52E-01	-2.95E-01	4.48E-01	8.92E-02	-9.25E-01	.2267
-4.24E-01	2.23E-01	2.07E-01	2.62E-01	-2.68E-02	-9.69E-01	.2300
2.59E-01	7.05E-01	6.26E-01	-3.58E-01	-1.62E-01	-9.83E-01	.2333
1.44E-01	8.02E-01	7.80E-01	-2.13E-01	-1.03E-01	-9.91E-01	.2367
-2.62E-01	3.21E-01	8.04E-01	2.59E-01	7.51E-02	-6.00E-01	.2400
5.10E-02	-1.13E-01	9.07E-01	2.59E-02	3.18E-01	-7.05E-02	.2433
6.53E-02	5.67E-01	9.91E-01	-4.93E-02	1.24E-01	-6.01E-01	.2467
1.27E-02	9.98E-01	9.97E-01	1.24E-02	2.50E-02	-9.95E-01	.2500
-1.68E-01	8.35E-01	9.07E-01	1.41E-01	-7.16E-02	-9.84E-01	.2533
-5.38E-01	6.12E-01	7.88E-01	4.11E-01	-2.30E-01	-9.62E-01	.2567
-3.09E-01	8.28E-01	9.10E-01	2.04E-01	-1.49E-01	-9.80E-01	.2600
-2.36E-02	9.96E-01	1.00E-00	1.47E-02	-9.03E-03	-9.97E-01	.2633
-2.14E-01	8.13E-01	7.02E-01	-2.14E-01	4.30E-02	-5.41E-01	.2667
-6.30E-01	5.38E-01	2.90E-01	-4.45E-01	2.83E-02	7.95E-02	.2700
-2.59E-01	6.25E-01	6.76E-01	-7.20E-02	1.43E-01	-4.18E-01	.2733
2.86E-01	6.45E-01	9.47E-01	1.63E-01	4.72E-01	-7.19E-01	.2767
-2.47E-01	5.27E-01	5.18E-01	4.61E-01	3.94E-01	-8.50E-01	.2800
-8.32E-01	-2.20E-02	4.08E-02	6.06E-01	5.81E-02	-6.90E-01	.2833
-9.22E-01	-1.66E-01	5.51E-01	4.68E-01	-5.52E-01	-3.64E-01	.2867
-8.00E-01	-4.35E-02	9.05E-01	3.06E-01	-5.77E-01	-2.24E-01	.2900
-5.95E-01	-1.81E-01	9.04E-01	-1.40E-01	-4.95E-01	2.60E-01	.2933
-6.44E-01	1.80E-01	4.49E-01	-2.66E-01	-4.29E-01	-9.24E-02	.2967
-8.83E-01	1.83E-02	-4.82E-02	1.62E-01	-8.35E-02	-4.42E-01	.3000
-8.89E-01	5.34E-02	1.63E-01	2.33E-02	-3.93E-01	9.74E-02	.3033
-7.53E-01	3.30E-01	-1.86E-02	-1.69E-01	-4.73E-01	4.81E-01	.3067
-8.69E-01	8.49E-03	4.42E-01	9.05E-02	-7.29E-01	1.58E-01	.3100
-6.55E-01	1.43E-01	5.49E-01	9.49E-02	-5.65E-01	3.51E-01	.3133
2.28E-01	5.51E-01	1.74E-01	3.10E-01	3.13E-01	4.22E-01	.3167
4.37E-01	2.08E-01	3.11E-01	2.67E-01	5.65E-01	-3.12E-01	.3200
-3.15E-01	-5.55E-02	1.44E-01	5.84E-01	1.79E-01	-8.66E-01	.3233
-2.09E-01	2.71E-01	3.87E-01	3.80E-01	2.94E-01	-8.99E-01	.3267
2.59E-01	-1.48E-01	1.89E-01	-2.56E-01	5.56E-01	-8.01E-01	.3300
-3.34E-01	-5.96E-01	-3.24E-01	1.54E-01	2.10E-01	-7.96E-01	.3333
-8.55E-01	-4.12E-01	3.89E-02	7.84E-01	-3.58E-01	-7.78E-01	.3367
-5.18E-01	-2.14E-02	4.32E-01	7.52E-01	-2.93E-02	-7.18E-01	.3400
4.80E-01	2.73E-01	7.48E-01	4.19E-01	7.27E-01	-2.85E-01	.3433
7.30E-01	5.95E-01	7.73E-01	5.58E-01	9.68E-01	-6.43E-02	.3467
3.22E-01	8.76E-01	7.73E-01	5.84E-01	7.15E-01	-4.37E-01	.3500
2.11E-01	7.26E-01	4.80E-01	1.78E-01	7.19E-03	-7.45E-01	.3533
3.11E-01	3.08E-01	-5.00E-02	-1.20E-01	-6.46E-01	-6.32E-01	.3567
-2.16E-01	6.37E-02	4.90E-01	1.47E-01	-7.56E-01	-3.12E-01	.3600
9.43E-03	-3.17E-01	6.75E-01	1.73E-01	-5.84E-01	5.85E-04	.3633
2.84E-01	7.63E-02	4.64E-01	-2.26E-01	-3.54E-01	-5.75E-01	.3667
-2.15E-01	9.83E-02	4.45E-01	3.45E-01	-5.00E-01	-6.78E-01	.3700
-8.40E-02	-6.52E-01	2.66E-01	8.61E-01	-8.21E-01	8.56E-03	.3733
8.53E-02	-9.81E-01	2.32E-01	4.34E-01	-4.89E-01	2.03E-01	.3767
1.06E-01	-9.75E-01	-1.04E-01	-1.01E-01	2.25E-02	-2.82E-01	.3800
1.28E-01	-5.69E-01	-4.36E-01	3.24E-01	-4.47E-01	-1.40E-01	.3833
5.14E-01	2.27E-01	-7.51E-01	8.67E-02	-6.77E-01	2.19E-01	.3867
5.23E-01	4.02E-01	-3.79E-01	-3.26E-01	-6.31E-01	-3.72E-01	.3900
1.08E-01	4.22E-01	5.63E-01	-1.63E-01	-2.19E-01	-7.48E-01	.3933
1.60E-01	1.62E-01	9.06E-01	-2.93E-01	1.42E-01	-4.09E-01	.3967
-1.64E-01	-1.83E-01	4.85E-01	-2.62E-01	-4.72E-01	-1.35E-01	.4000

APPENDIX B

SOIL MEASUREMENTS AND ANALYSIS

B.1 INTRODUCTION

In Reference 1 a model representation of yielding surface (soil) behavior under the dynamic action of the passage of a vehicle was formulated. This model plus data describing vehicle structural characteristics enables a theoretical computation to be made of vehicle motions induced by rough terrain. The theoretical vehicle response is necessarily dependent upon advanced knowledge of the undisturbed surface roughness along the intended track. In addition, use of the model requires information defining certain surface (soil) properties and the nature of the vehicle-surface contact.

The subject investigation is concerned with predicting the dynamics of two test vehicles (truck and trailer) and making comparisons with vehicle runs conducted over a surveyed course. The model which is applied (theoretical calculations) is based partly on direct field measurements of surface layer characteristics and partly on best estimates of other surface physical descriptive constants. Investigations performed by the U.S. Army Engineer Waterways Experiment Station, which determined the detail of tire deformations in soil, also were influential in forming the model. (12)(13)(14)

B.2 SURFACE MODEL

It was postulated⁽¹⁾ that the dynamic soil reaction force acting on a vehicle wheel opposing its sinkage may be expressed by Equation (B-1).

$$R_s = \theta_1(z) + \theta_2(\dot{z}) + \theta_3(\ddot{z}) \quad (B-1)$$

R_s is the soil reaction force. $\theta_1(z)$, $\theta_2(\dot{z})$, and $\theta_3(\ddot{z})$ are functions dependent, respectively, upon soil penetration (z) by the wheel, rate of

change of soil penetration (\dot{z}), and rate of change of soil penetration rate (\ddot{z}). $\phi_1(z)$, as formulated, is time independent and, therefore, is considered identically equal to soil reaction to static load.

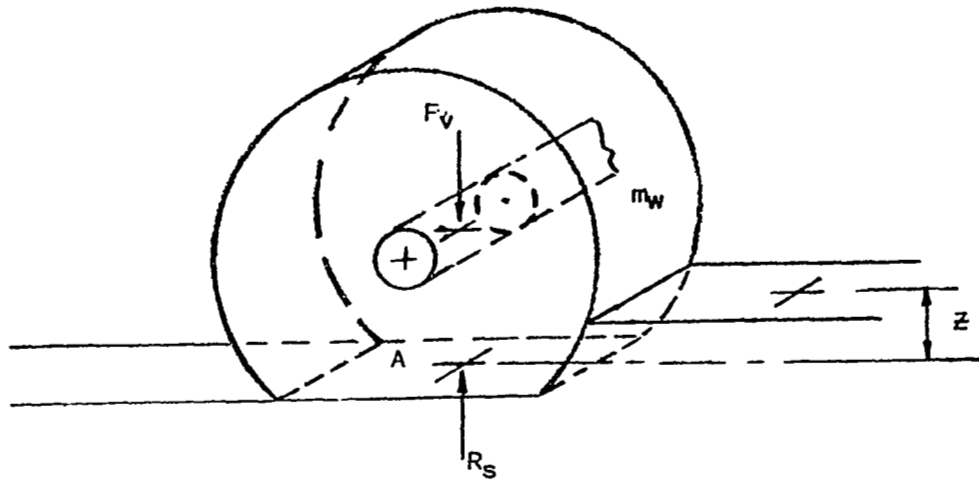


Figure B-1 WHEEL-SOIL INTERACTION

The contact interface between wheel and soil is considered to be a flat plate area "A". From Figure B-1, the equation* determining wheel motion on a yielding surface is:

$$m_w \ddot{z} + \phi_1(z) + \phi_2(\dot{z}) + \phi_3(\ddot{z}) = F_v \quad (B-2)$$

where m_w is wheel mass, and F_v is the dynamic force imparted by the vehicle body to the wheel.

*wheel flexing ignored (here) for simplicity.

Explicit expressions may be obtained for $\phi_2(\dot{z})$ and $\phi_3(\ddot{z})$ if the elastic properties of the surface layer are considered influential. This approach is suggested by the theory for vibrating foundations supported by soils. (1)(15)(16)(17)(18) If an analogy between a dynamically loaded footing and a dynamically loaded wheel is accepted, $\phi_2(\dot{z})$ is a damping action opposing wheel penetration associated with the propagation of stress waves throughout the soil; $\phi_3(\ddot{z})$ is a retardation to wheel penetration caused by the inertia of soil in proximity to wheel-soil contact area.

$$\phi_2(\dot{z}) = \frac{A}{\pi} b_0 \sqrt{\frac{E\rho}{2(1+U)}} \dot{z} \quad (B-3)$$

$$\phi_3(\ddot{z}) = c_1 \rho \left[\frac{A}{\pi} \right]^{\frac{3}{2}} \ddot{z} \quad (B-4)$$

<u>Soil Properties</u>	<u>Footing Characteristic</u>	<u>Elastic Theory Coefficients</u>
ρ , mass density	A , contact area	b_0 , soil damping
E , Youngs Modulus		c_1 , soil effective mass
U , Poissons Ratio		

With respect to $\phi_1(z)$, it was proposed in Reference 1 that a definition be obtained from standard plate penetrometer tests (static loading) of soil. Techniques for correlation of plate-sinkage versus static load occur frequently in the literature. (19)(20)(21)

For the purpose of the subject study, it was considered appropriate and expedient to obtain the form of $\phi_1(z)$ directly using the simple test vehicle (trailer) plus ballast weights at the test site rather than indirectly using penetrating plates. A remarkably simple expression for $\phi_1(z)$ representing stiffness of the field course surface layer was determined from the mean data

of several sampling measurements (Equation B-5).

$$\theta_j(z) = kz \quad (B-5)$$

B.3 LOAD SINKAGE MEASUREMENTS

The layout of the yielding surface test course, located at the northeast corner of the Chrysler Chelsea (Michigan) Proving Ground, is shown in Figure B-2. The actual course was 300 ft. in length and divided into six 50 ft. segments. On November 7, 1967, surface layer stiffness measurements were conducted with the single wheel test trailer plus ballast weights within each zone at offsets approximately 10 ft. south of the track centerline. On November 8, 1967, dynamic test runs were conducted with truck and trailer over the track. Table B-1 presents average cone index readings* taken each day within the six zones both inside the track and at the locations of the surface stiffness tests. Each reading tabulated is the mean of 5 probes randomly spaced. The readings indicate small surface property change within any one zone and small change over 24 hours. However, a gradient increase in resistance to probe penetration (a 1.6 factor) is indicated in the run direction (west to east) from end to end of the course.

The surface layer stiffness tests were a measurement of trailer hub movement versus load. The technique is given in Figure B-3. Tire sinkage was not a direct observation because of tire deflection in the soil. Grid lines traverse to the rolling wheel, spaced approximately 18 inches apart, were marked on the undeformed surface. The wheel path was projected and surface elevations

*Cone Index Reading - the average pressure (psi) required to maintain movement of a cone shaped probe (30 degrees total apex angle - 1/2 square inch base area) normal to soil surface through the layer from zero to 6 inches depth.

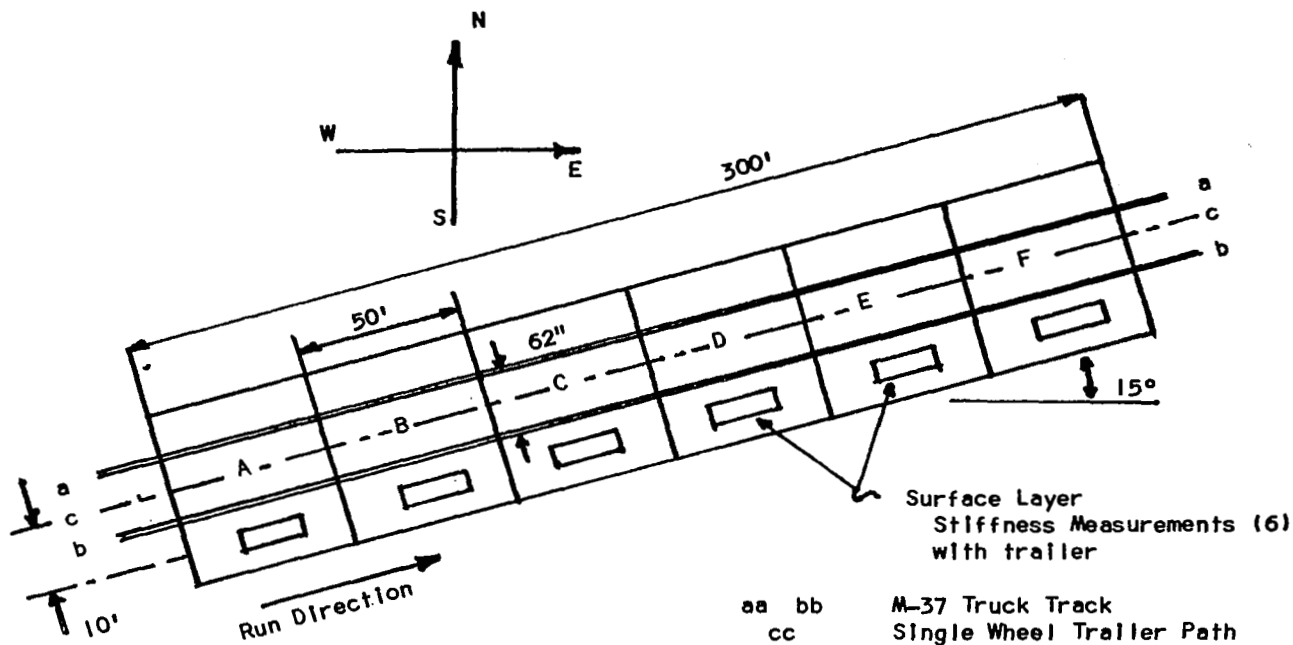
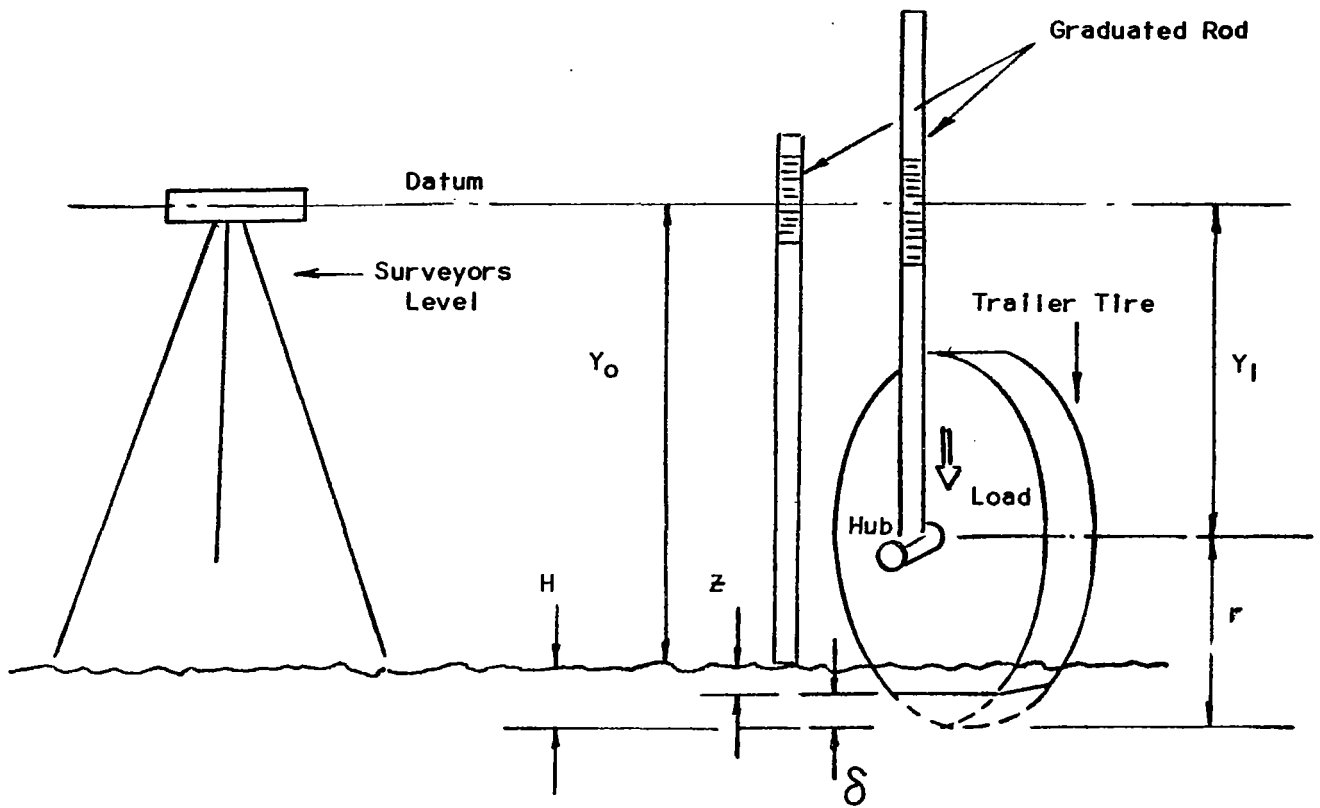


Figure B-2 YIELDING SURFACE TEST COURSE
CHELSEA, MICHIGAN

Table B-1			
CONE INDEX READINGS (psi)			
YIELDING SURFACE TEST COURSE			
(Average to 6 Inches Depth)			
ZONE	November 7, 1967 Within Track	November 8, 1967 Within Track	November 7, 1967 10 ft. South of Track
A	44	48	47
B	44	46	51
C	61		55
D	69	75	62
E	69		72
F	73	77	76
Average	60	61	60
Dates: November 8, 1967 November 7, 1967		Dynamic Test Runs with Vehicles Surface Layer Stiffness Measurements (with trailer plus ballast weights)	



$$H = Y_1 + r - Y_0$$

H = hub movement under static load

Y_1 = hub center location from level datum

Y_0 = undeformed surface location from level datum

r = tire radius (undeflected)

δ = tire deflection

z = tire sinkage in soil

Figure B-3 DETERMINATION OF HUB MOVEMENT - TRAILER
(Surface Layer Stiffness Measurement)

noted at the grid intersections. The wheel, under a prescribed load, was rolled to, and centered on an intersection. The elevation of the wheel hub center was recorded. The difference between undeflected tire radius and hub location above surface is called hub movement.

A tire sinkage (Z) was calculated by subtracting tire deflection (δ) obtained on a non-yielding surface** from hub movement (H).

$$Z = H - \delta \quad (B-6)$$

This procedure is based on fundamental behavior of pneumatic tires. Consider Figure B-4.

A) TIRE AT REST
Non-Yielding Surface

B) TIRE AT REST
Yielding Surface

C) ROLLING TIRE
Yielding Surface

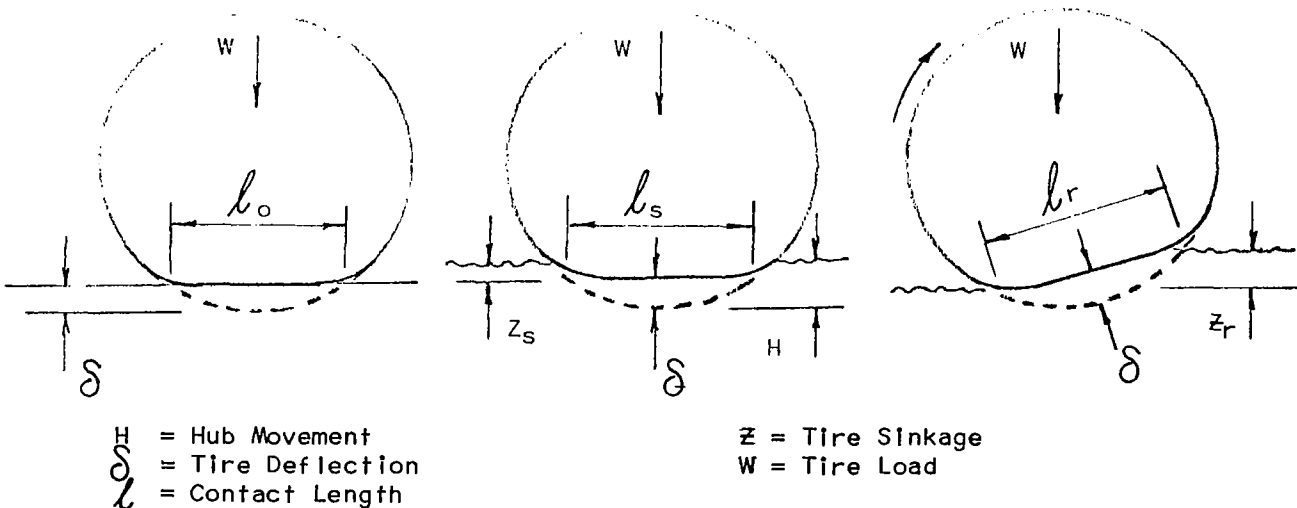


Figure B-4 DEFORMATION OF A PNEUMATIC TIRE

**Standard tire information furnished by manufacturer.

For constant load and pneumatic pressure, it is suspected that tire deformations for all three conditions cited are nearly equal since surface contact pressures are nearly equal. In order to check this expectation, the lengths of lines of contact (ℓ) for rolling tires on soft soil and stationary tires on non-yielding surfaces were calculated from Table I information of Reference 14. The comparison, shown in Figure B-5, indicates equal contact occurred, within $\pm 5\%$, for the bulk of the data; the data describes various tires at different internal pressures and loads. It is concluded that the primary effect of "rolling-yielding surface" versus "at rest-yielding surface" is inclination of contact - see Figure B-4. Although tire deformations (δ) may be considered approximately the same, tire sinkages are unequal ($z_r \neq z_s$). Figure B-6 presents expressions for "at rest" sinkage (z_s) and "rolling" sinkage (z_r) related to hub movement (H) for the trailer test vehicle; H is a field site measurement. z_r is determined from the constraint that lines of contact (ℓ) for "at rest" and "rolling" conditions are equal.

The foregoing discussion poses the question: What sinkage (z_s , z_r) should be applied to vehicle dynamics computation? The model requires that soil reaction be related to tire position below soil surface and its time derivatives. The " θ " terms of Equation (B-1) are derived from a concept of constant depth contact. Therefore, z_r appears inappropriate. From Figure B-6 it may be seen that z_s is always a representative mean depth for rolling contact; hence, for simplicity, sinkage as determined by Equation (B-6) has been selected.

A summary of surface layer stiffness measurements (hub movement - H) obtained with the trailer test vehicle at six field site locations (zones) is presented in Figure B-7. The actual measurements are given in Table B-2.

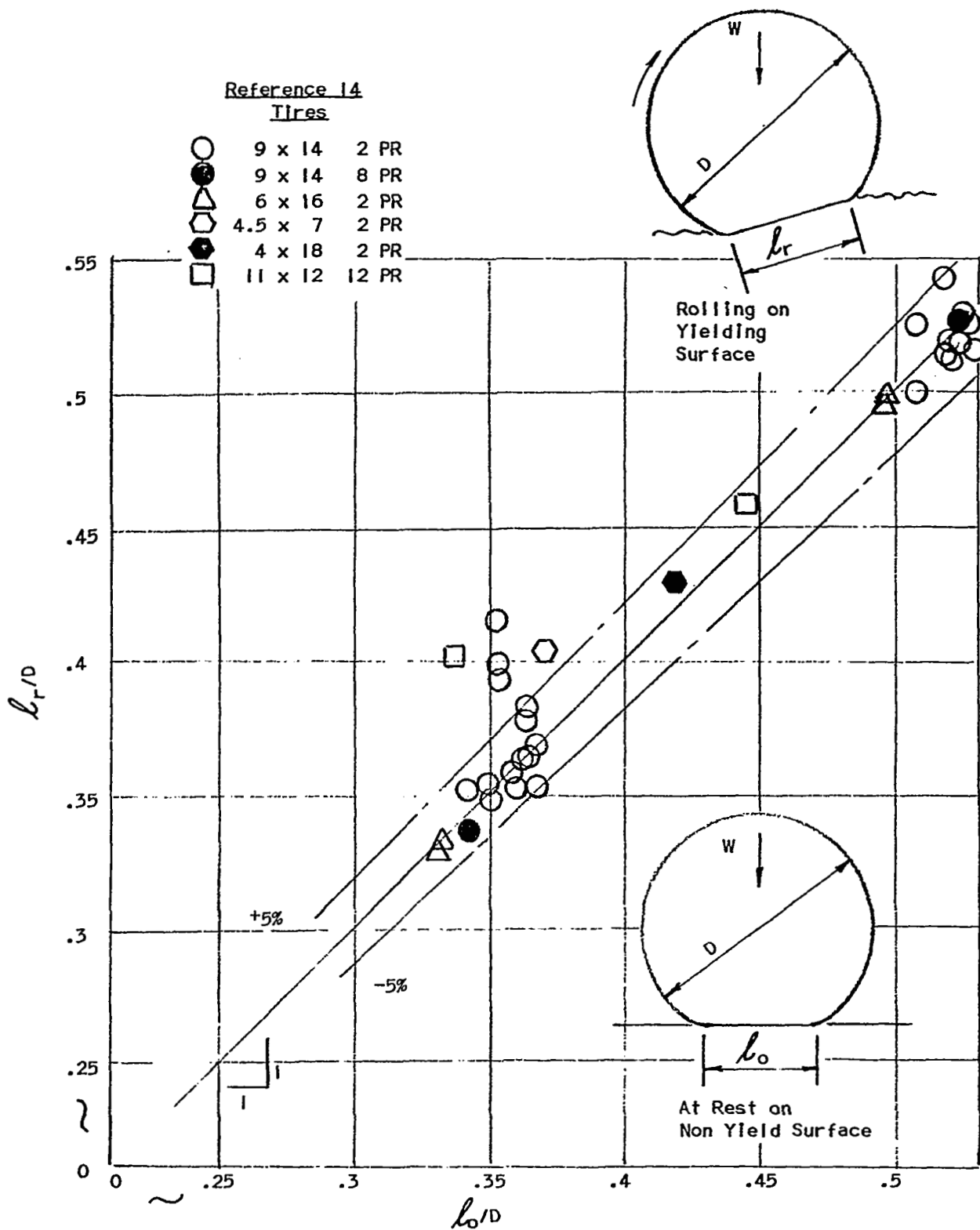


Figure B-5 TIRE CONTACT - ROLLING ON YIELDING SURFACE
VERSUS AT REST ON NON-YIELDING SURFACE

B-10

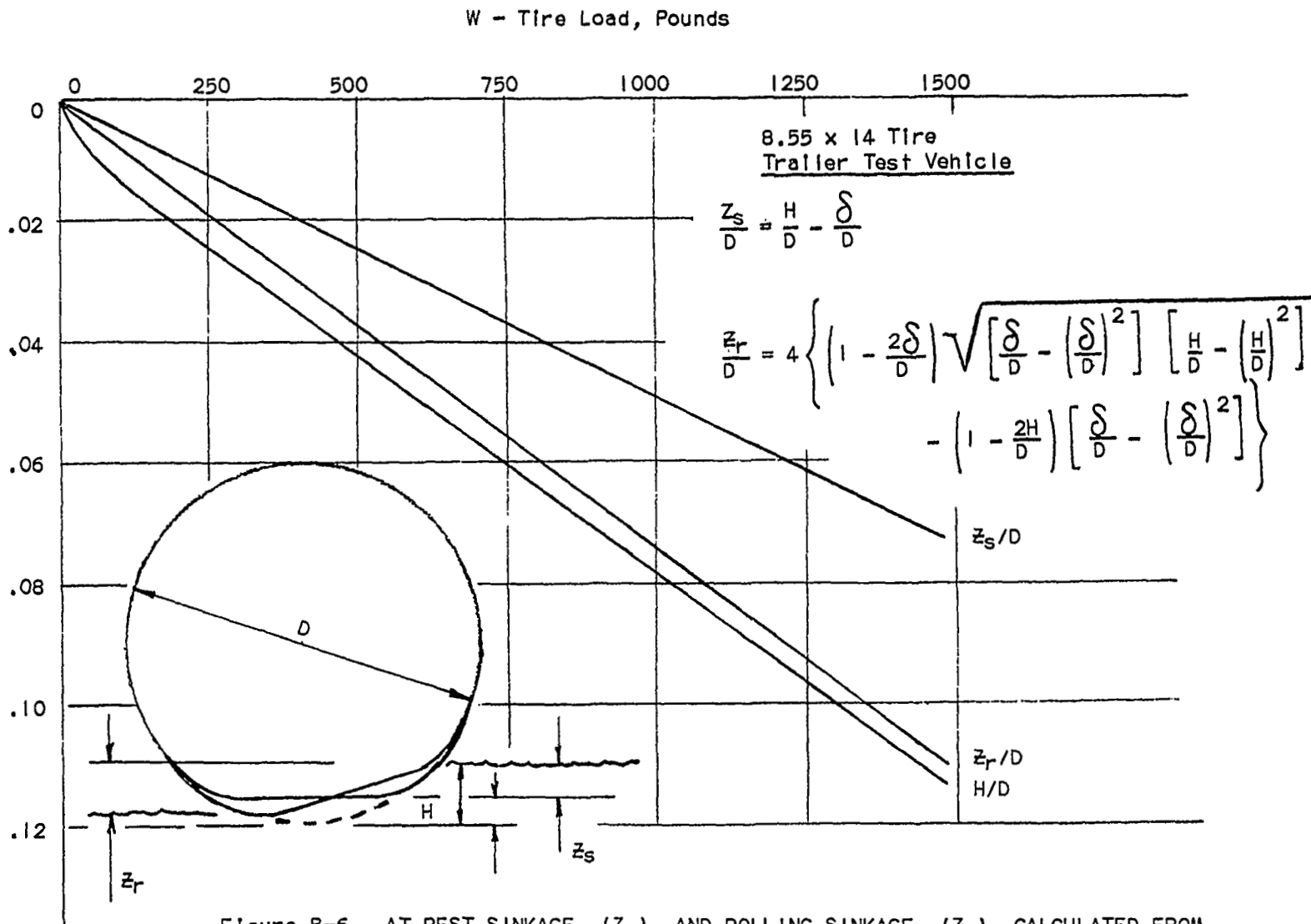


Figure B-6 AT REST SINKAGE (z_s) AND ROLLING SINKAGE (z_r) CALCULATED FROM HUB MOVEMENT (H) MEASURED AT TEST SITE AND TIRE DEFLECTION (δ)

B-11

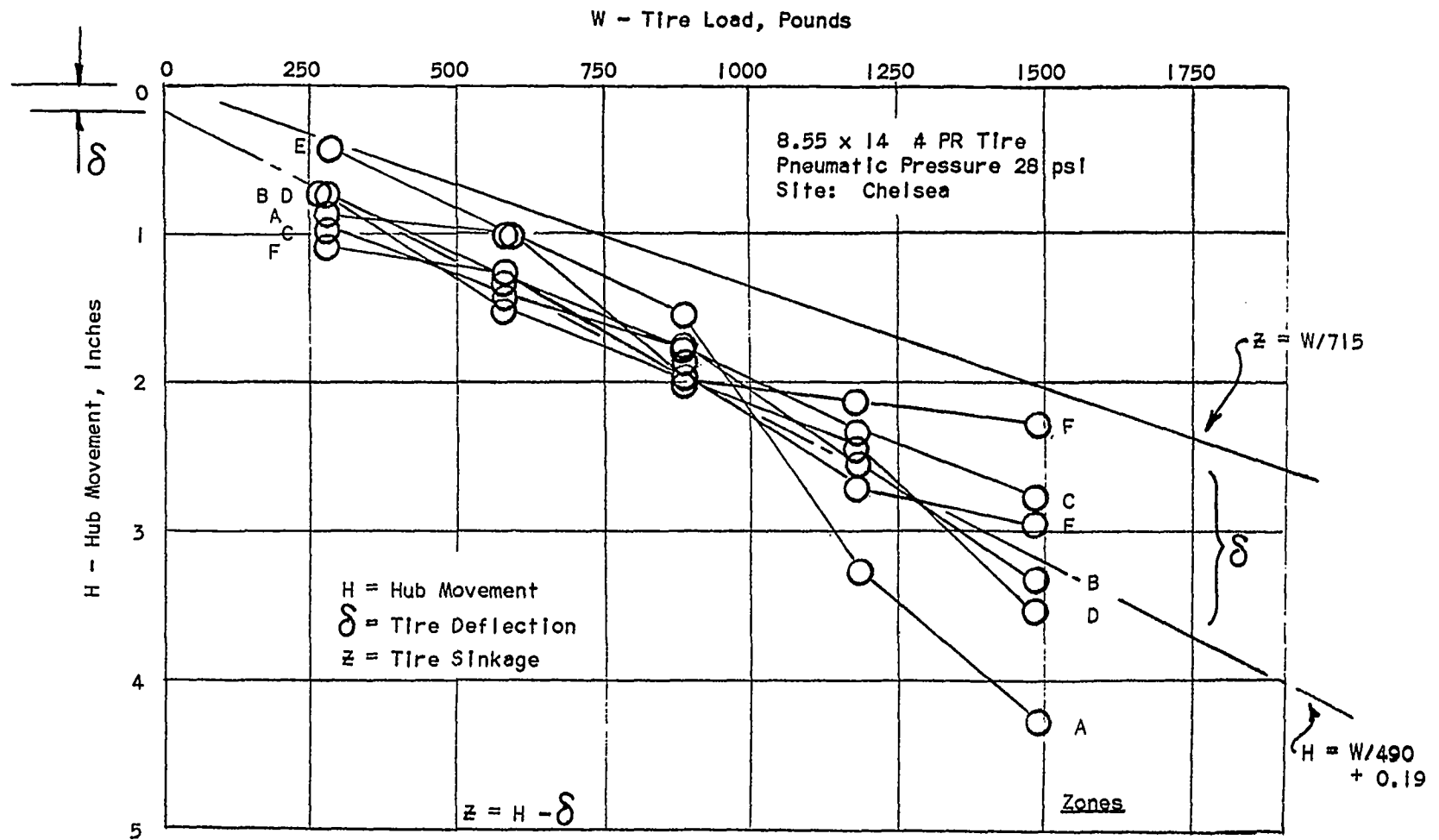


Figure B-7 HUB MOVEMENT VERSUS TIRE LOAD - TRAILER TEST VEHICLE
(Surface Layer Stiffness Measurement)

Table B-2 TRAILER HUB SINKAGE DATA					
Total Load Pounds	280	582	883	1185	1486
Ballast Load Pounds	(0)	(302)	(603)	(905)	(1206)
Position	Sinkage in Inches				
A	.87	1.01	1.56	3.28	4.32
B	.75	1.33	1.80	2.55	3.38
C	.92	1.42	1.79	2.34	2.77
D	.74	1.50	1.93	2.45	3.55
E	.42	1.01	1.93	2.71	2.96
F	1.08	1.27	1.98	2.16	2.30
Total	4.77	7.54	10.99	15.49	19.28
$H = \text{Avg } \delta + z$	0.795	1.26	1.831	2.582	3.213
$-\delta$	- 0.38	- 0.56	- 0.76	- 0.95	- 1.14
$= z$.415	.70	1.071	1.632	2.073

Applied tire load varied from net trailer weight of 280 lbs to 1486 lbs gross weight with ballast. An attempt to correlate results with the previously mentioned cone index gradient along course length was not successful; hence, the total data was lumped together to determine a mean linear variation of H versus W based on least squares. Subtracting tire deflection (δ) from hub movement (H) yields sinkage (z) as shown in Figure B-7 and Table B-2.

$$H = W/490 + 0.19$$

$$z = W/715$$

$$\phi_1(z) = 715 z \quad \text{Trailer Test Vehicle}$$

It is interesting to note that the predicted soil consolidation spring rate is actually a spring "constant" of 715 pounds per inch. Attempts to fit non-linear lines through the data resulted in negligible higher order terms either for exponentials or polynomials. This is attributed to the fact that while the soil gets softer with increased penetration, the tire loading area increases and the two factors seem to cancel over the limited range of penetration of interest in these tests.

It was not practical to obtain $\theta_1(z)$ for the truck by a similar method because the four wheel loads unevenly distributed on rough terrain could not be measured accurately. Instead, the correlation obtained in Reference 13 between tire sinkages, "z/D," and the numeric,* " $\frac{W}{C_1 \delta \pi \sqrt{D w}}$ " was applied to infer θ_1 . Denoting truck and trailer by the subscripts 1 and 2, respectively,

$$\frac{z_1}{D_1} \frac{D_2}{z_2} = \frac{W_1}{W_2} \frac{\delta_2}{\delta_1} \sqrt{\frac{D_2 W_2}{D_1 W_1}}$$

Inserting $W_1 = k_1 z_1$; $W_2 = k_2 z_2$ (B-5)

$$k_1 = k_2 \frac{\delta_1}{\delta_2} \sqrt{\frac{D_2 W_1}{D_1 W_2}}$$

$$k_1 = 715 \times \frac{0.90}{0.66} \times \sqrt{\frac{28.2}{35.1} \times \frac{10.75}{8.3}} = 1000 \frac{\text{lb}}{\text{in}}$$

$\theta_1(z) = 1000 z$ Truck Test Vehicle

B.4 EVALUATION OF DYNAMIC TERMS

Table B-3 presents a list of physical constants required to establish magnitudes of $\theta_2(\ddot{z})$ and $\theta_3(\ddot{z})$ - see Equations (B-3)(B-4). A discussion follows.

Soil Properties

Soil at the test site was analyzed as a moist sand-clay mixture.

A soil specific gravity of 1.6 was found from the weighing of samples.

*w equals tire carcass width
C1 equals surface cone index

Table B-3 PHYSICAL CONSTANTS YIELDING SURFACE

<u>Soil Properties</u>	
Mass Density	3.1 lb sec ² /ft ⁴
Poissons Ratio	0.4
Youngs Modulus, E	
Maximum	1.0 x 10 ⁶ lb/ft ²
Minimum	0.4 x 10 ⁶ lb/ft ²
<u>Coefficients</u>	
Damping, b _o	
Trailer	5.9
Truck	5.9
Effective Mass, c _l	
Trailer	1.6
Truck	1.6
<u>Tire Characteristic</u>	
Contact Area, A ... l _g	
8.55 x 14 (Trailer)	0.21 ft ²
9.00 x 16 (Truck)	0.27 ft ²

The weights measured are shown in Table B-4.

Poissons Ratio (ν) for earth soils varies from 1/3 (sand) to 1/2 (clay).⁽¹⁵⁾ An intermediate value (0.4) was chosen.

The measurement of Youngs Modulus (E), which requires special technique and laboratory (soils) equipment, was not undertaken. Maximum (moist sand) and a minimum (wet clay) values were selected (Table B-3) from the data cited in Reference 15 (Chapter 1). E is estimated to be uncertain by a factor of 2.5; therefore, theoretical soil damping due to elastic effects is uncertain by a factor $\sqrt{2.5}$ equal 1.58. Computer simulation shows a negligible effect of these uncertainties on vehicle motion.

Table B-4

MEASUREMENTS FOR DETERMINING SOIL DENSITY

Location	Volume cu. ft.	Weight lbs.	Density lb/cu. ft.	Specific Gravity
A1	.01625	1.245	76.6	1.23
A2	.01750	1.360	77.7	1.24
B1	.01250	1.210	96.8	1.55
B2	.01050	0.960	91.4	1.46
C1	.01250	1.380	110.4	1.77
C2	.01450	1.915	132.1	2.12
D1	.01100	1.540	140.0	2.24
D2	.02275	1.990	87.5	1.40
E1	.01925	1.600	83.1	1.33
E2	.01675	1.555	92.8	1.49
F1	.01625	1.490	91.7	1.46
F2	.01400	1.330	95.0	1.52
Average			97.93	1.57

Coefficients

The damping coefficient (b_0) and effective mass coefficient (c_1) are theoretically dependent upon Poissons Ratio (ν). Values are tabulated in References 16 and 1.

Tire Contact Area "A"

Tire contact area (A) varies in a complicated way with tire sinkage (z). This behavior may be best appreciated from relations of A and z to tire deflection (δ).

A Versus δ

Reference 22 suggests Equation (B-7)

$$A = C \delta \sqrt{(D-\delta)(w-\delta)} \tag{B-7}$$

D = tire diameter

w = tire carcass width

δ = tire deflection

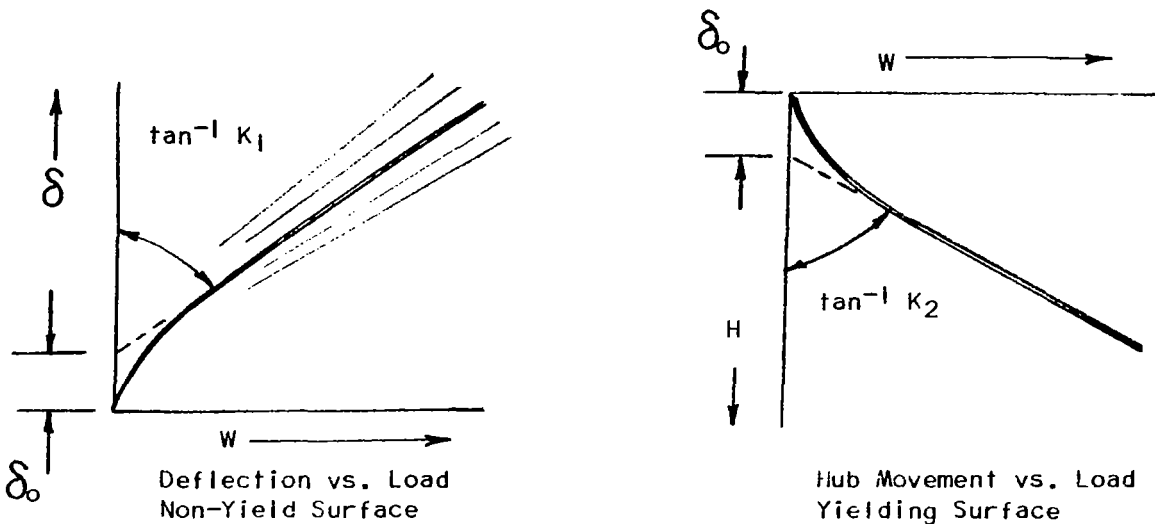
C = dimensionless coefficient

Figure B-8 shows that Equation (B-7) can be fitted approximately to actual tire characteristics for the two test vehicles.

δ Versus z

Manufacturer's tire data and surface stiffness results

(Figure B-7) are indicated by the following sketches.



$$A = C \delta \sqrt{(D-\delta)(W-\delta)}$$

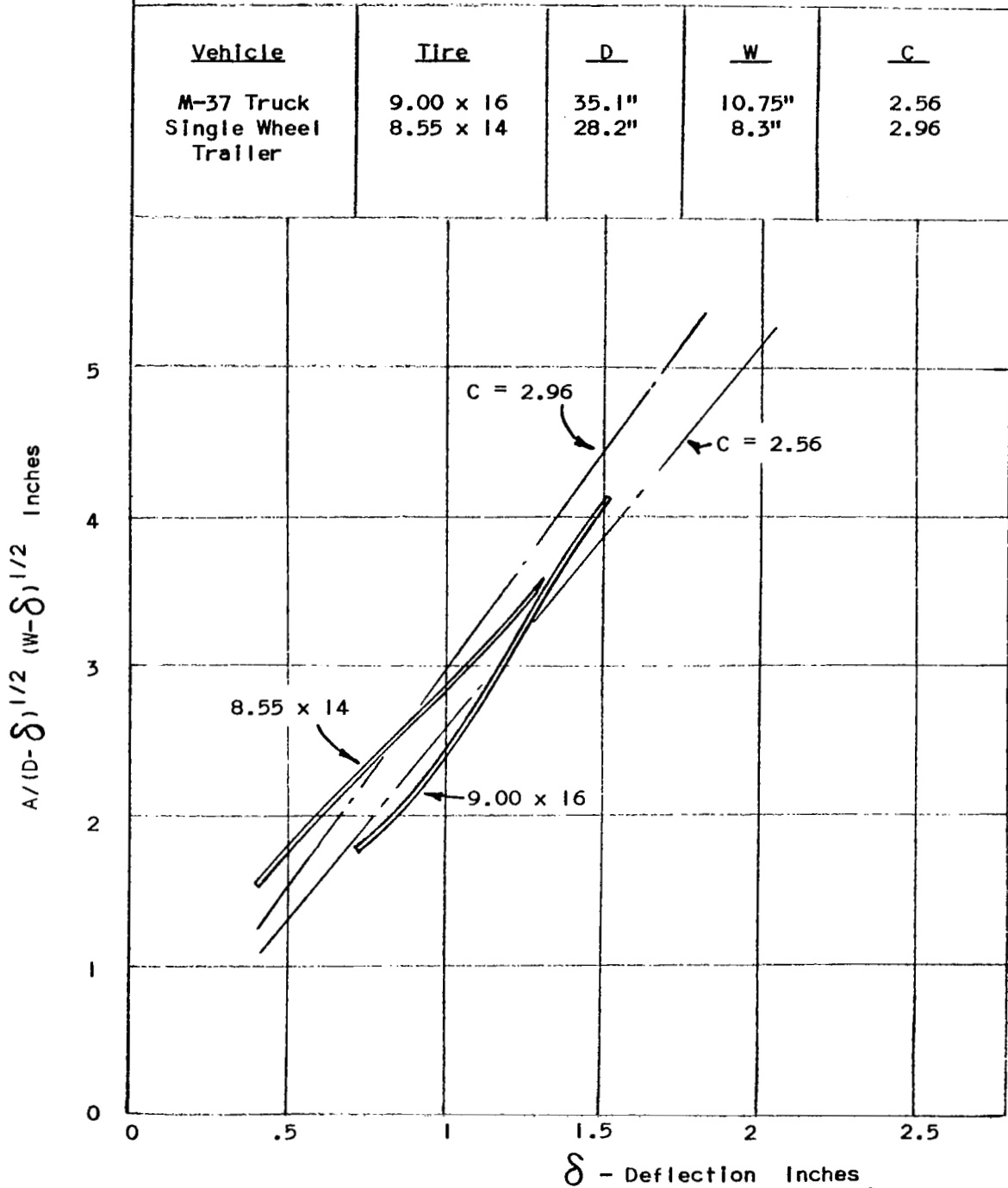


Figure B-8 TIRE CONTACT AREA (A) VERSUS TIRE DEFLECTION (δ)

APPENDIX C

VEHICLE FIELD TEST MEASUREMENTS AND ANALYSIS

C.1 TESTS

Measurements were obtained from six dynamic tests of the two vehicles in the form of acceleration records. The truck, a standard M-37, was operated unloaded. The specially designed single wheel trailer which featured a long tow arm to reduce coupling of the towing vehicle, the truck, required a ballast load to have the sprung mass c.g. directly above the center of the tire patch. The trailer had a G.V.W. of 800 pounds using an 8.55 x 15" automotive tire. The dynamic test runs were conducted as follows:

- a) Truck alone over rough yielding (SOFT) surface at 3 mph.
- b) Truck alone over rough non-yielding (HARD) surface at 3 and 6 mph - two consecutive runs.
- c) Trailer towed by truck over rough SOFT surface at 3 mph.
- d) Trailer towed by truck over rough HARD surface at 3 and 6 mph - two consecutive runs.

A single run was used on the soft surface since the profile measurements had to be made prior to each run, and the surface profile was significantly altered by the vehicle passage. The profiles were selected so that the truck wheels followed the same tracks whether carrying the trailer or not. In other words, the truck, while carrying the trailer over the soft surface, followed the same ruts it had left from the previous test, and the trailer followed between these ruts on a virgin profile.

C.2 INSTRUMENTATION

Due to the low test speeds, the standard truck speedometer was impossible to use for determining vehicle speed and maintaining a constant test speed.

In order to obtain a constant speed, which is essential for the statistical processing of accelerometer data as necessitated in this verification, a tachometer was placed upon the hood of the truck. The tachometer was clearly visible to the driver as he followed a course, and by monitoring engine rpm it was demonstrated through repeated runs on a level surface, that he could maintain quite accurately a constant speed.

The gear ranges were selected for the tests so that the tachometer reading was approximately 2000 rpm. Specifically, for the 3 mph run, the transmission was operated in low gear and the transfer case also in the low ratio, which resulted in 2100 rpm for the soft surface and, due to less wheel slippage, 2030 rpm for the hard surface. For 6 mph on the hard surface, the transmission was operated in low gear and the transfer case in high or 1:1 ratio, an engine speed of 2080 rpm was used. Timing the test over the course between designated pole markers showed that the speed was held reasonably constant, and was felt adequate for the required test speeds.

Standard Kistler force-balance accelerometers were used to instrument both the towing vehicle and the trailer. The truck had five accelerometers mounted on it located as shown in Figure C-1. One accelerometer was mounted on the floor pan at the location of the vehicle c.g. The front accelerometer was attached onto the winch support to monitor the furthestmost forward point from the c.g. possible on the centerline of the truck. A third accelerometer was mounted at the rear near the trailer hitch point. The other two accelerometers were positioned to the left and right of the c.g. location. The trailer accelerometer placements during the field tests are indicated in Figure C-2. One was at the front of the towing arm near the hitch point. One was mounted at the wheel spindle to measure wheel motions, and the third

Figure C-1 ACCELEROMETER LOCATIONS ON M-37

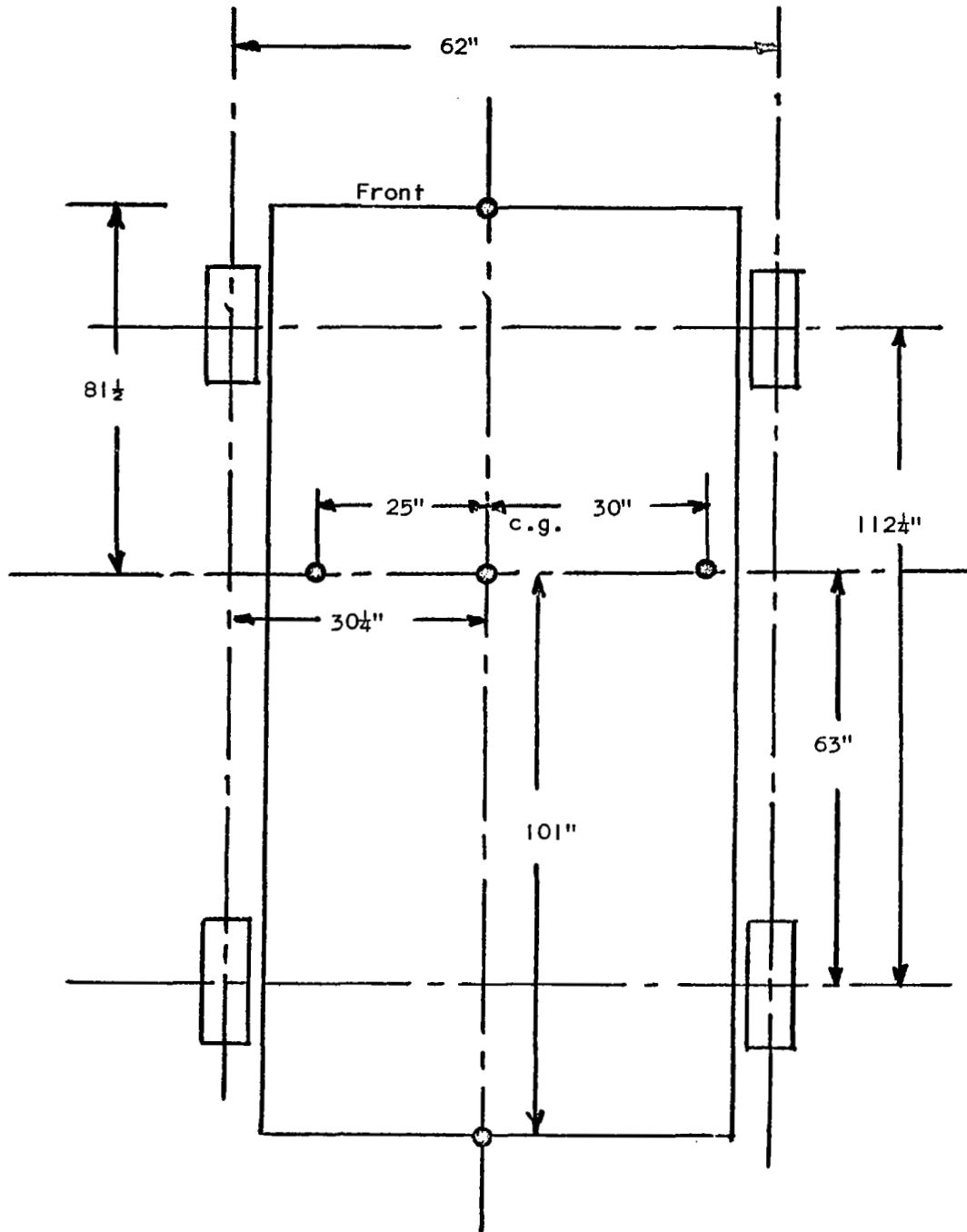
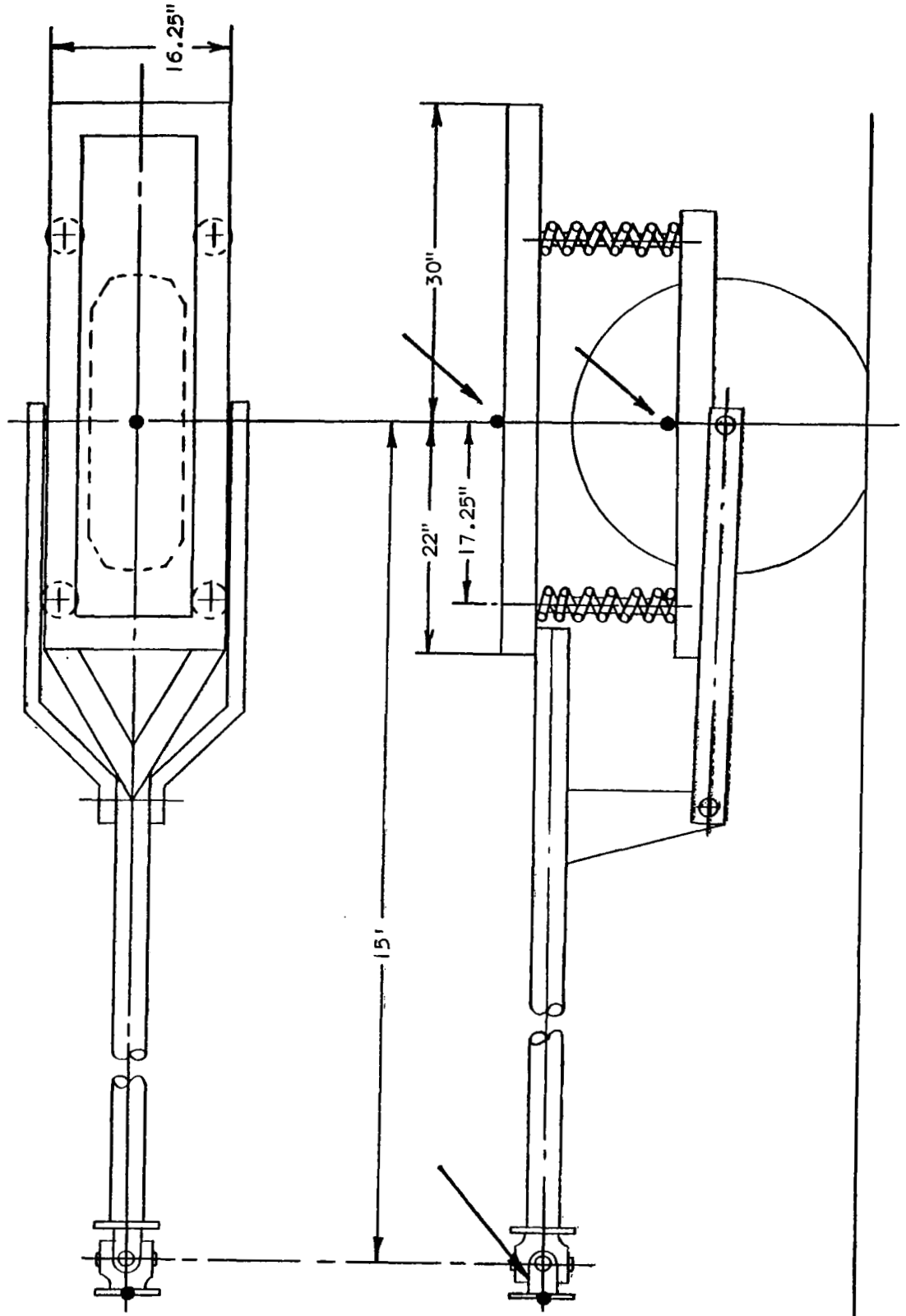


Figure C-2 ACCELEROMETER LOCATIONS ON SINGLE WHEEL TRAILER



was at the c.g. directly above the center of the tire patch on the trailer bed.

The output of all accelerometers during testing were recorded directly on an f.m. multi-channel tape recorder which also allowed an audio recording. The recording of the experimenter's comments directly with the data allowed easy verification of the site and knowledge of any extenuating circumstances which existed during that test sequence.

Figure C-3 shows some of the instrumentation as used on the M37 vehicle. The tachometer is mounted on the hood in front of the windshield clearly in the view of the driver. The front accelerometer can be seen on the winch support. Figure C-4 shows the f.m. tape recorder inside the vehicle and the accelerometer mounted above the frame on the left sill used to calculate roll acceleration.

C.3 PRE-PROCESSING OF DATA

With a proper combining of fore and aft, and left and right accelerometer recordings, it was possible to calculate roll and pitch motions of the truck assuming rigid body motion. The assumption of rigid body motions was verified in the frequency range of interest by comparing the sum of the left and right accelerometers with twice the acceleration at the c.g. The same procedure was used to verify the bending mode of the vehicle by comparing the sum of the fore and aft accelerometers with two times the c.g. acceleration. It was determined that the fundamental bending and torsional modes of the truck frame-body combination were above the dynamic range of interest in this study. Likewise the trailer pitch motion was determined through translational motions of the hitch and c.g. However the rigid body assumption was not as valid in

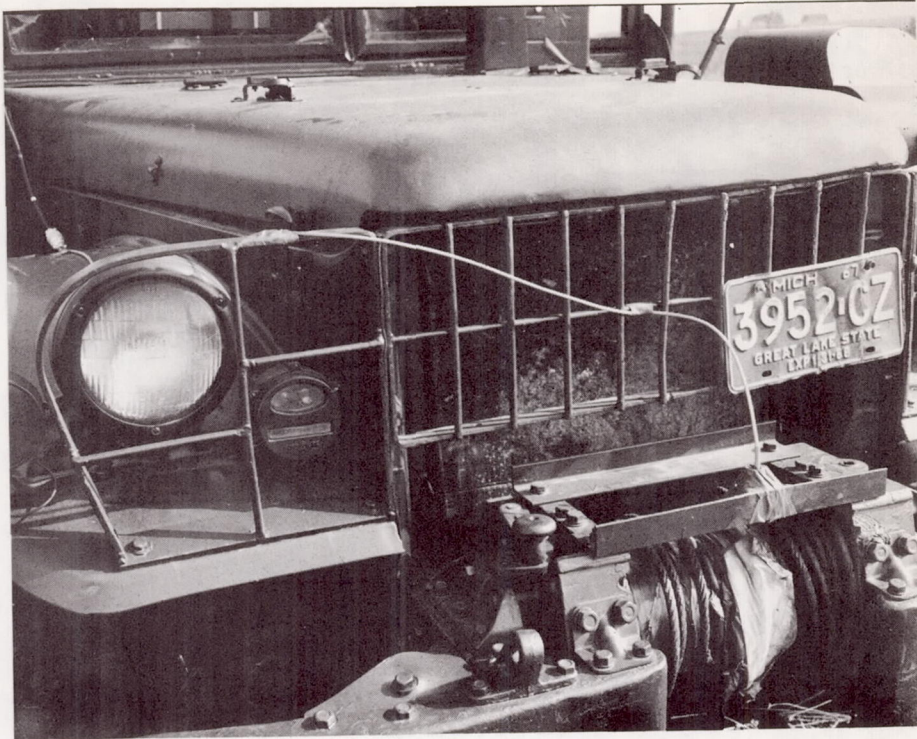


Figure C-3 View Showing Tachometer Mounted on M37 Hood and Front Accelerometer Mounted on Winch Support

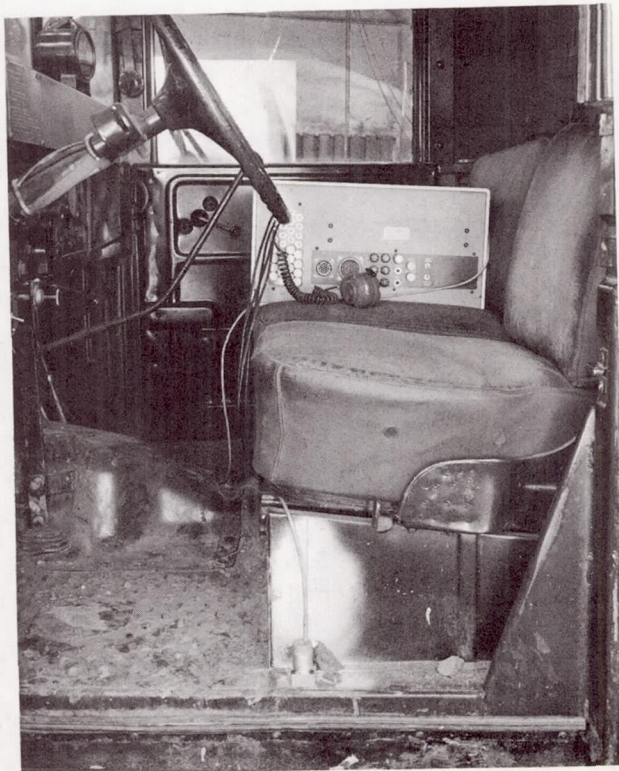


Figure C-4 View Showing Accelerometer Mounted on M37 Sill and Tape Recorder in Vehicle

this case due to the bending of the long tow arm.

The five truck and three trailer accelerometer recordings were combined as described above, and the resulting signals re-recorded on tape loops. This resulted in six loops for the three test conditions of the two vehicles. Each loop had three signals per vehicle, i.e., bounce (vertical motion), pitch and roll for the truck; or c.g. bounce, pitch and wheel bounce for the trailer. These 18 signal recordings were processed, using a standard analog computer, to yield the power spectral density and amplitude probability distribution plots according to the procedures of Reference 10.

C.4 STATISTICAL DATA ANALYSIS

A random signal is best described in the frequency domain by means of its power spectral density which expresses the average variance of a waveform as a function of frequency. The direct analog calculation of PSDs for the frequency range from $\omega = 2$ to 200 radians per second ($f = .318$ to 31.8 cps) for the selected signals was performed.

The first step in this process is to form the tape record of the signals into a long tape loop. These repeating signals are then processed by the analog computer network shown in Figure C-5. The initial portion of the circuit is a high pass filter which has a 3 db per octave cutoff below .3 radians per second. This circuit is included to attenuate any instrumentation drift below this frequency which is not of interest in this random vibration analysis. The second section of the computer PSD circuit is a constant Q bandpass filter which was set for a value of Q equal to 10. This value was determined in order to yield the desired resolution in the frequency domain. The frequency of this bandpass filter is determined by the loop gain which is

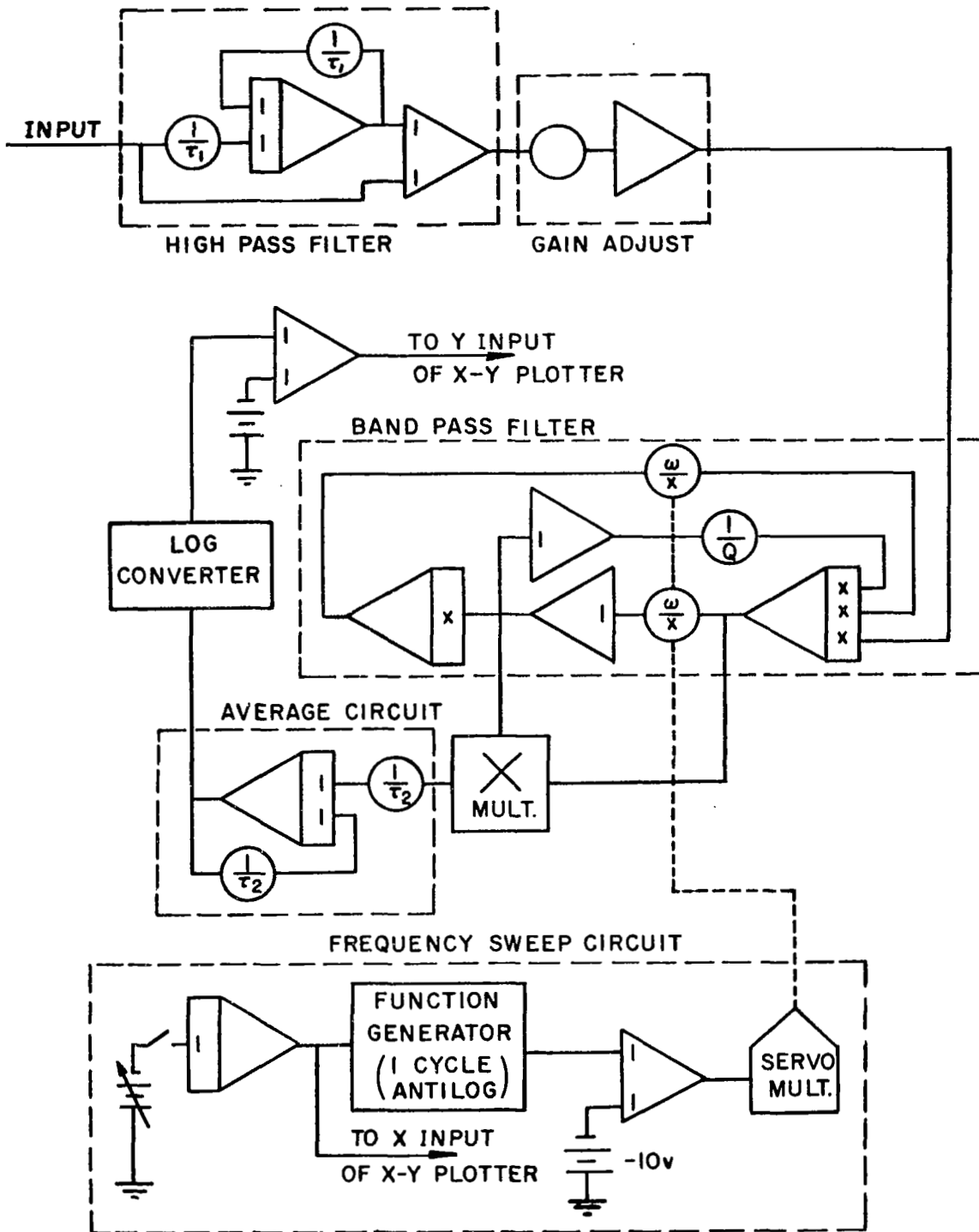


Figure C-5 ANALOG COMPUTER POWER SPECTRAL DENSITY CIRCUIT

adjusted by the two potentiometers of the servo-multiplier. As the tape loop is continuously repeated, the servo-multiplier is used to slowly change the center frequency of the filter so that the mean square value of the filtered function can be plotted versus frequency directly on an X-Y recorder. A one cycle, antilog function generator is used to drive the servo-multiplier to produce a scan of the bandpass filter that changes in such a manner that the speed of sweep is proportional to the bandwidth of the filter. After scanning through one decade, the frequency sweep circuit is reset and the loop gain of the bandpass filter is changed by a factor of 100 to allow scanning of the subsequent frequency decade. The initial speed of sweep of the filter was set so that three tape loop passes were completed before the filter advanced through one bandwidth.

The signal, after being filtered, was passed through a multiplier and averaging circuit to obtain the mean square value of the filtered function in the pass band. The two different points are brought to the multiplier so that the squared value becomes independent of the changing bandwidth of the filter. The averaging time was adjusted to be equal to the time of one tape loop length. The voltage corresponding to the mean square value is passed through a logarithmic converter in order to make a direct log-log plot of the desired function.

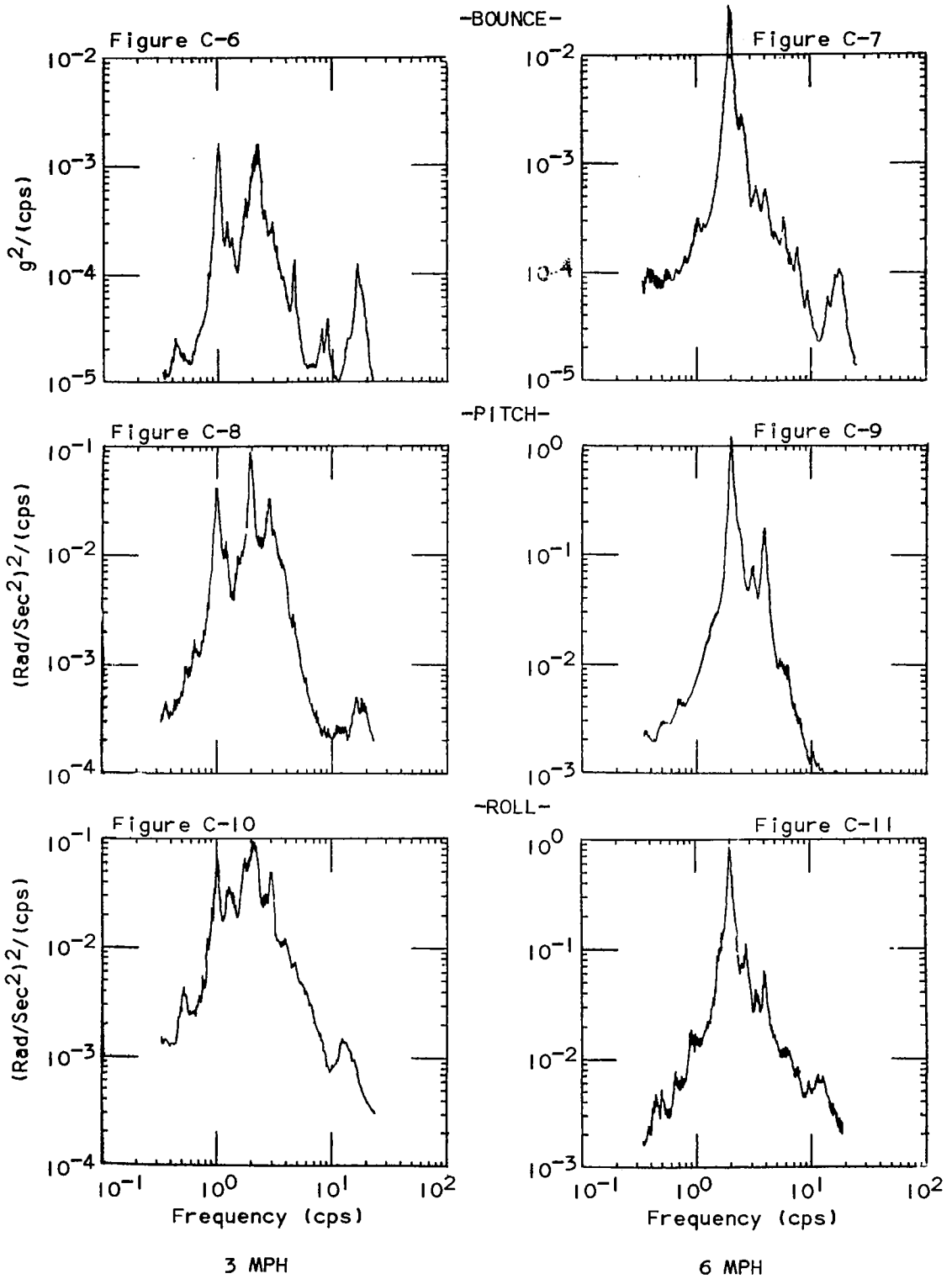
The power spectral density functions obtained from acceleration signals are plotted in Figures C-6 through C-23.

The square root of the area under a PSD curve corresponds to the root mean square (RMS) value or the standard deviation of a Gaussian random process. However, neither the RMS value nor the PSD function can indicate how closely

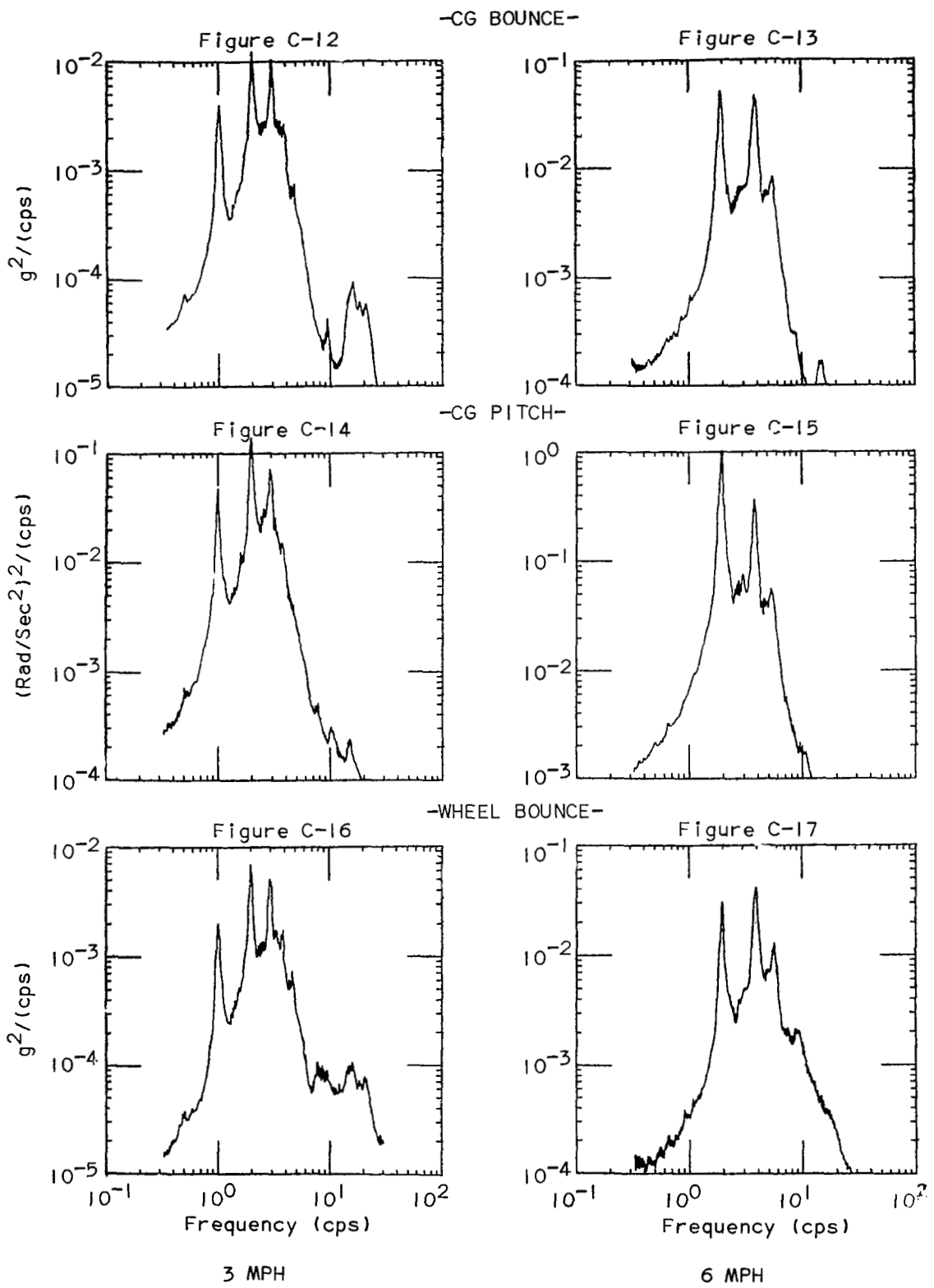
the random process approaches the important Gaussian case. The amplitude probability distribution (APD) functions were plotted to test for the Gaussian case. Figures C-24 through C-31 show example APD plots for the truck and trailer on both hard and soft surfaces. It can be seen from these plots that the truck motion was very close to Gaussian. The trailer, however, shows a substantial deviation from Gaussian which tends to accentuate high accelerations. This might be due to the limited wheel travel on the trailer. These results are summarized in Table C-1 which gives the value of RMS acceleration determined from the APD curves.

Table C-1 RMS ACCELERATIONS DETERMINED FROM FIELD TEST APD PLOTS							
VEHICLE		M-37 TRUCK			SINGLE WHEEL TRAILER		
TEST	Surface	Bounce (g's)	Pitch ($\frac{\text{Rad}}{\text{Sec}^2}$)	Roll ($\frac{\text{Rad}}{\text{Sec}^2}$)	Bounce (g's)	Pitch ($\frac{\text{Rad}}{\text{Sec}^2}$)	Wheel Bounce
3 MPH	Soft	.062	.395	.428	.144	.206	.250
3 MPH	Hard	.038	.262	.312	.064	.212	.064
6 MPH	Hard	.080	.580	.520	N/A	.638	.181

PSD'S OF TRUCK ON HARD SURFACE

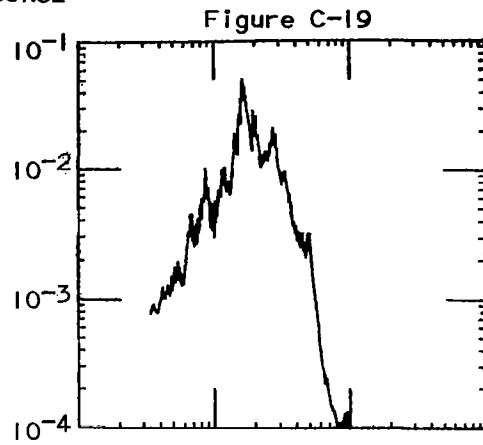
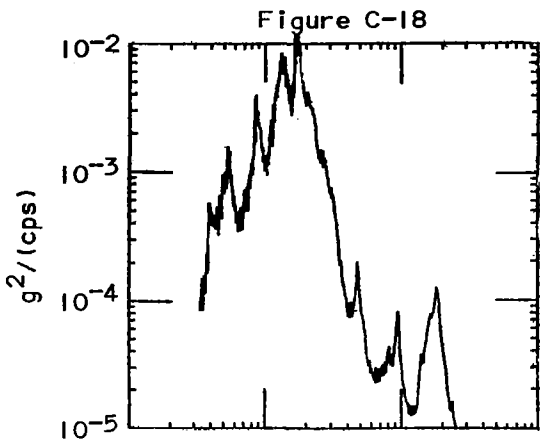


PSD'S OF TRAILER ON HARD SURFACE

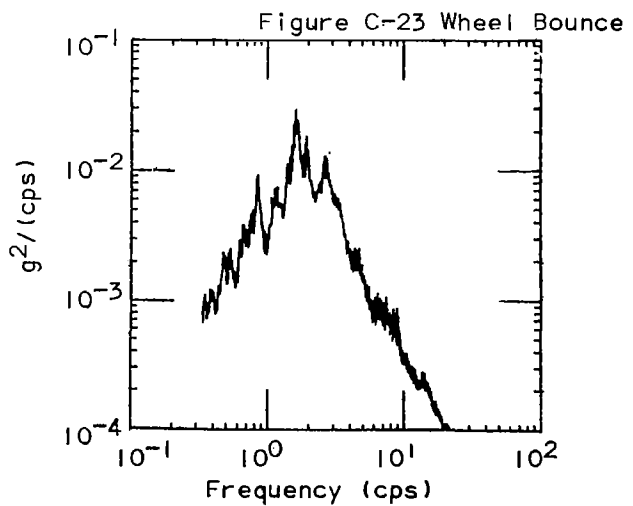
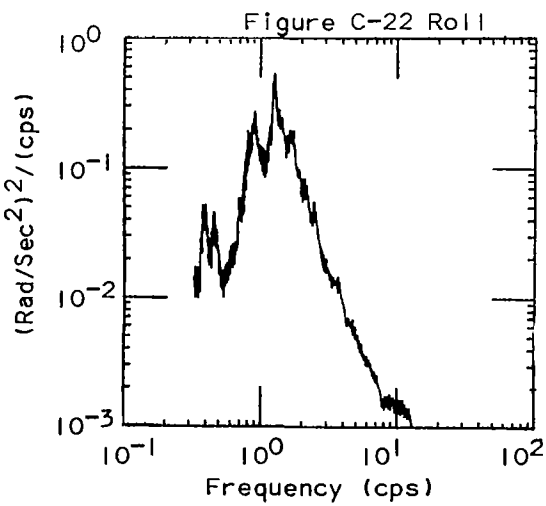
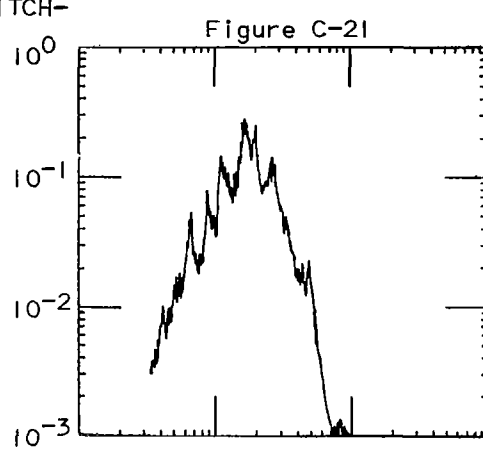
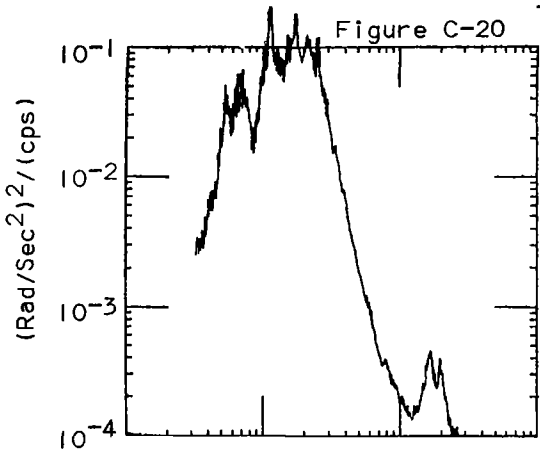


VEHICLE PSD'S ON SOFT SURFACE AT 3 MPH

-CG BOUNCE-



-CG PITCH-

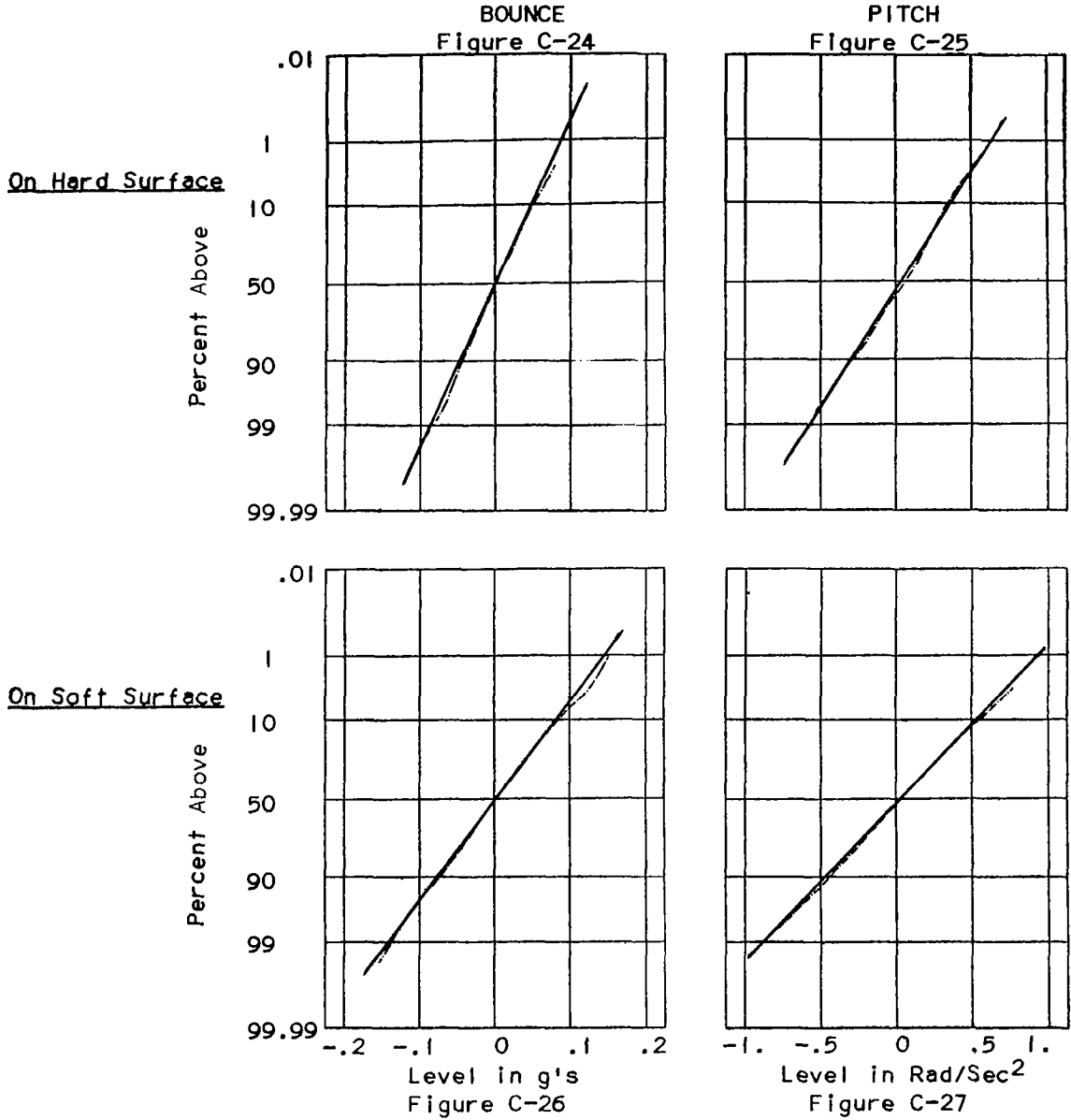


TRUCK

TRAILER

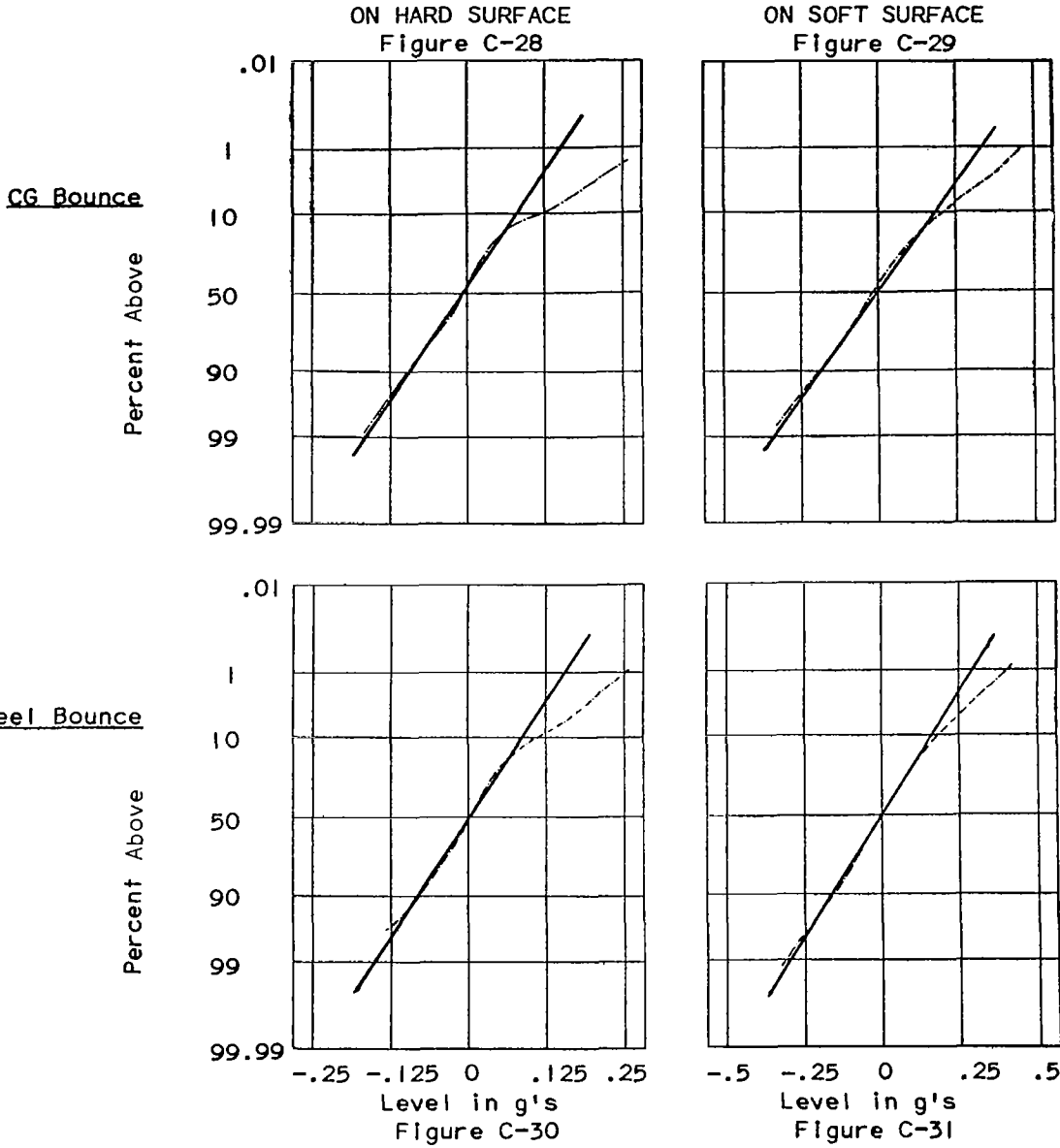
APD'S OF TRUCK ACCELERATIONS @ 3 MPH

Measured — · — · — ·
 Gaussian —————



APD'S OF TRAILER ACCELERATIONS @ 3 MPH

Measured
 Gaussian



APPENDIX D

LINEAR MODEL - FREQUENCY DOMAIN APPROACH

The M-37 vehicle and the trailer were modeled mathematically. The M-37 model had seven degrees of freedom, and the trailer model had two degrees of freedom. Laboratory measurements were made to determine numerical data for the truck and trailer. Both vehicles were weighed and the center of gravity was determined from tilt measurements on the truck. Pneumatic tire spring rates were statically determined from measurements of the deflections for various loads. Other quantities were determined from the literature.⁽²³⁾⁽²⁴⁾

A right hand coordinate system was used in the development of the equations of motion, which is shown in Figure D-1.

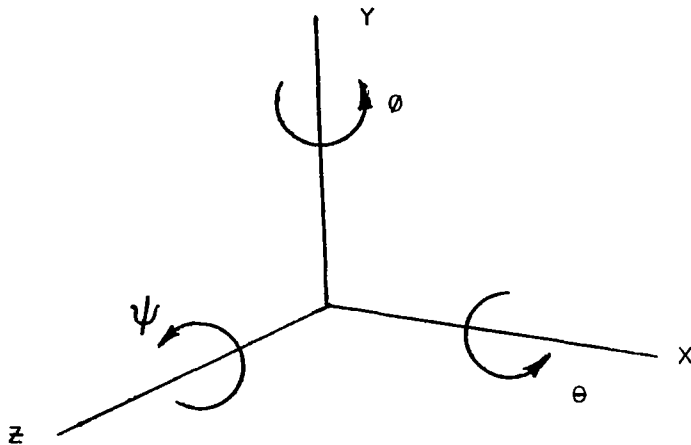


Figure D-1 COORDINATE SYSTEM

This coordinate system is located in the vehicle such that the positive X-axis is toward the rear of the vehicle, the Y-axis is in the vertical direction and the positive Z-axis is towards the left of the vehicle.

D-1 M-37 TRUCK MODEL

A line drawing of the truck model is shown in Figure D-2. The M-37

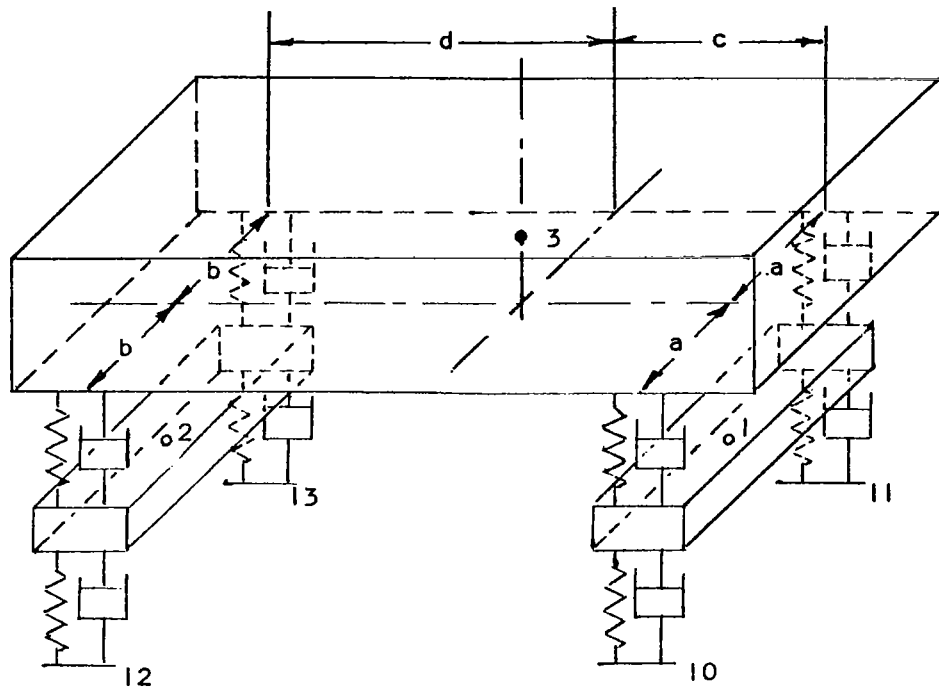


Figure D-2 TRUCK MODEL

vehicle is a 3/4 ton military cargo carrier with four driven wheels and solid axles front and rear. Left to right symmetry was assumed and the principal axes of inertia coincided with the coordinate axes. The model consists of three masses connected by linear springs and dampers (representing the suspension system). Linear springs and dampers representing the tires were also connected to the ground (input points) from the axle masses. Specific points identified in the model are shown below. The numbers are arbitrary "bookkeeping" symbols used in the computer program.

1. Center of gravity of the front axle
2. Center of gravity of the rear axle
3. Center of gravity of the vehicle body
10. Right front wheel ground contact area
11. Left front wheel ground contact area
12. Right rear wheel ground contact area
13. Left rear wheel ground contact area

Since only vertical inputs were considered, compliances were defined for vertical motions. The degrees of freedom considered, included bounce and roll motion for the two axles, and bounce, pitch and roll for the vehicle body. The M-37 vehicle model input data is shown in Table D-1

The seven resonant frequencies for this model are listed in Table D-2. These are approximate frequencies computed from undamped uncoupled systems.⁽²³⁾

D-2 TRAILER MODEL

The trailer was modeled as a simple two degree of freedom system consisting of two mass elements, the sprung mass and the unsprung mass, which included the wheel, tire and undercarriage connected by linear springs and dampers. The pneumatic tire was also represented by a linear spring and

Table D-1 M-37 VEHICLE MODEL DATA

Tire spring constant lb./in.	1700
Tire damping coefficient lb.sec./in.	0.35
Front suspension spring constant lb./in	370
Rear suspension spring constant lb/in.	330
Front and rear shock absorber damping coefficient lb.sec./in.	7
Vehicle sprung mass lb.sec. ² /in.	13.30
Pitch moment of inertia sprung mass lb.sec. ² in.	38000
Roll moment of inertia sprung mass lb.sec. ² in.	5800
Front axle assembly mass lb.sec. ² /in.	1.825
Rear axle assembly mass lb.sec. ² /in.	1.56
Roll moment of inertia front axle lb.sec. ² in.	1250
Roll moment of inertia rear axle lb.sec. ² in.	1070
Distance from vehicle centerline to front suspension attachment in.	23.10
Distance from vehicle centerline to rear suspension attachment in.	27.40
Distance from sprung mass c.g. to point above front axle in.	63.30
Distance from sprung mass c.g. to point above rear axle in.	48.70

Table D-2 RESONANT FREQUENCIES - TRUCK

Sprung mass bounce	1.37 cps
Sprung mass pitch	1.65 cps
Sprung mass roll	1.83 cps
Front axle bounce	7.20 cps
Rear axle bounce	7.50 cps
Front axle roll	7.70 cps
Rear axle roll	8.30 cps

damper element. Vertical inputs through the tire were considered, and since the sprung mass center of gravity was directly above the tire, no rotational motion was excited. The two degrees of freedom were the bounce motions of the sprung and unsprung mass elements. The trailer model data is presented in Table D-3.

Sprung mass	lb.sec. /in.	1.63
Unsprung mass	lb.sec. /in.	.363
Suspension spring rate	lb./in.	320
Suspension damping coefficient	lb.sec./in.	16
Tire spring rate	lb./in.	915
Tire damping coefficient	lb.sec./in.	0.9

The two resonant frequencies for the trailer model are given in Table D-4.

Sprung mass	1.95 cps
Unsprung mass	8.50 cps

Initial computer runs were made with the truck and trailer tied together. The effect of truck motion on the trailer and trailer motion on the truck was determined. This coupling effect showed less than 1% change in predicted values, and therefore for subsequent runs, it was assumed that the trailer was uncoupled from the towing vehicle (the M-37 truck). The hitch point at the end of the boom was taken as fixed, and therefore the trailer experienced pitching motion about the hitch point. This pitching motion is therefore predicted to be directly proportional to the bounce motion of the sprung mass.

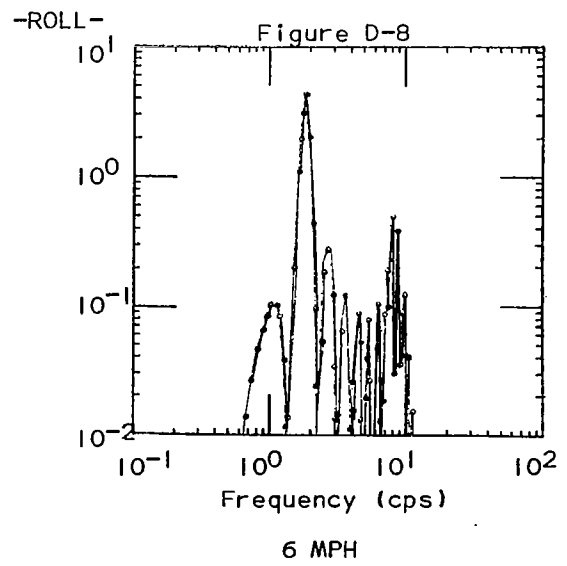
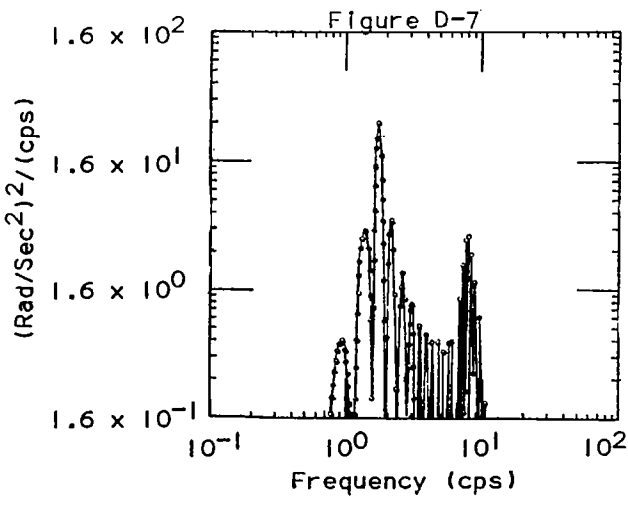
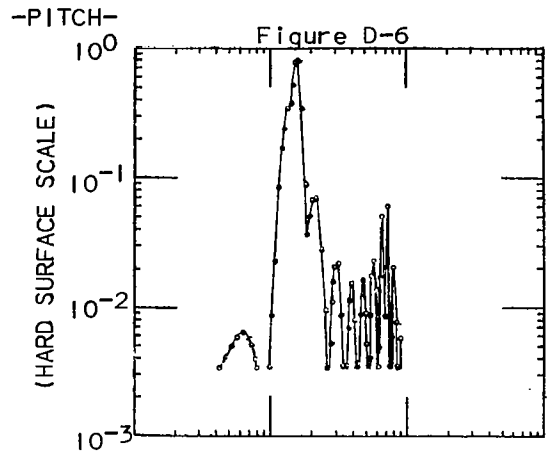
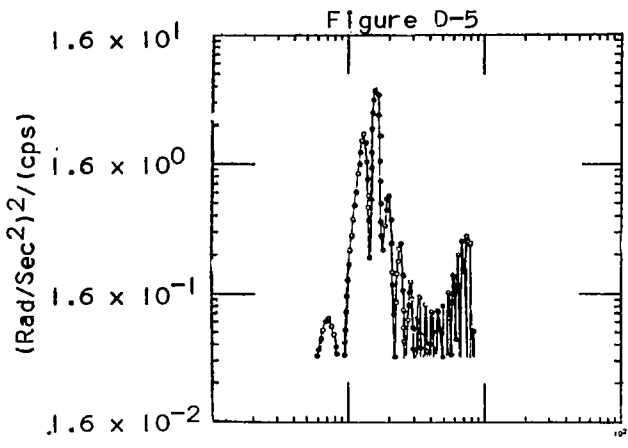
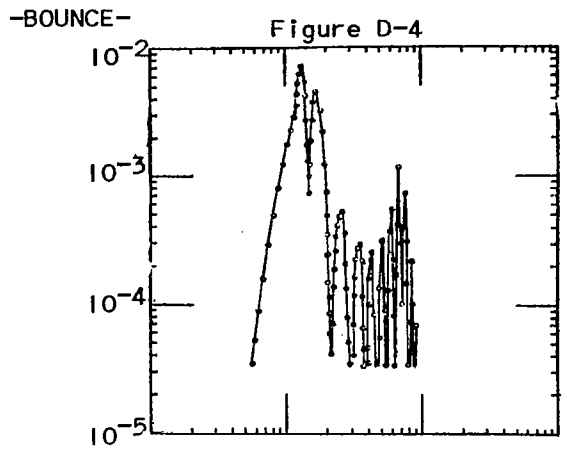
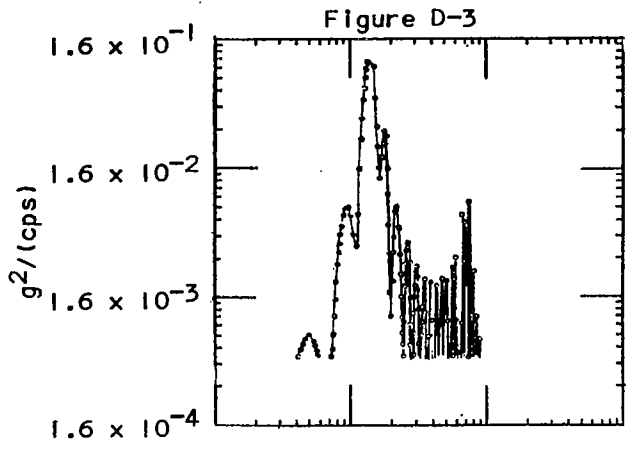
D-3 ANALYSIS OF VEHICLE VIBRATION

Transfer functions for the truck and trailer were determined for each input separately (that is, a sinusoidal vertical input at each tire contact with the ground). Transfer functions for a very similar M-37 model have previously been published.⁽²³⁾ These transfer functions were combined, taking into account vehicle velocity, wheel spacing (wheelbase) and the idealized power spectral density of the input with the cross correlation of parallel traces assumed to be zero. The resulting computed power spectral densities for each degree of freedom measured in the field are presented in the following series of graphs (Figures D-3 through D-11). Through the linearity assumption it is possible to present the graphs showing different scales for the ordinates corresponding to a surface roughness and/or vehicle speed from the field tests. For example, Figure D-3 presents the acceleration spectral density of the truck c.g. bounce motion at 3 miles per hour over either the hard or soft surface as characterized by the change in vertical scales. The RMS acceleration values given in Table D-5 were determined from the square root of the area under the corresponding PSD curves.

VEHICLE		M-37 TRUCK			SINGLE WHEEL TRAILER		
TEST	Surface (C in Ft)	Bounce (g's)	Pitch $\left(\frac{\text{Rad}}{\text{Sec}^2}\right)$	Roll $\left(\frac{\text{Rad}}{\text{Sec}^2}\right)$	Bounce (g's)	Pitch $\left(\frac{\text{Rad}}{\text{Sec}^2}\right)$	Wheel Bounce (g's)
3 MPH	Soft (C=.000232)	.139	1.013	2.344	.304	.656	1.029
3 MPH	Hard (C=.000014)	.110	.254	.586	.077	.164	.257
6 MPH	Hard (C=.000014)	.137	.372	.880	.108	.230	.364

PSD'S OF TRUCK CG ACCELERATIONS

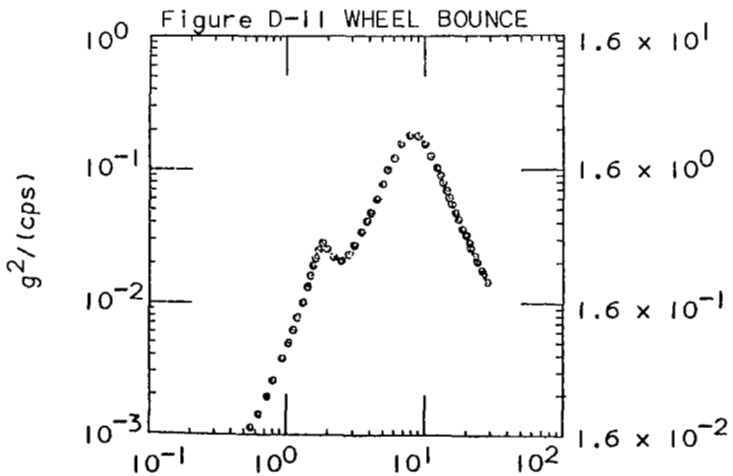
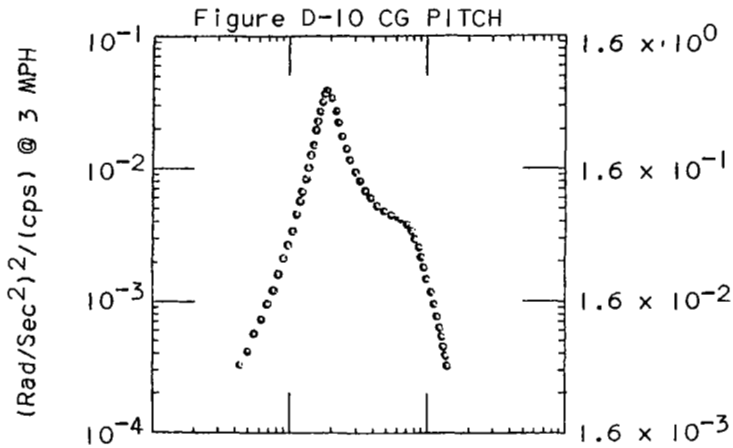
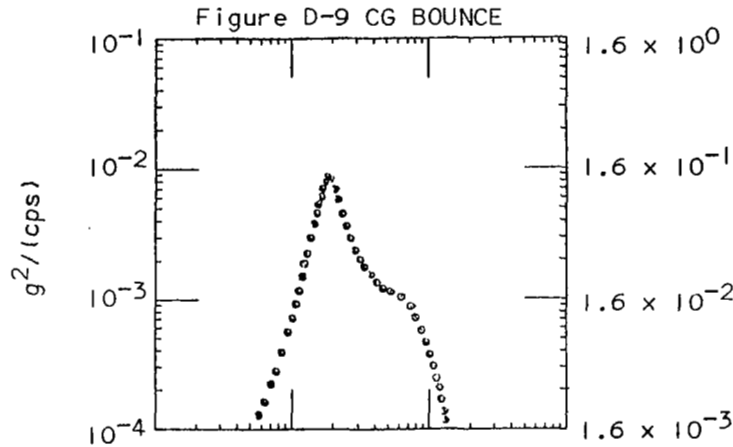
(SCALE FOR SOFT SURFACE RANDOM INPUT)



PSD'S OF TRAILER ACCELERATIONS

SCALE FOR HARD SURFACE INPUT AT 6 MPH

2×10^{-1}
 2×10^{-2}
 2×10^{-3}
 2×10^{-4}
 2×10^{-1}
 2×10^{-2}
 2×10^{-3}
 2×10^{-4}
 2×10^0
 2×10^{-1}
 2×10^{-2}
 2×10^{-3}



SCALE FOR SOFT SURFACE INPUT AT 3 MPH

1.6×10^0
 1.6×10^{-1}
 1.6×10^{-2}
 1.6×10^{-3}
 1.6×10^0
 1.6×10^{-1}
 1.6×10^{-2}
 1.6×10^{-3}
 1.6×10^1
 1.6×10^0
 1.6×10^{-1}
 1.6×10^{-2}

Frequency (cps)

APPENDIX E
TIME DOMAIN ANALYSIS

This appendix presents the results of the time domain simulation technique used to analyze vehicle models. The technique is described in detail in Appendices C and E of Reference I. The distinction between the program of Reference I and that utilized herein is the conversion of the analog computer circuits and analysis to digital analysis. The simulation was accomplished using the MIMIC Program with the corresponding statistical analysis via digital computer programs similar to those described in Appendix A of Reference I. The MIMIC language is thoroughly covered in Reference II.

Standard linearized equations of motion featuring linear springs and linear (viscous) dampers acting only in the vertical plane were used for this simulation. Since it was felt that the accelerations to cause encounter of jounce and rebound bumpers could not be obtained at the low test speeds, the corresponding non-linear feature was excluded. However, the non-linearity of wheel-surface separation was present in all model simulations. This was accomplished by allowing the tire force to take on only compressive values through the use of the MIMIC limiting function (LIM). The physical values relating the models to the test vehicles can be found in Appendix D. The soil model and data used appears in the summary of Appendix B.

The models were subjected to two different types of input. In the first case, actual profile height data was used as an input by reading directly from digital magnetic tape through a subroutine external to the MIMIC program. The second case made use of the more general representation of random surfaces. This was accomplished through the use of the Gaussian random number generator (RNG) which had a standard deviation determined by the vehicle speed and

surface roughness coefficient corresponding to field test conditions. The output of the random number generator was integrated in a manner analogous to the analog computer integration of the white noise generator described in Reference 1. In this case, the timing between new random number points was selected to be identical to the printout interval, once each .01 seconds, while the MIMIC integration step size was automatically controlled to achieve a minimum error criteria. Since the input points of either method were spaced relatively far apart for digital integrations, it was necessary to extrapolate in some fashion. A linear extrapolation of the slope of the line was selected. Thus, the velocity input was piecewise continuous while the profile was a continuous straight-line segment profile. This technique caused some difficulty due to the discontinuity at the ends of the line segments. In order to partially minimize this effect, a frequency filter was incorporated into the input portion of the simulation. This filter was essentially a "leaky" integrator; that is, the high frequency components of the segmented input were filtered out with a 3 db per octave standard RC filter simulated in the MIMIC program. The cutoff frequency of the filter was set at 200 radians per second or 31.8 cps. This filtering minimized the effects of the end point discontinuities without degrading the simulation results.

Tables E-1 and E-2 are the MIMIC source-language programs for the truck and trailer. Table E-1 lists the truck with a soil model excited by a random input. This shows the method used to generate random surface roughness inputs to four wheels using four random number generators. The generators are identical except for their starting numbers and starting time. When given the same starting numbers, two generators produce identical results. However, having different starting times, these generators yield an effective time delayed result for inputting to in-line following wheels. With different

starting numbers, the random number generator outputs will be different, that is, uncorrelated. However, the statistical properties will be the same. This fact is used to produce left and right inputs to the truck. The listing in Table E-1 also demonstrates how the maximum penetration of the soil was time delayed to allow the surface penetration to be properly computed at the rear wheels. Table E-2 gives the source language program for the trailer and soil model. In this example, the input is read directly from digital magnetic tape through an external subroutine (RED). This was the technique used to input actual profile measurements for comparison with the random generated profile as well as the field test results. All other computer simulations were either subsets or combinations of these two examples.

The results of the simulation consisted of time sampled data; that is, results each printout time were recorded directly on digital tape from the MIMIC program. In all cases, the simulation was allowed some time, approximately 5 seconds, for the start-up transients to die out before results were recorded. The simulation was then allowed to run until 2,000 points of data per variable of interest had been generated; this corresponds to 20 seconds of simulated test time. The recorded time sampled vehicle acceleration data was fed back into statistical processing programs to yield estimates such as the power spectral densities shown in the figures at the end of this appendix. Another estimate of interest is the RMS acceleration values which appear in Table E-3. In addition to the computer runs which were identical to field measurements, several changes were made to show the effects of various influences. The most interesting of the variations, that of with and without a soil model, has been included in the results shown in this appendix. It should be pointed out that simulations of the hard surface or without a

Table E-3 RMS ACCELERATIONS FROM MIMIC SIMULATION

VEHICLE		M-37 TRUCK			SINGLE WHEEL TRAILER		
TEST	Surface (C in Ft)	Bounce (g's)	Pitch (Rad / Sec ²)	Roll (Rad / Sec ²)	Bounce (g's)	Pitch (Rad / Sec ²)	Wheel Bounce (g's)
3 MPH	Soft (C=.000232)	.132	1.004	2.107	.342	.733	.796
3 MPH	Soft-No Soil (C=.000232)	.180	1.470	3.049	.435	.933	1.091
3 MPH	Hard (C=.0000145)	.045	.360	.772	.109	.235	.274
6 MPH	Hard (C=.0000145)	.069	.444	1.135	.154	.331	.388
3 MPH	Soft	{ Actual Profile Measurements as Input to Trailer Model }			.219	.470	.209
3 MPH	Soft-No Soil				.273	.585	.309
3 MPH	Hard				.058	.122	.055
6 MPH	Hard				.173	.370	.153

soil model were achieved by setting the dependent variables of the soil model (see Table E-1 or E-2) to zero.

The results as shown in the figures of this appendix are all acceleration power spectral density estimates. Figures E-1 through E-6 show the truck response on a hard random surface at the two test speeds. Figures E-7 through E-12 are also truck motions on a random surface; however the speed was held constant at 3 MPH while the input was allowed to represent the soft surface with and without the soil model. The rest of the figures are trailer results. Figures E-13 through E-18 represent trailer response at two speeds on the hard random surface. The trailer motions as determined on the soft surface with and without a soil model are shown in Figures E-19 through E-24. A comparison of actual versus random inputs at 3 MPH may be obtained in Figures E-25

through E-30. The last set of trailer results, shown in Figures E-31 through E-36, are only c.g. bounce acceleration for all the test conditions; that is, hard and soft surfaces at the test speed of 3 and 6 MPH, with actual and random generated profiles as inputs.

A PSD of the MIMIC generated random surface profile used for the left lane of the M37 truck is plotted in Figure E-37. This profile was generated for the 3 MPH run with the soft surface roughness coefficient. The same random number sequence was used for the left track of the truck and all trailer runs. The only distinction being made was the timing of the random generator output and the amplitude of the random points as dictated by the surface roughness coefficient. A second independent random generator was used for the right track of the truck model with its corresponding PSD shown in Figure E-38.

Table E-1 TRUCK COMPUTER PROGRAM

MIMIC SOURCE-LANGUAGE PROGRAM

* M-37 TRUCK WITH RANDOM PROFILE INPUT.

CON%DT ,DTMX,DTMN,SECS,STRT, G □
 CON%X01 ,X02 ,Z01 ,Z02 ,Z1LS,Z1RS□
 CON%Z2LS,Z2RS,Z1LW,Z1RW,Z2LW,Z2RW□
 CON% MO, M1, M2, IO, I1, I2□
 CON% C1S, C2S, K1S, K2S, K1W, K2W□
 CON% ISI, C1W, C2W,OVY0,OVSI,OVTO□
 CON%OY0 , OY1, OY2, OT0, OT1, OT2□
 CON% OSI,OVY1,OVY2,OV11,OV12,XXXX□
 CON%VELC, XO,OPTN,CNT1,CNTR,SWIT□
 CON%PM37,RF37,BM37,CS37,SM37,RM37□
 CON%OS10,OS11,OS20,OS21,OY10,OY11□
 CON%2PIE, SCR, ST1, ST2, ST3, ST4□
 CON%NTAU□

TEQO FSW%T,TRUE,TRUE,FALS□
 12DG 12./G
 TEQO 1DMO 1./MO
 TEQO SGMA 2PIE*SQR%SCR*VELC/%2.*DT□□
 TEQO RECV -2.*VELC/RM37
 TFQO PDVB PM37/BM37
 TEQO REST 1.0-PDVB/RF37
 TEQO MS37 -1./SM37

SWIT RST%XXXX,T□
 NUDT FSW%T-SWIT,FALS,TRUE,FALS□
 DLAY FSW%T&NTAU,FALS,TRUE,TRUE□
 OUT3 FSW%T-STRT,FALS,TRUE,TRUE□
 WRT3 AND%NUDT,OUT3□
 REAR AND%NUDT,DLAY□
 WRT3 CNT1 CNT1&1.
 XD1S INT%VELC,XO□

THE INPUT DISPLACEMENTS Y10, Y11, Y20, AND Y21 ARE GENERATED HERE.

NUDT 1LLL RNG%0.0,SGMA,ST1□
 NUDT 1RRR RNG%0.0,SGMA,ST3□
 REAR 2LLL RNG%0.0,SGMA,ST2□
 REAR 2RRR RNG%0.0,SGMA,ST4□

Y10P INT%1RRR,OY10□
 Y11P INT%1LLL,OY11□
 Y20P INT%2RRR,OY10,TRUE,DLAY□
 Y21P INT%2LLL,OY11,TRUE,DLAY□
 D10P 200.*%Y10P-P10P□
 P10P INT%D10P,OY10□
 D11P 200.*%Y11P-P11P□
 P11P INT%D11P,OY11□
 D20P 200.*%Y20P-P20P□
 P20P INT%D20P,OY10□
 D21P 200.*%Y21P-P21P□
 P21P INT%D21P,OY11□
 Q1DR TDL%10MX, NTAU,214.□
 Q1DL TDL%11MX, NTAU,214.□

Table E-1 (Continued)

M-37 BODY EQUATIONS

A $Y0 - \%X01 * SI \& Y1 \square$
 E $1DY0 - \%X01 * 1DSI \& 1DY1 \square$
 F $Y0 \& X02 * SI - Y2$
 D $1DY0 \& X02 * 1DSI - 1DY2$

F1LS IS THE FORCE ON THE M-37 BODY FROM THE FRONT-LEFT SUSPENSION SYSTEM.
 F1LS $MAD\%K1S, \%Z1LS * T1 \& A \square - Z01 * T0, C1S, \%Z1LS * 1DT1 \& E \square - Z01 * 1CT0 \square$

F1RS IS THE FORCE ON THE M-37 BODY FROM THE FRONT-RIGHT SUSPENSION SYSTEM.
 F1RS $MAD\%K1S, \%Z01 * T0 \& A \square - Z1RS * T1, C1S, \%Z01 * 1DT0 \& E \square - Z1RS * 1CT1 \square$

F2LS IS THE FORCE ON THE M-37 BODY FROM THE REAR-LEFT SUSPENSION SYSTEM.
 F2LS $MAD\%K2S, \%Z2LS * T2 \& F \square - Z02 * T0, C2S, \%Z2LS * 1DT2 \& D \square - Z02 * 1CT0 \square$

F2RS IS THE FORCE ON THE M-37 BODY FROM THE REAR-RIGHT SUSPENSION SYSTEM.
 F2RS $MAD\%K2S, \%Z02 * T0 \& F \square - Z2RS * T2, C2S, \%Z02 * 1DT0 \& D \square - Z2RS * 1DT2 \square$

THE VERTICAL FORCE DUE TO THE SUSPENSION ELEMENTS AND WEIGHT ACTING ON THE M-37 BODY IS F1.

* F1 $-\%M0 * G \& \%F1LS \& F1RS \& F2LS \& F2RS \square$

THE M-37 BODY ACCELERATION, VELOCITY, AND DISPLACEMENT ARE SOLVED FOR HERE.

2DY0 $-\%F1LS \& F1RS \& F2LS \& F2RS \square * 1DM0 \& G \square$
 1DY0 $INT\%2DY0, 0VY0 \square$
 Y0 $INT\%1DY0, 0Y0 \square$

THE TORQUES DUE TO THE SUSPENSION ELEMENTS ACTING ON THE M-37 BODY IS TT.

TT $\%X01 * \%F1LS \& F1RS \square - X02 * \%F2LS \& F2RS \square$

THE M-37 BODY PITCH ACCELERATION, VELOCITY, AND ANGLE ARE SOLVED FOR HERE.

2DSI TT / ISI
 1DSI $INT\%2DSI, 0VSI \square$
 SI $INT\%1DSI, 0SI \square$

THE M-37 BODY ROLL ACCELERATION, VELOCITY, AND ANGLE ARE SOLVED FOR HERE.

2DTO $MAD\%Z01, F1LS - F1RS, Z02, F2LS - F2RS \square / I0$
 1DTO $INT\%2DTO, 0VTO \square$
 TO $INT\%1DTO, 0TO \square$

F1RW IS THE FORCE ON THE FRONT-RIGHT WHEEL OF THE M-37.

P101 $Y1 - \%YS10 \& P10P \square$
 Q101 $Z1RW * T1 \& P101$
 P102 $1DY1 - \%1S10 \& D10P \square$
 Q102 $Z1RW * 1DT1 \& P102$
 L1RW $-\%MAD\%K1W, Q101, C1W, Q102 \square$
 F1RW $LIM\%L1RW, 0., L1RW \square$

F1LW IS THE FORCE ON THE FRONT-LEFT WHEEL OF THE M-37.

P103 $YS11 \& P11P - Y1$
 Q103 $Z1LW * T1 \& P103$
 P104 $1S11 \& D11P - 1DY1$
 Q104 $Z1LW * 1DT1 \& P104$
 L1LW $MAD\%K1W, Q103, C1W, Q104 \square$
 F1LW $LIM\%L1LW, 0., L1LW \square$

Table E-1 (Continued)

F2RW IS THE FORCE ON THE REAR-RIGHT WHEEL OF THE M-37.

P105 Y2-%YS20&P20P□
 Q105 Z2RW*T2&P105
 P106 1DY2-%1S20&D20P□
 Q106 Z2RW*1DT2&P106
 L2RW -MAD%K2W,Q105,C2W,Q106□
 F2RW LIM%L2RW,0.,L2RW□

F2LW IS THE FORCE ON THE REAR-LEFT WHEEL OF THE M-37.

P107 YS21&P21P-Y2
 Q107 Z2LW*T2&P107
 P108 1S21&D21P-1DY2
 Q108 Z2LW*1DT2&P108
 L2LW MAD%K2W,Q107,C2W,Q108□
 F2LW LIM%L2LW,0.,L2LW□

THE M-37 FRONT-AXLE ACCELERATION, VELOCITY, AND DISPLACEMENT ARE SOLVED FOR HERE.

2DY1 %F1LS&F1RS&F1LW&F1RW□/M1-G
 1DY1 INT%2DY1,0VY1□
 Y1 INT%1DY1,0Y1□

THE M-37 REAR-AXLE ACCELERATION, VELOCITY, AND DISPLACEMENT ARE SOLVED FOR

2DY2 %F2LS&F2RS&F2LW&F2RW□/M2-G
 1DY2 INT%2DY2,0VY2□
 Y2 INT%1DY2,0Y2□

THE M-37 FRONT-AXLE ROLL ACCELERATION, VELOCITY, AND DISPLACEMENT ARE SOLVED FOR HERE.

2DT1 %MAD%71RS,F1RS,Z1RW,F1RW□-MAD%Z1LS,F1LS,Z1LW,F1LW□/I1
 1DT1 INT%2DT1,0VT1□
 T1 INT%1DT1,0T1□

THE M-37 REAR-AXLE ROLL ACCELERATION, VELOCITY, AND DISPLACEMENT ARE SOLVED FOR HERE.

2DT2 %MAD%Z2RS,F2RS,Z2RW,F2RW□-MAD%Z2LS,F2LS,Z2LW,F2LW□/I2
 1DT2 INT%2DT2,0VT2□
 T2 INT%1DT2,0T2□

M-37 SOIL EQUATIONS

THE SOIL ACCELERATION, VELOCITY, AND DISPLACEMENT UNDER THE M-37 FRONT-RIGHT WHEEL ARE SOLVED FOR HERE.

2S10 %CS37*1S10&KS10&F1RW□*MS37
 1S10 INT%2S10,0.0□
 YS10 INI%1S10,0S10□
 10ON FSW%10MX-YS10,FALS,FALS,TRUE□
 1D10 RFCV*10MX
 10MX INT%1D10,YS10,10ON,FALS□
 P110 PDVB*10MX
 KS10 RF37*%YS10-10MX□&P110

Table E-1 (Continued)

THE SOIL ACCELERATION, VELOCITY, AND DISPLACEMENT UNDER THE M-37 FRONT-LEFT WHEEL ARE SOLVED FOR HERE.

2S11 %CS37*1S11&KS11&F1LW□*MS37
 1S11 INT%2S11,0.0□
 YS11 INT%1S11,0S11□
 11ON FSW%11MX-YS11,FALS,FALS,TRUE□
 1D11 RECV*11MX
 11MX INT%1D11,YS11,11ON,FALS□
 P111 PDVB*11MX
 KS11 RF37*%YS11-11MX□&P111

THE SOIL ACCELERATION, VELOCITY, AND DISPLACEMENT UNDER THE M-37 REAR-RIGHT WHEEL ARE SOLVED FOR HERE.

2S20 %CS37*1S20&KS20&F2RW□*MS37
 1S20 INT%2S20,0.0□
 YS20 INT%1S20,0S20□
 200N FSW%NU20&OLDR-YS20,FALS,FALS,TRUE□
 1D20 RECV*NU20
 NU20 INT%1D20,YS20-OLDR,200N,FALS□
 20MX OLDR&NU20
 PI20 PDVB*20MX
 KS20 RF37*%YS20-20MX□&PI20

THE SOIL ACCELERATION, VELOCITY, AND DISPLACEMENT UNDER THE M-37 REAR-LEFT WHEEL ARE SOLVED FOR HERE.

2S21 %CS37*1S21&KS21&F2LW□*MS37
 1S21 INT%2S21,0.0□
 YS21 INT%1S21,0S21□
 21ON FSW%NU21&OLDL-YS21,FALS,FALS,TRUE□
 1D21 RECV*NU21
 NU21 INT%1D21,YS21-OLDL,21ON,FALS□
 21MX OLDL&NU21
 PI21 PDVB*21MX
 KS21 RF37*%YS21-21MX□&PI21
 CNTR CNTR&1.

NUDT TIME T
 NUDT SWIT 2.*T
 NUDT ACCO 2DY0/G
 NUDT ACC1 2DY1/G
 NUDT ACC2 2DY2/G
 NUDT ACSI 2DSI*12DG

NOTE CNT3 IS THE RESTORED SOIL AFTER THE TRUCKS REAR WHEEL HAS PASSED

NUDT CNT3 REST*20MX&P20P
 NUDT ACT0 2DT0*12DG
 NUDT ACT1 2DT1*12DG
 NUDT ACT2 2DT2*12DG
 NUDT AS10 2S10/G
 NUDT AS11 2S11/G
 NUDT AS20 2S20/G
 NUDT AS21 2S21/G
 FIN%CNT1,2000.□
 FIN%TIME,SECS□
 WRT3 OUT%ACCO,ACSI,ACT0,P10P,P11P,CNT3□
 END

Table E-2 TRAILER COMPUTER MODEL

MIMIC SOURCE-LANGUAGE PROGRAM

* TRAILER ON SOFT SOII PROFILE 3 MPH POINTS ARE AT 5 IN. SPACING

```

.
$
      CON% DT,DTMX,DTMN,SECS,IB , G□
      CON% KW, CW, KT, CT, MB, MW□
      CON%VELC,OPTN,CNT3,P,SWIT,CNTR□
      CON%XO ,OYB ,OYW ,OVYB,OVYW,OYR□
      CON%RFT,P1,B,CS,MEF,RT□
. COMPUTE PROGRAM CONSTANTS ONLY AT TIME ZERO 180 IN. IS THE LENGHT OF BOOM
. FROM TRAILER BED CG. TO HITCH POINT
      TEQO FSW%T,TRUE,TRUE,FALS□
TEQO MBTG MB*G
TEQO EFFM 1./%MB&IB/%180.*180.□□
TEQO DIVG 1./G
TEQO D180 1./180.
TEQO 12DG 12.*DIVG
TEQO NVOR -2.*VELC/RT
TEQO PDVB P1/B
TEQO RECF 1.0-PDVB/RFT
. GET INPUT FROM TAPE AND SET UP CONTROL FOR WRITING OUTPUT TAPE EVERY DT.
      XDIS INT%VELC,XO□
      OOD2 RED%OPTN,XDIS,YRIN□
      YPP YRIN*12.
      1DYP 200.*%YPP-YP□
      YP INT%1DYP,OYR□
      SWIT RST%P,T□
      NUOT FSW%T-SWIT,FALS,TRUE,FALS□
      OUT3 FSW%T-4.99,FALS,FALS,TRUE□
      WRT3 AND%NUOT,OUT3□
WRT3 CNT3 CNT3&1.
. TRAILER EQUATIONS OF MOTION
THE VERTICAL FORCE ACTING ON THE TRAILER BODY IS F3.
      FS KW*%YW-YB□&CW*%1DYW-1DYB□
      F3 FS-MBTG
. THE ACCELERATION, VELOCITY, AND DISPLACEMENT
OF THE TRAILER BODY ARE SOLVED FOR HERE.
.
      2DYB F3*EFFM
      1DYB INT%2DYB,OVYB□
      YB INT%1DYB,OYB□
. FWR IS THE VERTICAL FORCE BETWEEN THE WHEEL AND RIM OF THE TRAILER.
      FWSL KT*%YP&YS-YW□&CT*%1DYP&1DYS-1DYW□
NOTE SEPERATION PUT INTO MODEL BY LIMITING THE FORCE INPUT TO POSITIVE VALUES
      FWR LIM%FWSL,0.,FWSL□
. THE ACCELERATION, VELOCITY, AND DISPLACEMENT
OF THE TRAILER WHEEL ARE SOLVED FOR HERE.
      2DYW %FWR-FS□/MW-G
      1DYW INT%2DYW,OVYW□
      YW INT%1DYW,OYW□

```

Table E-2 (Continued)

THE ACCELERATION, VELOCITY, AND DISPLACEMENT
OF THE SOIL UNDER THE TRAILER ARE SOLVED FOR HERE.

2DYS -%CS*1DYS&KS&FWR/MEF
 1DYS INT%2DYS,0.0
 YS INT%1DYS,0.0
 YON FSW%YMAX-YS,FALS,FALS,TRUE
 1DYM NVOR*YMAX
 YMAX INT%1DYM,YS,YON,FALS
 PHI YMAX*PDVB
 KS RFT*%YS-YMAX&PHI
 CNTR CNTR&1.

COMPUTE THE FOLLOWING VALUES ONLY AT EACH PRINT OUT TIME I.E. EACH NEW DT

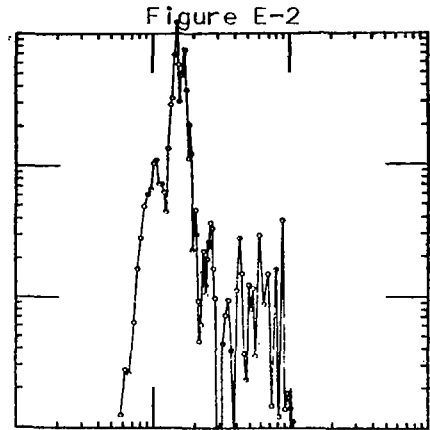
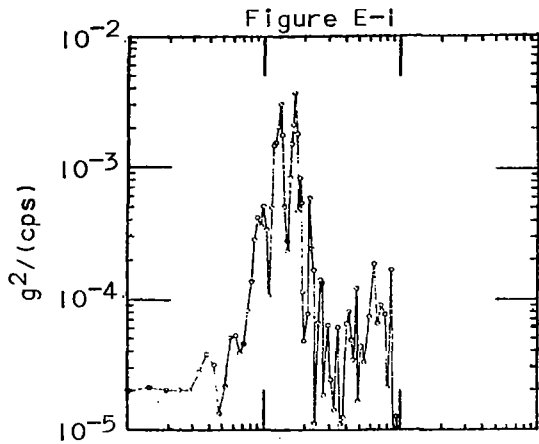
NUDT SWIT MPY%2.,T
 NUDT ACCB 2DYB*DIVG
 NUDT ACCW 2DYW*DIVG
 NUDT ACCS 2DYS*DIVG
 NUDT TIME T

THE TRAILER PITCH ACCELERATION AND ANGLE ARE SOLVED FOR HERE.

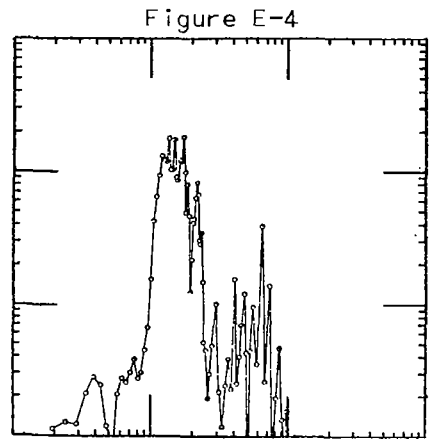
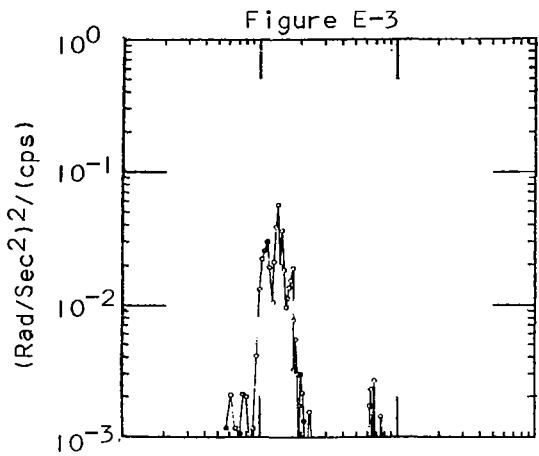
NUDT 2SIB 2DYB*D180
 NUDT ASIB 2SIB*12DG
 NUDT SIB YB*D180
 NUDT YRES RECF*YMAX&YP
 FIN%XDIS,3006.
 OUT%TIME,CNT3,ACCS,ASIB,ACCB,ACCW
 OUT% YP,1DYM,YS,YMAX,YB,YW
 OUT%YPP,1DYP,1DYS,CNTR,1DYB,1DYW
 OUT%XDIS,FWR,FWSL,YRES,KS,PHI
 OUT
 WRT3 OUT%ACCB,ACCW,ACCS,YP,YRES,CNT3
 END

TRUCK PSD'S FOR HARD RANDOM SURFACE INPUT

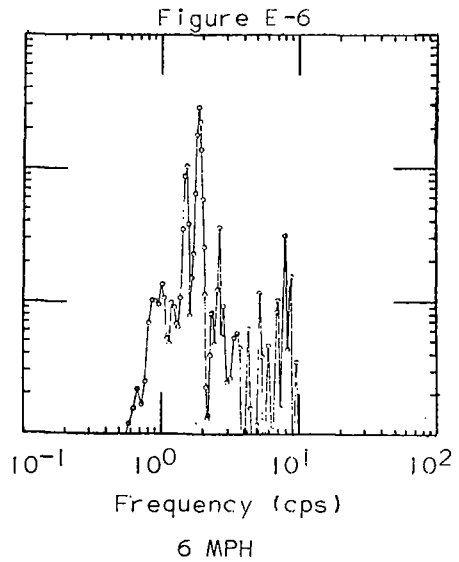
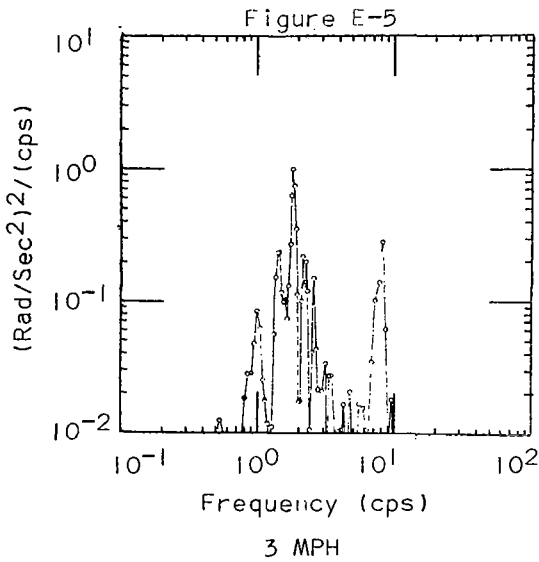
-BOUNCE-



-PITCH-

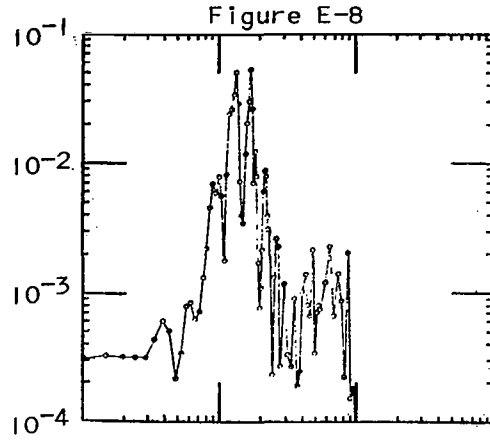
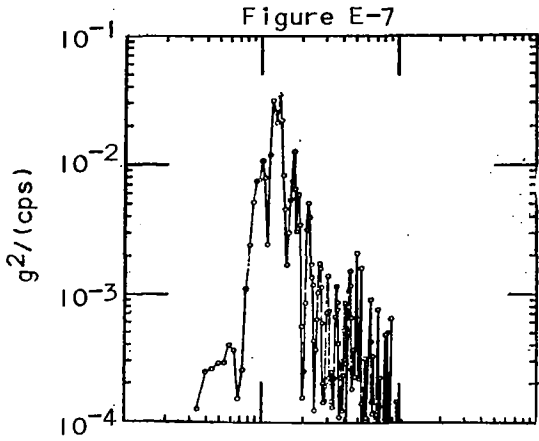


-ROLL-

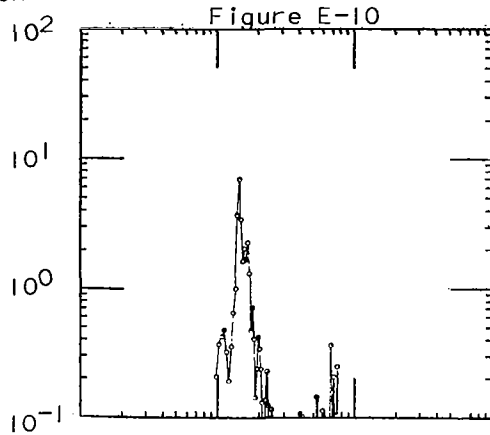
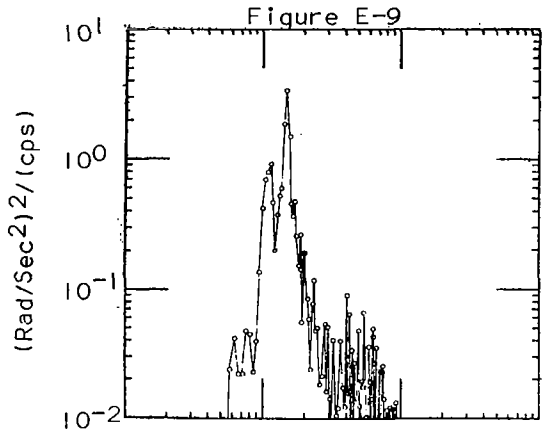


TRUCK PSD'S FOR SOFT RANDOM SURFACE INPUT @ 3 MPH

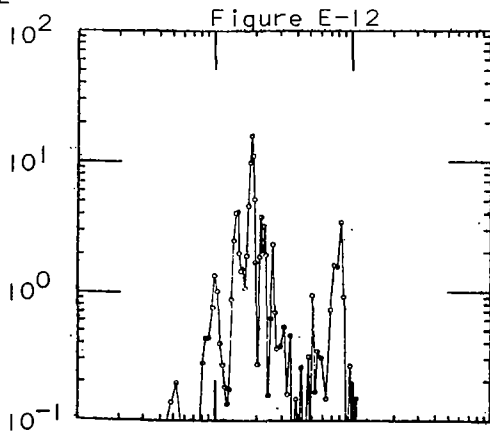
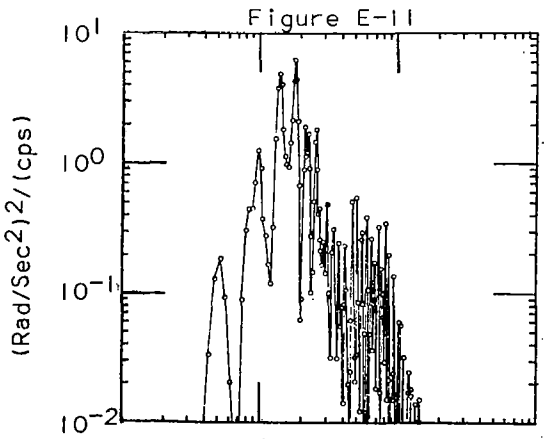
-BOUNCE-



-PITCH-



-ROLL-



Frequency (cps)

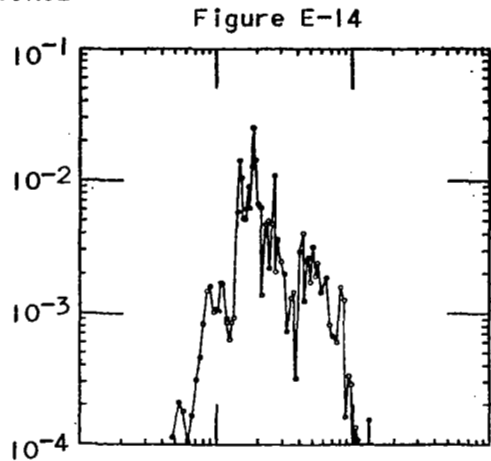
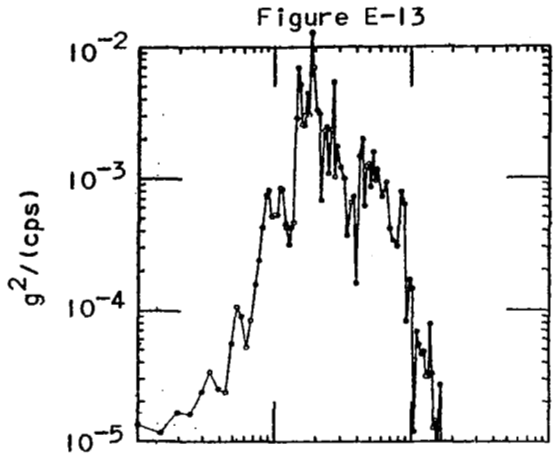
Frequency (cps)

WITH SOIL MODEL

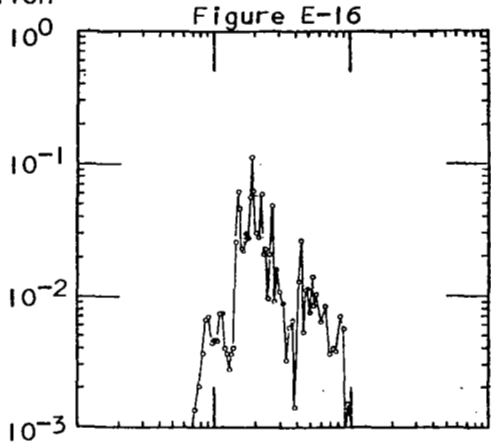
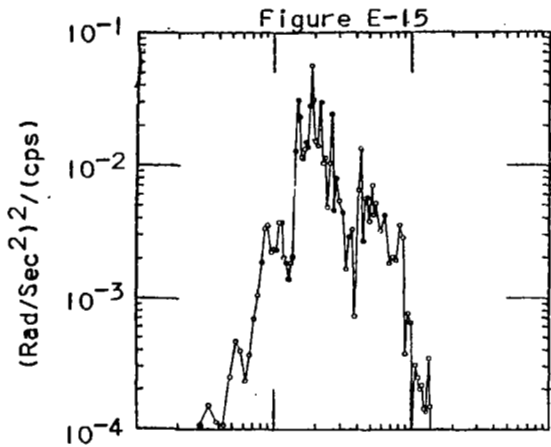
WITHOUT SOIL MODEL

TRAILER PSD'S FOR HARD RANDOM SURFACE INPUT

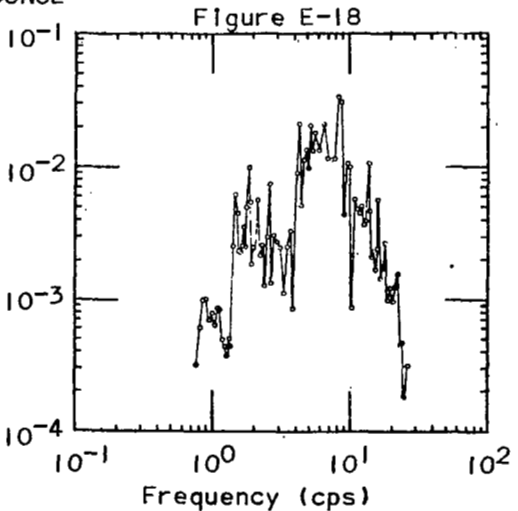
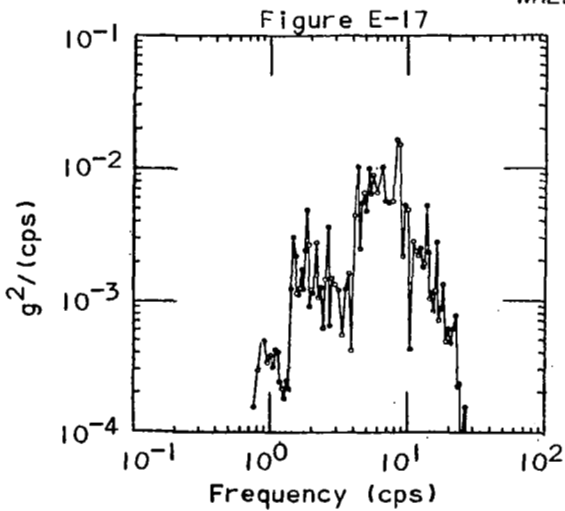
-CG BOUNCE-



-CG PITCH-



-WHEEL BOUNCE-



3 MPH

6 MPH

PSD'S OF TRAILER ON SOFT SURFACE AT 3 MPH

-CG BOUNCE-

Figure E-19

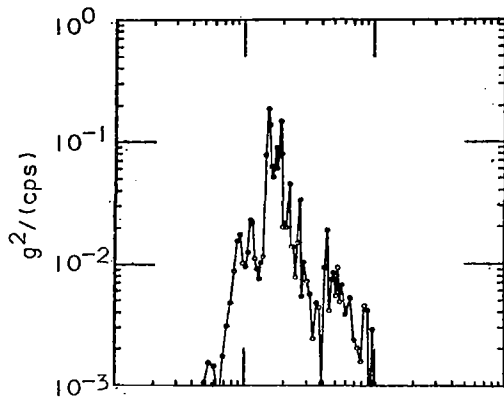
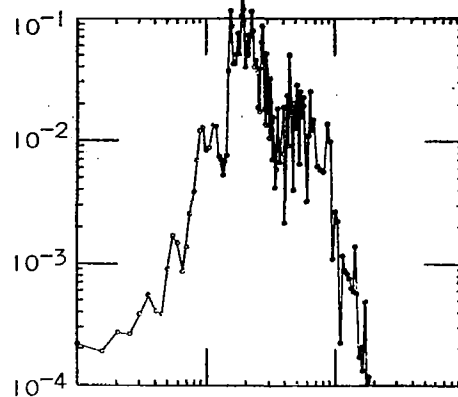


Figure E-20



-CG PITCH-

Figure E-21

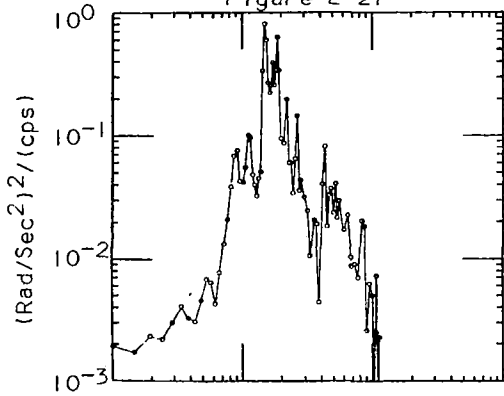
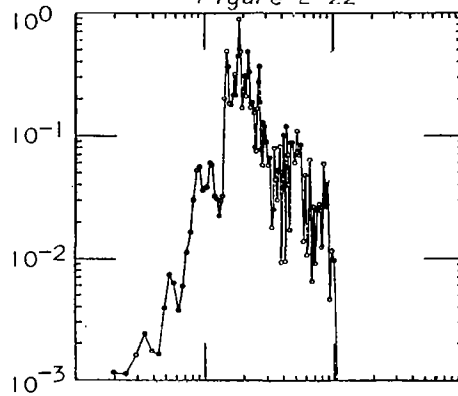


Figure E-22



-WHEEL BOUNCE-

Figure E-23

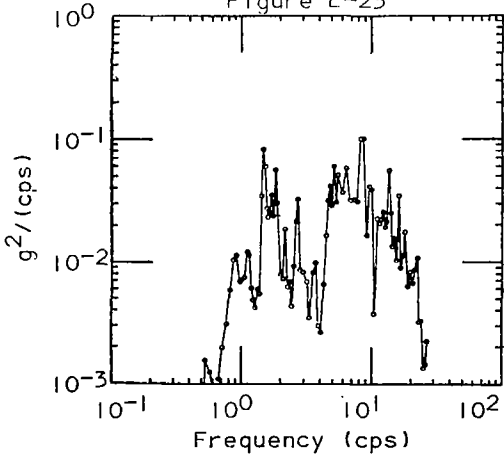
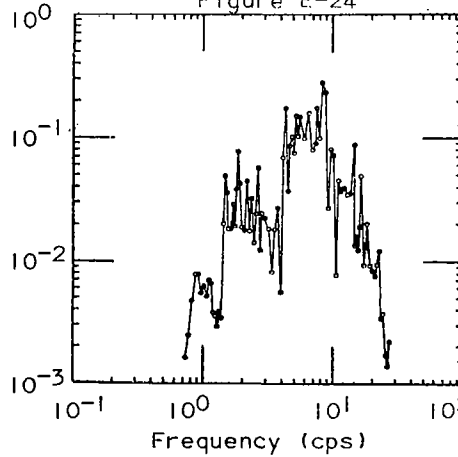


Figure E-24

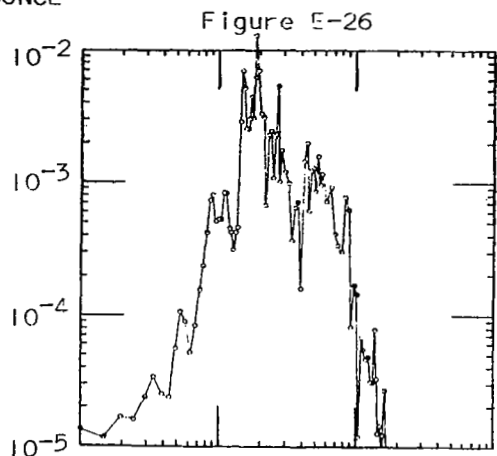
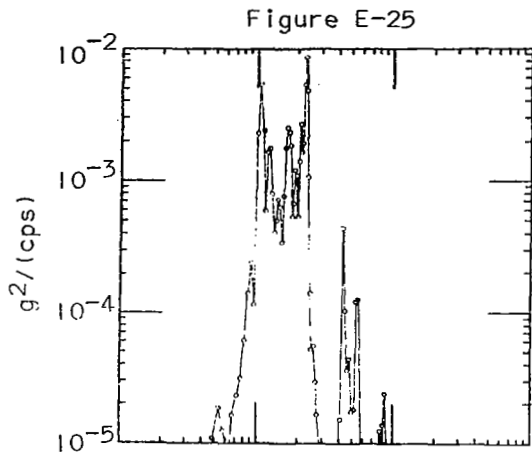


WITH SOIL MODEL

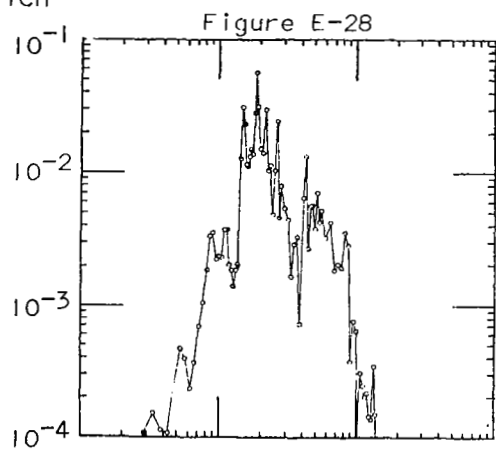
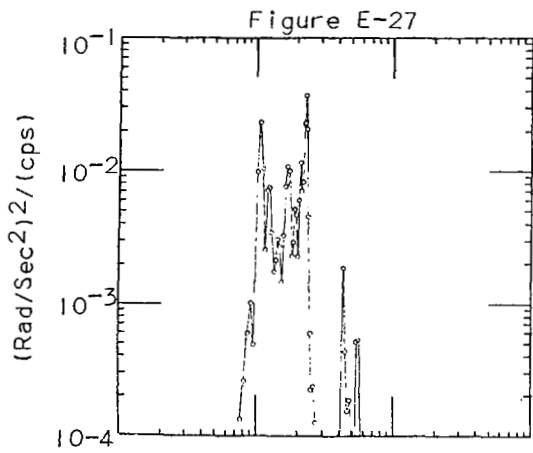
WITHOUT SOIL MODEL

PSD'S OF TRAILER ON HARD SURFACE AT 3 MPH

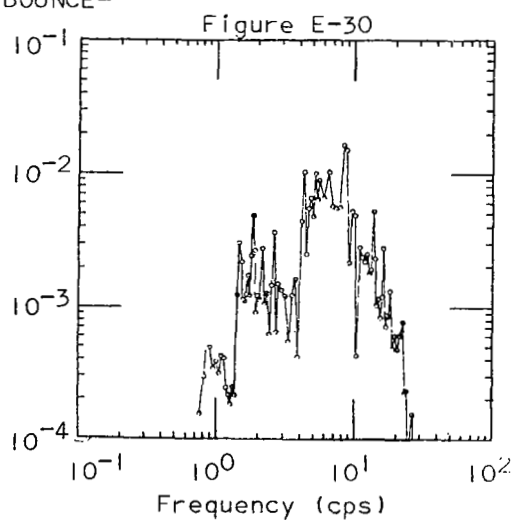
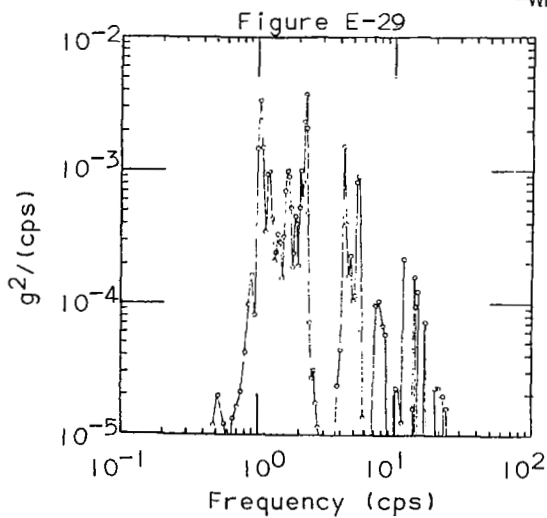
-CG BOUNCE-



-CG PITCH-



-WHEEL BOUNCE-

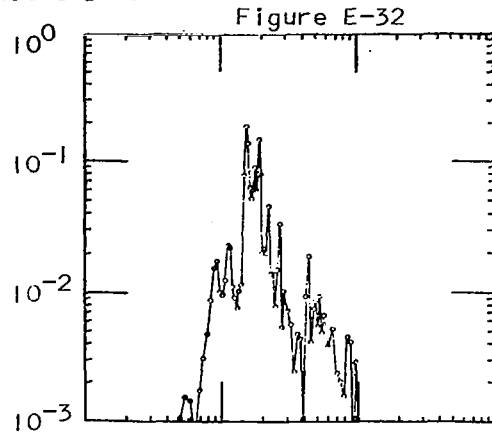
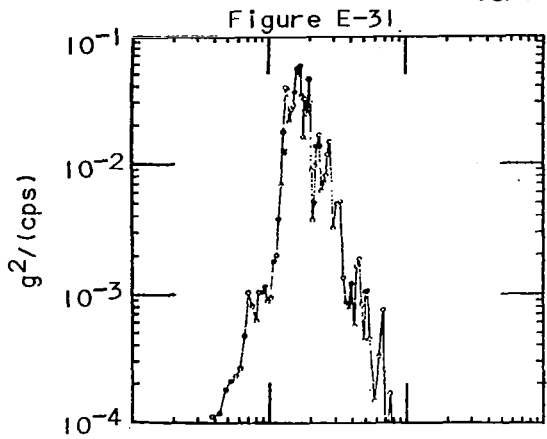


ACTUAL INPUT

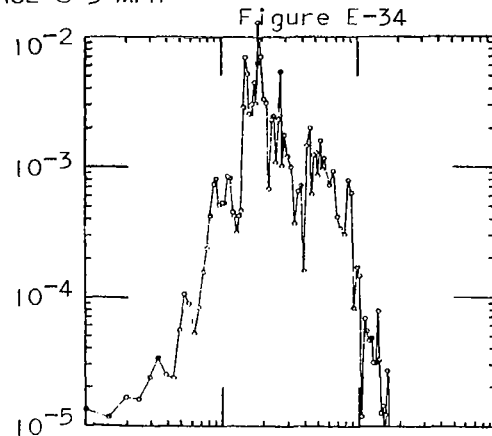
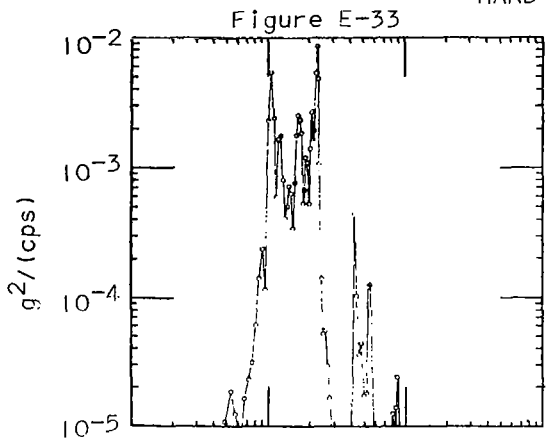
RANDOM INPUT

PSD'S OF TRAILER CG. BOUNCE ACCELERATIONS

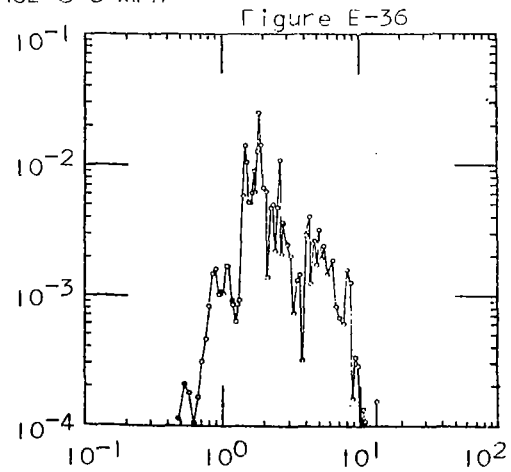
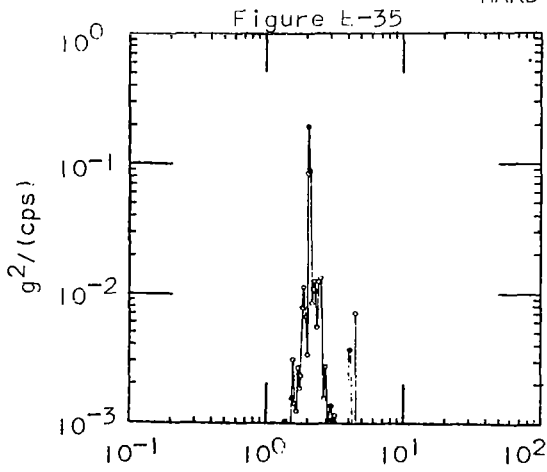
-SOFT SURFACE @ 3 MPH -



-HARD SURFACE @ 3 MPH -



-HARD SURFACE @ 6 MPH -



Frequency (cps)

Fréquency (cps)

ACTUAL INPUT

RANDOM INPUT

Figure E-37 PSD - RANDOM GENERATED SURFACE PROFILE - LEFT

Soft Surface C = 2.32×10^{-4}

TRUCK LEFT LANE AT 3 MPH

FREQUENCY (cycles/ft)

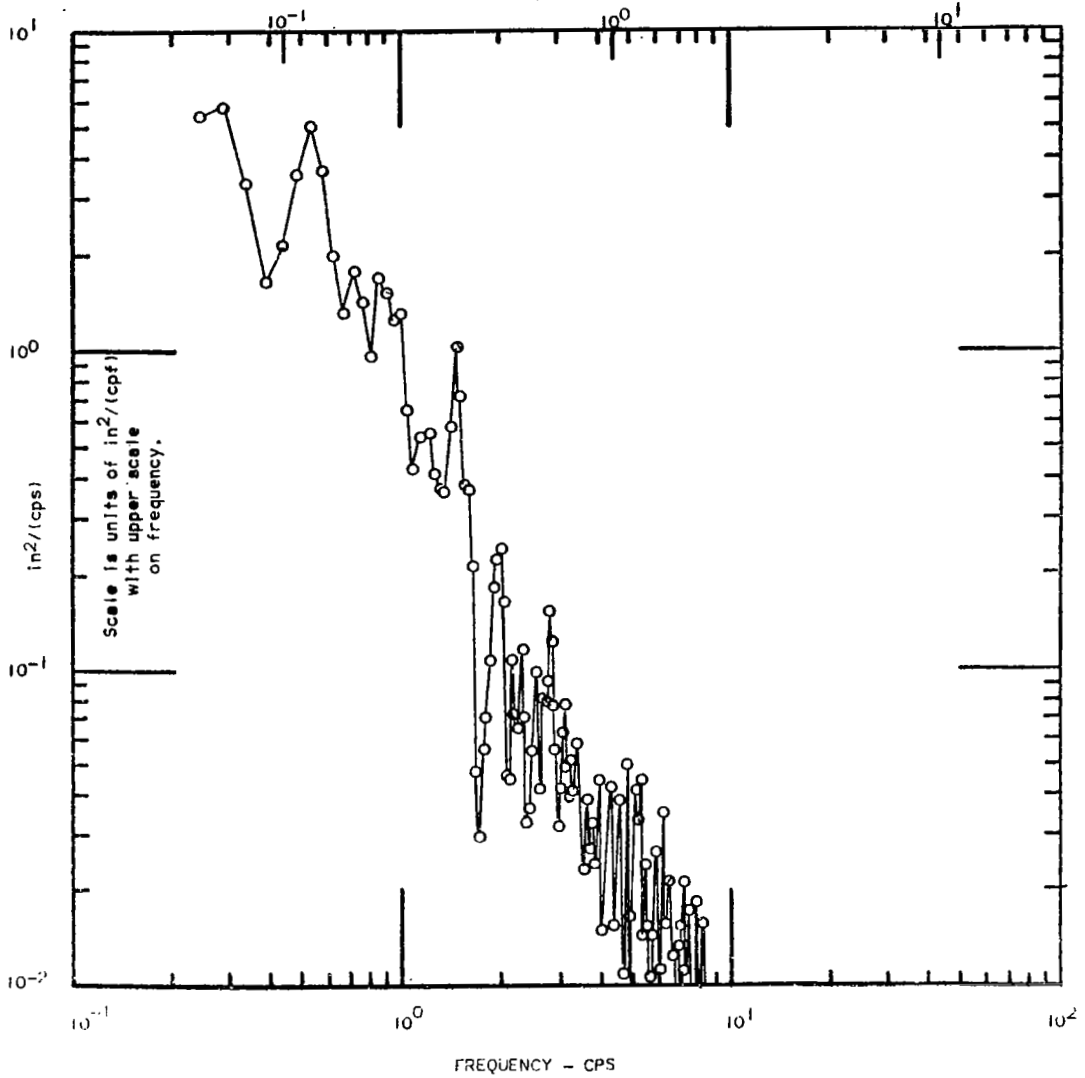


Figure F-38 PSD - RANDOM GENERATED SURFACE PROFILE - RIGHT

Soft Surface $C = 2.32 \times 10^{-4}$

TRUCK RIGHT LAND AT 3 MPH

FREQUENCY (cycles/ft)

